Rational Design, Synthesis and Evaluation of Novel Second Mitochondrial-Derived Activators of Caspase (Smac) Mimetics That Induce Apoptosis in Human MDA-MB-231 Breast Cancer Cell Line

By: Tasbir Cheema

Thesis submitted to the
Faculty of Graduate & Postdoctoral Studies
In fulfillment of the requirements for the
Masters of Science degree in Chemistry at the University of Ottawa

Candidate	Supervisor
_____	_____
Tasbir Cheema	Dr. Robert N. Ben

I dedicate this work, and all my life's achievements, to my wife, my family, and to all those who believed in me even when I did not believe in myself.

"*Education is the most powerful weapon which you can use to change the world*."

- **Nelson Mandela**

"*The most common way people give up their power is by thinking they don't have any*"

- Alice Walker

Table of Contents

List of Figures

List of Tables

List of Schemes

Abstract

Programmed cell death (apoptosis) is the most common mechanism of cell death in eukaryotes. The ability of cancer cells to evade and inhibit apoptosis has become a hallmark feature of cancer. This is accomplished through a family of proteins known as the inhibitor of apoptosis proteins (IAPs). X-Linked inhibitor of apoptosis protein (XIAP) is one of the best characterized IAPs. XIAP suppresses apoptosis by forming complexes with cysteine-aspartic proteases (caspase), through one of its baculovirus IAP repeat (BIR) domains. Its activity is endogenously antagonized by a second mitochondria derived activator of caspase (Smac). The anti-apoptotic behaviour of XIAP and the critical role it plays in the apoptotic program makes the Smac-XIAP interaction an important drug target. To this end, our laboratory is interested in synthesizing biologically related Smac mimetics which can induce apoptosis in a MDA-MB-231 cell line.

Efforts have focused on (1) understanding BIR domain binding sites which allow for this interaction, and (2) the design and synthesis of molecules which are much more effective at inducing apoptosis compared to other well known analogues.

Through the synthesis and evaluation of various divalent Smac mimetics we have been able to support the hypothesis that the likely binding site on XIAP is the BIR3 domain. As well, through the synthesis of a library of novel compounds, as described in the thesis, we have been able to assess the nature of the linker which joins the two tetrapeptide units. In our effort to understand which domains Smac binds with, various divalent analogues were synthesized containing MeAVPI-linker-IPVMeA (forward-reverse) and MeAVPI-linker-MeAVPI (forward-forward) sequence, which incorporated linkers with varying degrees of flexibility. We hypothesized that the forward-forward divalent mimetics would have decreased activity compared to the peptides synthesized in a forward-reverse fashion.

Lastly, information gathered from structure activity relationship (SAR) studies have shown that substituting the lysine (P2) and isoleucine residues (P4) in the AVPI protein can create more potent inducers of apoptosis than its native AVPI sequence. As one of the most potent Smac mimetic that has been previously made known contains an alkyne bridge at P2 and a large hydrophobic moiety at P4, we hypothesized that similar Smac mimetics containing a propargyl glycine residue at P2 and a bulky hydrophobic moiety at P4 will be much more potent in inducing apoptosis.

Acknowledgments

I would like to express my sincere appreciation to the following people. First and foremost I would like to thank Professor Robert N. Ben for allowing me the freedom to introduce and work on a new research field in his laboratory. I truly appreciate all of his support, guidance, and his flexibility on allowing me to contribute and pursue my own ideas on this project. As well for all the fun summer and Christmas parties at Dr. Bens' house, the place where the first brown Santa was introduced.

All my success, however, could not have been achieved without the support, love, encouragement, and at times extreme sacrifices made by my family. Not only in helping me achieve my goals in education but allowing me the freedom to grow, discover, and learn that the only limitations in life are those I impose on myself. I would also like to thank my wife who gave me the strength to continue, believed in me, and always reminded me that these tough times now are only small hurdles to a future full of success.

I would also like to thank Dr. Roger Tam, without whom I probably never would have gotten the opportunity to join Dr. Ben's lab. Dr. Tam has been a key inspiration for me in countless ways, and he was the only one who on a daily bases reminded me to always strive to better than myself and those around me but to remain humble. Also it was Dr. Tam who introduced me to the refined taste of single malt scotch, dark beers, and showed me how to get my money's worth at an all you can eat sushi bar. A friendship I hold dearly to my heart and one that I know will last a life time.

The challenges along the way, from my first day in the lab to the day I finished, could not have been made easier unless for the wisdom and invaluable research skills passed down to me by Dr. Mike Souweha, Dr. Mathiew Leclere, and Dr. Roger Tam. Also, Jacqueline Tokarew for guiding me and showing me countless times how to culture cells, how to use the hemocytometer, for keeping me calm when I was having difficulties with the cell line; also for providing a wall full of funny and memorable quotes. Lastly I

would like to thank Wendy Campbell for allowing me to share her fume hood while doing my honours project, and for making working by the stills fun.

My time in graduate school could not have been any more fun if it wasn't for all of the Tuesday wing and beer nights, Sushi nights, F&S lunch time beers, Honest Lawyer party nights, and house parties. All thanks to the memorable time created and shared by the following amazing friends: Dr. Burk Wilki, Jay-Eggfoo Yung, Idralyn Alacron and family, Sophie Rousseaux, Dr. Benoit Liegault, Mark Dornan, Christian Clavette, Dragana Petrovic, Jeffery Grainger, Taline Boghossian, Jacqueline Tokarew, Anna Balcerzak, Chantelle Capicciotti, Isabelle Dion, Matthew Whitmore, Tom Markiewicz, Dr. Sebastien Lethu, and all others I am currently drawing a blank on.

I would like to thank a few memorable and remarkable undergraduate students that I have had the pleasure to work with or around: Michela Fabbraro, Ross Mancini, and Bonnie Kwok. I also acknowledge all other lab members, past and present, for helping me through my studies.

Lastly, I would like to thank Dr. Herman Cheung, Dr. Eric LaCasse and the other members in the apoptosis research division located out of CHEO, for testing my earlier synthesized compounds. As well, Dr. Klemm Kazakoff for conducting Mass spectroscopy analysis on our samples, and the Dr. Moon lab for allowing me the use to their UV-Vis spectrometer at any time and helping me set up the machine.

List of Abbreviations

α	alpha
β	beta
γ	gamma
δ	delta
^{1}H	proton
^{13}C	carbon
Ac	acetyl
Ac_2O	acetic anhydride
Ala	alanine
All	Allyl
Asn	Asparagine
Asp	Aspartate
Atm	atmospheres
$BF_3 \bullet OEt_2$	boron trifluoride diethyl etherate
Bn	benzyl
Boc	*tert*-butyloxycarbonyl
Boc_2O	Di-*tert*-butyl dicarbonate
br	broad
brsm	based on recovered starting material
bs	broad singlet
Bz	benzoyl
$CaCl_2$	Calcium chloride
Cat.	Catalytic
$CDCl_3$	deuterated chloroform
CDI	1,1-carbonyldiimidazole
CD_3OD	deuterated methanol
CH_2N_2	diazomethane
cm^{-1}	wavenumber
CN	nitrile
$CuBr \cdot SMe_2$	copper bromide-dimethyl sulfide complex
d	doublet
D_2O	deuterium oxide
Dab	diaminobutanoate
dd	doublet of doublets
DCM	dichloromethane
DED	Death effector domain
DISC	Death inducing signalling complex
DIPEA	diisopropylethylamine
DMF	dimethyl formamide
DMSO	dimethyl sulfoxide
Dpr	diaminopropanoate
dt	doublet of triplets
ESI	electrospray ionization
Et	ethyl

Et_2O	diethyl ether
EtOAc	ethyl acetate
EtOH	ethanol
FADD	Fas adaptor death domain
Fmoc	9-fluorenylmethyloxycarbonyl
FmocOsuc	N-(9-Fluorenylmethoxycarbonyloxy) succinimide
Gly	glycine
HBTU	2-(1H-benzotriazole-1-yl)-1,1,3,3-tetramethylaminium hexafluorophosphate
HCl	hydrochloric acid
HCTU	2-(6-Chloro-1H-benzotriazole-1-yl)-1,1,3,3-tetramethylaminium hexafluorophosphate
HOBT	*N*-hydroxyl benzotriazole
HPLC	high performance liquid chromatography
IR	Infrared
IR resin	Amberlite ion exchange resin
Ile	Isoleucine
LiBr	lithium bromide
Leu	Leucine
Lys	Lysine
kDa	kiloDaltons
m	multiplet
M	molar
M^+	parent molecular ion
MALDI-TOF	matrix-assisted laser desorption/ionization – time of flight
Me	methyl
MeOH	methanol
MGS	mean grain size
$MgSO_4$	magnesium sulfate
MHz	mega Hertz
mM	millimolar
MS	mass spectrometry
MS	molecular sieves
NaH	sodium hydride
Na_2SO_4	Sodium sulfate
$NaHCO_3$	sodium bicarbonate
NaOH	sodium hydroxide
NaOMe	sodium methoxide
NMM	N-methylmorpholine
NIS	N-iodosuccinimide
O/N	overnight
OTf	trifluoromethane sulfonate
Phe	Phenylalanine
PIDA	phenyl iodine diacetate
PIFA	phenyl iodine di(trifluoroacetoxy)
PG	protecting group
Pd/C	palladium on carbon

$Pd(OH)_2$	palladium hydroxide
pKa	acid dissociation constant
ppb	parts per billion
ppm	parts per million
Pro	Proline
q	quartet
Rf	Retention factor
RT	room temperature
s	singlet
Ser	serine
SM	starting material
SPPS	solid-phase peptide synthesis
t	triplet
TBAF	*tert*-butylammonium fluoride
TBS	*tert*-butyldimethylsilyl
TEA	triethylamine
TFA	trifluoroacetic acid
THF	tetrahydrofuran
Thr	threonine
TIPS	triisopropylsilyl
TIS	triisopropylsilane
TMS	trimethylsilyl
TMSOTf	trimethylsilyl trifluoromethane sulfonate
TNF	Tumor necrosis factor
TRADD	TNF RI- associated death domain
TRAIL	TNF related apoptosis inducing ligand
Veh	Vehicle
VT-NMR	Variable temperature nuclear magnetic resonance

1.0 Introduction to Apoptosis

1.1 Defining Apoptosis

Apoptosis, also known as programmed cell death, is a vital cell process that occurs in normal development and homeostasis of multi-cellular organisms in order to eliminate damaged or mutated cells. DNA damage, chromosomal abnormalities, oncogene activation, viral infection, substrate detachment and hypoxia can all trigger apoptosis in a normal cell.[1] When a normal cell is no longer needed an intracellular death program is activated, which causes the cell to commit suicide. Apoptosis occurs on a daily basis, and the amount that occurs can sometimes be surprising. In an average human being billions of cells die in the bone marrow and intestine every hour,[2] even though most are perfectly healthy when programmed cell death occurs. This mode of cell death is an active and defined process which plays an important role in the development of multicellular organisms and in the regulation and maintenance of cell populations in tissues.

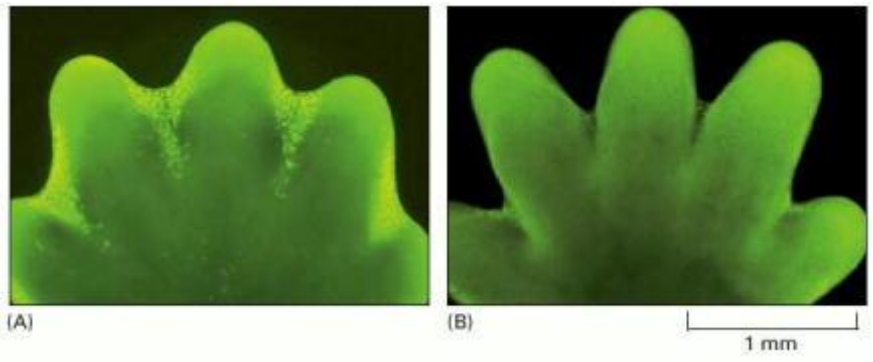

Figure 1.1 Sculpting of the digits in a developing mouse paw by apoptosis. (A) Apoptotic cells are bright green; (B) Cell death eliminates tissue between digials[3]

A prime example is in the sculpting of the digits in a developing mouse paw (Figure 1.1). Mouse paws are sculpted by cell death during embryonic development: they start out as spade like structures, and the individual digits separate only as the cells between them die. In other cases, cells die when the structure they form is no longer needed,[3] such as in the case of a tadpole developing into a frog. Throughout the development of multi-cellular organism there is always a fine balance between cell death and cell division. Only in a very few cases will there be more cell division than cell death, but this is short lived and occurs in response to environmental stimuli.[4]

As mentioned earlier apoptosis can be triggered by many events, either DNA damage, chromosomal abnormalities, and even hypoxia.[5] The general mechanism in which apoptosis occurs is simple, with the cytoskeleton disintegrating the nuclear envelope falls apart which causes the DNA to break into fragments. The process occurs in a neat and controlled manner, thus preventing neighbouring cell damage by cell necrosis.[6]

1.2 Mechanism of Action

1.2.1 General Mechanism

So how does such an efficient process occur, considering that billions of cells are killed every day? Apoptosis is controlled by an intracellular mechanism, involving a family of cysteine proteases. It is known that caspases, an acronym for Cysteine Aspartyl-specific Proteases, are responsible directly and indirectly for the morphologic and biochemical changes that characterize the phenomenon of apoptosis.[7] These

cysteine proteases are synthesized and present in all mammal cells as inactive precursors (procaspases), which can be activated by cleavage of their aspartic acids by other caspases. Once activated, caspases cleave, and thereby activate, other procaspases, resulting in an amplifying proteolytic cascade (Figure1. 2)[8].

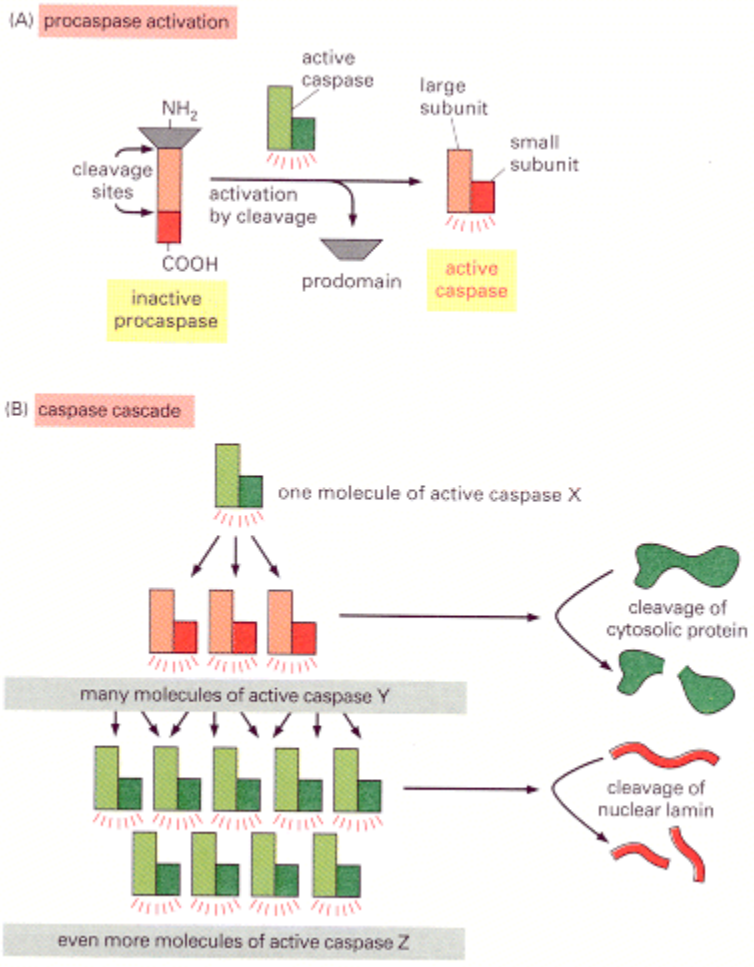

Figure 1.2. Caspase cascade involved in apoptosis[8]

The cascade of activating sequential caspases causes either an upstream initiator or downstream effector effect, and in the end serves as an irreversible-destructive pathway

for the suicidal cell. Given that the activation of caspases is an irreversible pathway, activation is firmly regulated.

1.2.2 Caspase Activation Pathway

Since the activation of each procaspases is regulated by other active caspases, one might wonder how the initial activation of a procaspases occurs to start the cascade in the first place. In general the cascade initiation is caused by protein-protein interactions, which is accomplished with the aid of adaptor proteins. These proteins play an integral role in intracellular signalling by both recruiting various proteins to specific locations and by assembling networks of proteins particular to a cascade.[9] A vast number of adaptor proteins exist and each one has a particular function. Once a procaspases protein is initiated by the adaptor proteins there is an immediate effect downstream, which causes amplification in the death signal and results in cell death. There are two known ways of caspase activation, the extrinsic pathway and the intrinsic pathway. The extrinsic pathway is initiated by ligation of transmembrane death receptors (Fas, TNF receptor, and TRAIL receptor) with their respective ligands (FasL, TNF, and TRAIL) to activate membrane-proximal caspases (caspase-8 and –10), which in turn cleave and activate effector caspases such as caspase-3 and –7.[10] The intrinsic pathway requires disruption of the mitochondrial membrane and the release of mitochondrial proteins. Cytochrome c, released from the mitochondrial intermembrane space to cytoplasm, works together with two other cytosolic protein factors, Apaf-1 (apoptotic protease activating factor-1) and procaspase-9,[11] to promote the assembly of a caspase-activating complex termed the apoptotosome, which in return induces

activation of caspase-9 and thereby initiates the apoptotic caspase cascade[12] (Figure 1.3).[13]

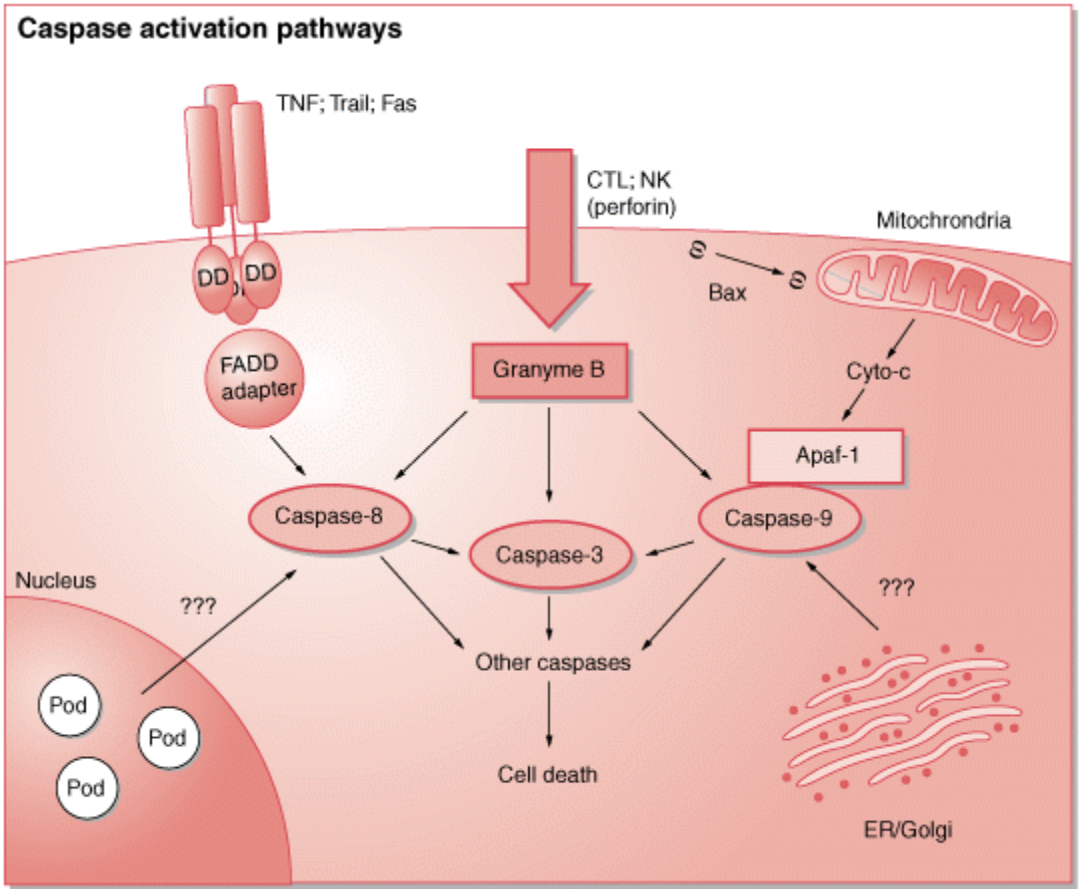

Figure 1.3. Activation of apoptosis through the extrinsic pathway caused by the initiation through TNF to activation of caspase-8; or intrinsic pathway which releases cytochrome-c to activate caspase 9.[13]

The activation of apoptosis from outside the cell causes recruitment and clustering of several intracellular proteins, forming a “death-inducing signalling complex” (DISC)[14] which causes caspase-8 or caspase-10 to be summoned. Caspase-8 and Caspase-10 are thought to contain a death effector domain (DEDs) located in the N-terminal domain, and these DEDs are believed to bind with corresponding DEDs in Fas associated death

domain (FADD). Aside from releasing cytochrome-c into the cytosol when apoptosis is activated from inside the cell, the mitochondria release several other proteins of relevance to apoptosis as well, Endonuclease G, Smac (Diablo) and Omi (HtrA2), which are antagonists of a family of caspase-inhibitory proteins known as the inhibitors of apoptosis proteins (IAPs).[15] In the end, it does not matter if it is the extrinsic pathway or intrinsic pathway that is activated by cell stress, the end result for a normal cell is death.

1.3 A Brief Overview of Cancer

1.3.1 Summarizing the complexity of Cancer

To understand how apoptosis occurs in a healthy normal cell, as described in Section 1.2, we need to comprehend how controlled and regulated such a process is. Cancer on the other hand is a complete failure of these controls, defined by its uncontrolled growth and deregulation of apoptosis.

For multi-cellular organism that are able to show hereditary distinction in reproductive ability will usually evolve by natural selection. Genotypes that reproduce faster or more extensively will amount to dominate later generations, only to be supplanted in turn by yet more efficient reproducers.[16] This exact same process applies to the population of cells that constitutes a multi-cellular organism such as humans. Cellular proliferation is under genetic control, and if somatic mutation creates a variant that proliferates faster, the mutant clone will tend to take over the organism.[17] This does not mean that a human will turn into a tumour because the cancer cells are

proliferating faster than normal cells, but that mutations in cells lead to survival of the fittest; meaning those that can avoid apoptosis. In a healthy cell the mechanism of natural selection is not present, instead self sacrifice for the organism exists. It is because of this self sacrifice that there is always a constant balance between growth, rest, and death. Cancer conversely has no balance. With repeated rounds of mutation, competition, and natural selection operating within the population of somatic cells cause matters to go from bad to worse. The basic traits of cancer are what allow individual mutant clones of cells to begin prospering at the expense of their neighbours; however, in the end destroy the whole cellular society. Cancer cells are defined by two heritable properties: they and their progeny (1) reproduce in defiance of the normal restraints on cell division and (2) invade and colonize territories normally reserved for other cells. It is the combination of these actions that makes cancers peculiarly dangerous.[18]

1.3.2 Characteristics of Cancer

There are many characteristics that define a cancer cell. One common characteristic of a cancer cell is its ability to produce its own growth factors, which can cause proliferation into neighbouring cells. [19] This uncontrolled growth allows for the cancer to expand and take over. Growth of normal cells is controlled by cell-cycle checkpoints[20] which allows control over the cell division cycle. Cancer cells however will by-pass these checkpoints and remain in the growth phase. It is estimated that 10^{16} cell divisions take place in a normal human body in the course of a lifetime, thus every

single gene is likely to have undergone mutation on about 10^{10} separate occasions in any individual human being.[21] However it takes more than just one mutation in a healthy cell to convert into a cancerous cell. It is estimated that it takes between six to ten mutations to occur in the same cell in order for a cancerous cell to develop, which occurs over the course of 20 years. If a single mutation were responsible, occurring with a fixed probability per year, the chance of developing cancer in any given year should be independent of age (Figure 1.14). [22] In fact, for most types of cancer the incidence rises steeply with age—as would be expected if cancer is caused by a slow accumulation of numerous random mutations in a single line of cells.[23]

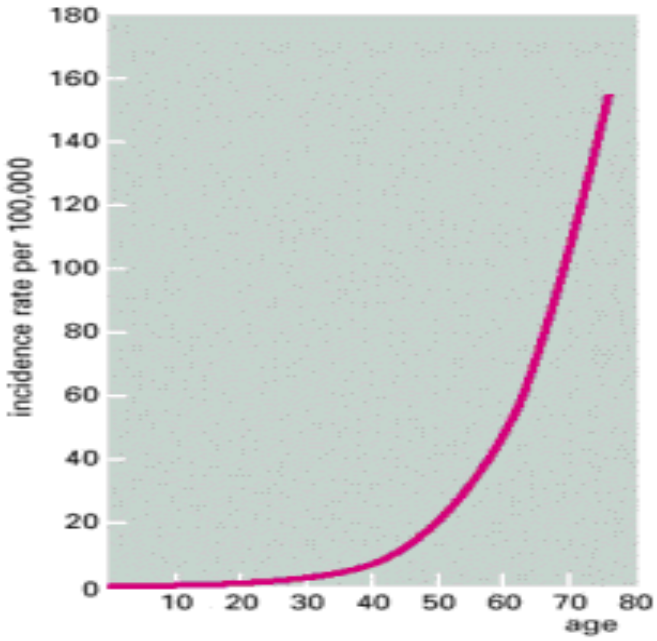

Figure 1.4. Prevalence of cancer based on age, with an incidence rate of 100, 000 people[22]

It is without a doubt that for a cancer cell to survive and proliferate, it must be able to acquire a range of adaptation skills as it evolves. There are six key properties that

make cells capable of cancerous growth: (1) they disregard the external and internal signals that regulate cell proliferation, (2) they tend to avoid suicide by apoptosis, (3) they circumvent programmed limitations to proliferation, escaping replicative senescence and avoiding differentiation, (4) they are genetically unstable, (5) they escape from their home tissues (that is, they are invasive) and (6) They survive and proliferate in foreign sites (that is, they metastasize).[24]

1.4Inhibitors of Apoptosis Proteins (IAPs)

1.4.1 IAPs and BIR Domains

A cell's fate cannot be determined by the mere presence of activated caspases but rather the amount and where in a cell they are localized. There are many different proteins involved in controlling the intrinsic and extrinsic pathways leading to apoptosis. Interactions among these proteins are commonly mediated by domains that are intimately associated with apoptosis regulation, including caspase recruitment domains (CARDs), Death Domains (DDs), Death Effector Domains (DEDs), Bcl-2 Homology (BH) domains of Bcl-2 family proteins, and Baculovirus IAP Repeat (BIR) domains of IAP-family proteins.[25] Although each of the listed proteins has a specific function toward regulating apoptosis, the remainder of this section will focus on the Inhibitors of Apoptosis Proteins and the Baculovirus IAP repeat domains of the IAP-family.

The IAPs represent a family of evolutionarily conserved apoptosis suppressors. Though these proteins can interact with a variety of biochemical pathways in cells, the fundamental mechanisms of action of IAP-family proteins is direct suppression of

caspases, thus acting as endogenous inhibitors of the cell death proteases.[26] A key defining feature of the IAPs is that they contain a Baculovirus repeat domain (BIR) with at least one to maximum three copies (BIR1, 2, and 3), and in some cases a RING-finger domain which contains ubiquitin-ligase activity, allowing the IAP to tag caspases for degradation (figure 1.5)[27].

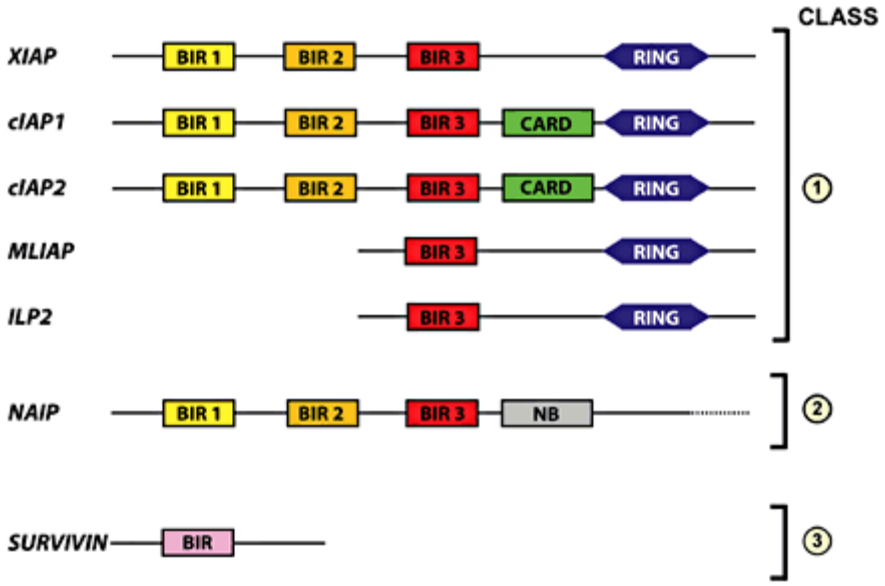

Figure 1.5. Domain structures of the mammalian IAP Family[27]

The BIR domains are zinc-binding domains which consist of ~80 amino acids that are necessary for IAP binding to and consequent inhibition of activated caspases.[28]

1.4.2 Governing Initiator and Effector Caspases

All IAPs contain at least one BIR domain, but the mere presence of a BIR domain alone does not necessarily reflect the IAPs anti-apoptotic activity. Such as the case in BIR containing proteins which regulate mitosis and meiosis, but which have no apparent

effect on cell death regulation, have been described in yeast and *C. elegans*.[29] There are several proteins within the IAPs that have been discovered which bind and inhibit activated caspases. Proteins such as the X-linked IAP (XIAP), Livin/ML-IAP, cIAP-1 and cIAP-2, are believed to inhibit apoptosis through direct inhibition of caspases[30] and some of these proteins are believed to be involved in additional pathways. Among the IAP-family members listed, XIAP and cIAP-1 and 2 are the most important. It is believed that within XIAP alone it is the effect of the BIR domains that dictates whether caspase-9, -3, or -7 will be inhibited, which is regulated by 80 amino acid sequences within the BIR domains. [31] The BIR2 domain has been shown to bind to and inhibit caspase 3 and 7, whereas BIR3 has been shown to inhibit caspase-9.[32] It is through these BIR domains that XIAP is able to prevent apoptosis, by governing the initiator and effector caspases in both pathways (Figure 1.6).[33]

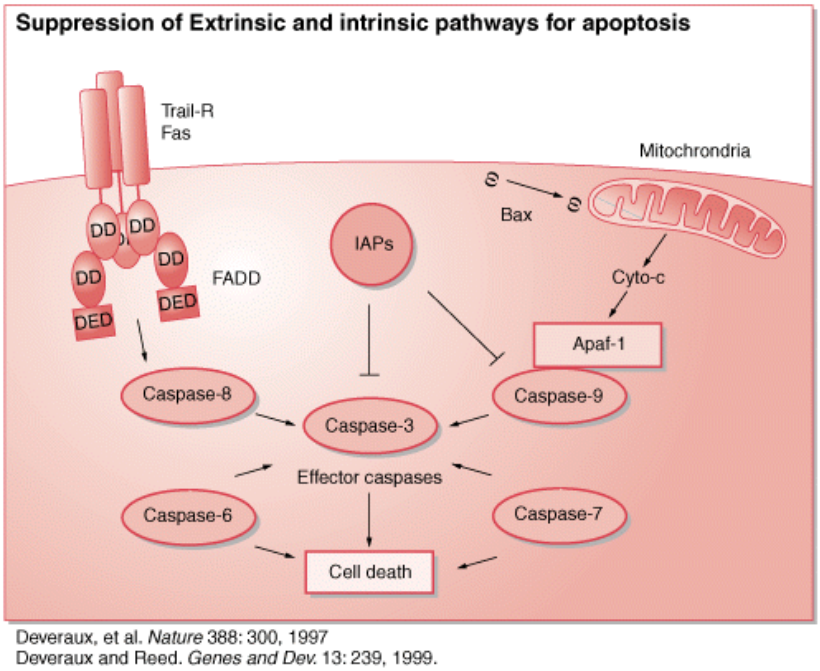

Figure 1.6. Suppression of Extrinsic and Intrinsic pathways by inhibiton of Caspases by IAPs.[33]

Ultimately the purpose of Inhibitors of Apoptosis Proteins (IAPs) is to regulate apoptosis within a cell, thus the antagonism of XIAP-mediated inhibition of caspase is required for efficient caspase-dependent cell death.[34]

1.5 IAPs in Cancer

1.5.1 Amplified Expression of XIAP and Survivin

In cancer cells there is an over expression of IAPs, in particular XIAP and another IAP family member known as Survivin. Survivin is highly expressed in the developing fetus but largely absent from normal adult tissues. Through unclear mechanisms, Survivin becomes over-expressed in cancers.[35] Elevated levels of XIAP allow a cancer cell to resist apoptosis and many anticancer drugs - giving cancer its anti-apoptotic activity.

1.5.2 Release of Smac from the mitochondria

In the mammalian cells two naturally occurring endogenous IAP-antagonist proteins are released when increased amounts of XIAP are detected. Both Smac (Second mitochondria-derived activator of caspases) also known as DIABLO (Direct IAP binding protein with low pI) and HtrA2 (High temperature resistant A2) also known as Omi are released from the mitochondria and into the cytosol in response to apoptotic

stimuli.[36] Smac, like cytochrome c, is released during the early stages of apoptosis. When Smac is released into the cytosol its N-terminal leader sequences are removed by proteolysis, exposing a tetra-peptide motif that binds the BIR domains of IAPs (figure 1.7).[37] It is this conserved tetra amino-acid IAP-binding motif (IBM) that serves the pro-apoptotic function of Smac. Structural studies have demonstrated that it is this four amino acid terminal peptide that binds to a shallow surface groove on select BIR domains of the IAPs in an extended conformation.[38] This IAP-antagonist competes with caspases for binding to IAPs, thus freeing caspases from the grip of the IAPs and promoting apoptosis.[39]

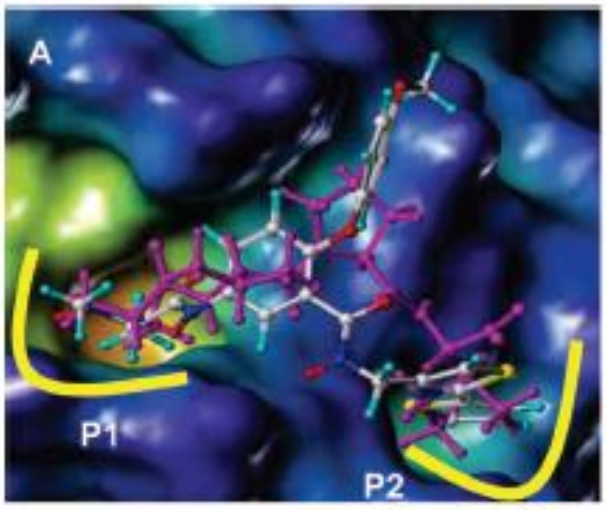

Figure 1.7. Superposition between the X-ray structure of AVPI (magenta) in complex with BIR3 domain of XIAP[37]

Based on structural and chemical studies it has been shown that Smac binds to the BIR3 domain via its four amino acid residue Alanine-Valine-Proline-Isoleucine (AVPI) tetrapeptide motif. The peptide binds across the third β-strand of the BIR3 domain in an

extended conformation with only the first four residues of Smac in contact with the protein. The complex is stabilized by four intermolecular hydrogen bonds, an electrostatic interaction involving the N-terminus of the peptide, and several hydrophobic interactions.[40]

Recently, HtrA2/Omi was identified as yet another mitochondrial protein that could bind to XIAP and induce apoptosis. HtrA2 is a serine protease whose mitochondrial targeting signal is proteolytically removed upon import into the mitochondrion to reveal an N-terminus conserved IAP (Ala-Val-Pro-Ser) binding site. During apoptosis HtrA2 is released from the mitochondrion and inhibits the function of XIAP in an analogous manner to Smac.[41] Figure 1.8[42] shows a 3D structure of the HtrA2/Omi trimeric serine protease.

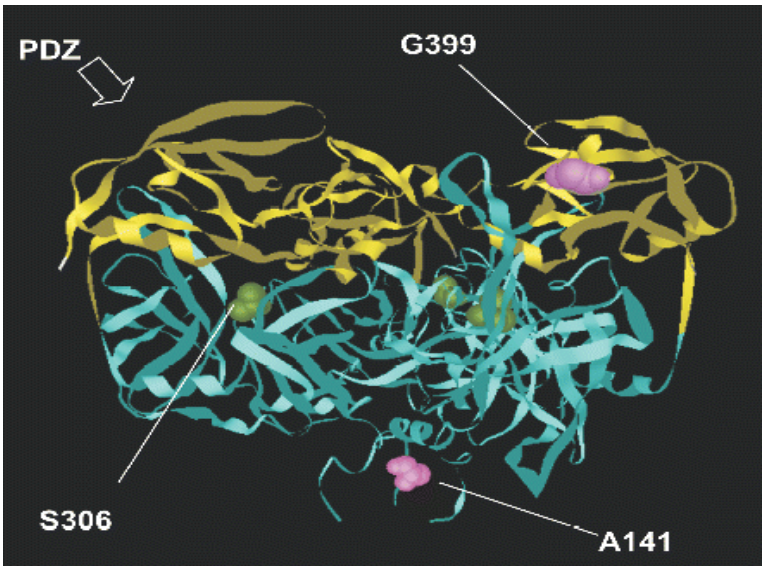

Figure 1.8.The figure shows the predicted 3D structure of the trimeric serine protease Omi/HtrA2. S306 represents the active center of the serine protease.[32]

In 2007 Jin Q. Cheng et al. discovered that HtrA2 was directly regulated by protein kinase B (Akt), and provided a mechanism by which Akt induced cell survival at post mitochondrial level.[43] Akt has been shown to inhibit apoptosis at both pre-mitochondrial and post-mitochondrial levels. The first Akt target identified was the pro-apoptotic protein BAD. BAD is a member of the Bcl-2 family that initiates apoptosis by binding to Bcl-xL and BcL2 on the outer mitochondrial membrane, causing the release of cytochrome *c* into the cytosol. At the post-mitochondrial level, it has been shown that Akt phosphorylates and inactivates caspase-9.[44] Thus in response to Akt, the mitochondria releases HtrA2/Omi protein into the cytosol where it binds and cleaves the IAPs, analogous to Smac (Figure 9).[45]

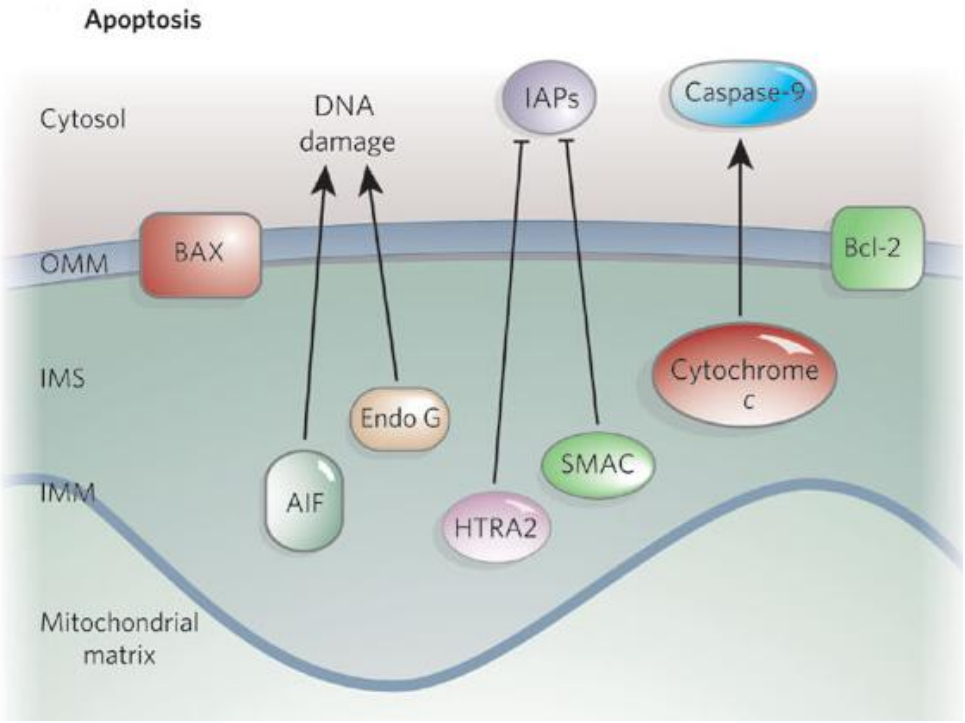

Figure 1.9. Release of Smac and HTRA2 by the mitochondria in response to apoptotic stimuli, which induces apoptosis.[35]

However, accumulated evidence indicates that HtrA2/Omi also initiates caspase-independent apoptosis in a process that relies entirely on its ability to function as an active protease.[46] In the mitochondria of a healthy cell HtrA2/Omi is synthesized as a premature complex, following apoptotic stimuli HtrA2 gets transformed into the mature complex and is then released. Since HtrA2/Omi is still a relatively newly discovered protein, its activity and exact mechanism is yet to be fully characterized.

1.6 Starting point for the Design of Smac mimetics

1.6.1 Structural basis for IAP recognition

In 2000 Shi et al.[47] were able to crystallize the wild-type Smac in complex with either the BIR2 or the BIR3 domain of XIAP. Their original complexes were unable to diffract X-rays well due to the poor nature of the crystals. In order to obtain X-ray crystals that could diffract well, they reconstituted binary complexes using a monomeric Smac protein and in doing so were able to generate X-ray structures which gave insight into the binding of Smac and the BIR domains of XIAP. What they discovered was that Smac was able to recognize BIR3 of XIAP in two different ways. First, the initial tetra-amino acid sequence located at the N-terminus (Ala-Val-Pro-Ile) is able to bind to a surface groove on BIR3 which are formed by beta strands and alpha helixes (figure 1.10). Secondly, helices from two different Smac promoters are able to contact the same BIR3 domain in XIAP. All of these interactions conducted through a combination of hydrogen-bond interactions, with eight causing inter- and three intra-hydrogen bonds, and van der Waals interations. Through the use of both crystal structures and NMR

solution structures it was validated that Smac recognizes and binds to the surface groove of BIR3 through its leader sequence AVPI.[48]

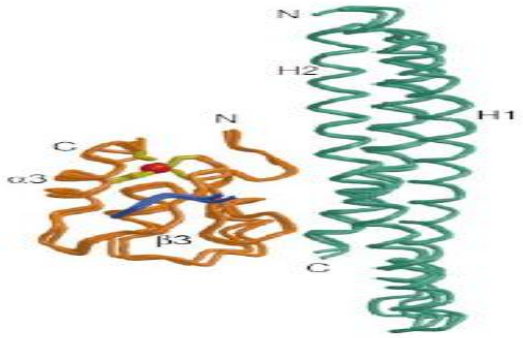

Figure 1.10. Stereo view (3D) of superimposition of Smac and BIR3 shown in green and orange respectively

1.6.2 Structural-activity relationship of Smac mimetics

Since the initial discovery of the Smac amino acid sequence in 2000 a variety of compounds, designed to mimic the N-terminus of Smac (AVPI), have been synthesized. It is from these diverse compounds, synthesized over the past eleven years, that a general picture of the structural activity relationship (SAR) has emerged (figure 1.11).[49]

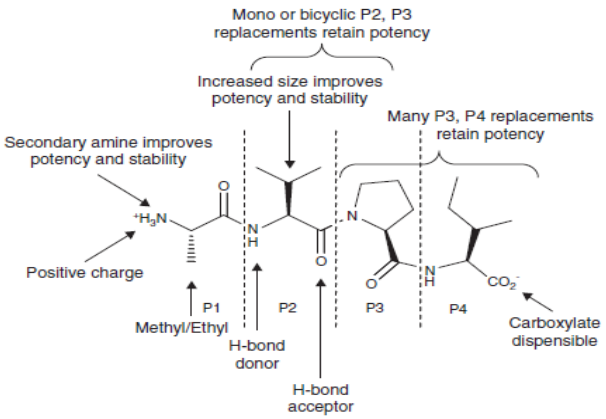

Figure 1.11. Schematic summary of the SAR of Smac mimetics[49]

From the data gathered, a number of key and important SARs have come into view. Foremost, the Alanine residue located at position one (P1) only tolerates small changes without disrupting all binding. One such modification consists of the mono-methylation of the amine terminus of P1, creating N-methylalanine. It is believed that this methylation aids in the protection from proteases while still allowing critical hydrophobic and charge-charge interactions with the IAP BIR domain.[50] However, dimethylation of the amine terminus decreases binding to XIAP-BIR3 by a factor greater than 100 fold. The un-methylated version of alanine is known to form strong hydrogen bonds to the glutathione residues at positions 314 and 319 on BIR3, and the backbone carbonyl group forms a suboptimal hydrogen bond to the indole NH group in tryptophan residue at position 323.[51] The side chain of P1 can tolerate one beneficial modification, where the methyl group can be replaced with an ethyl side chain causing an increase in binding.[52]

Secondly, the Valine residue in position two (P2) can be modified in many ways as long as the hydrogen-bond donor and acceptor in the molecule are retained; since

they are used to create hydrogen bonds with the carbonyl and amino groups of the threonie residue at position 308. The only exception being that P2 cannot be replaced with glycine, since glycine leads to a greater than 30 fold loss in binding affinity.[53] The side chain of valine has no interactions with the BIR domains and is exposed into the cytosol. Modifications done to the side chain through substitutions with bulkier groups or stereospecific cyclizations have shown to improve not only potency but also stability of the compound as well. In 2004, Wang et al. [54] were the first to report such conformationally constrained bicylic Smac mimetics, where stereospecific cyclizations onto C4 of the pyrrolidine ring lead to compounds with nanomolar activity.[55]

Third, the pyrrolidine ring at position three (P3) cannot be replaced since it creates van der Waal interactions with the side chains of the tryptophan residues at positions 323 and 324.[56] It has been shown that replacing the five-membered ring with four- or six-membered rings results in a 7 fold loss in binding affinity, and even greater loss with other residues. However, modifications around the five-membered ring are tolerated and in some cases have improved binding.

Fourth, the Isoleucine residue at position four (P4) has displayed the greatest tolerance to modifications. Hydrophobic moieties have been the preferred choice for such modifications, since they have displayed an increase in binding affinity. Studies have shown that isoleucine forms hydrogen bonds with the carbonyl group of glycine residue at position 306, and its hydrophobic side chain inserts into a hydrophobic pocket which is formed by the side chains of leucine residues at position 292 and valine residue at position 298 as well as the hydrophobic portion of the side chains in lysine at position 297 and 299.[57] Lastly, the importance of the stereochemistry at each of the

amino acids in the amino-terminal four residues of the tetrapeptide was established by Armstrong et al. [58] through peptide libraries in which each of the amino acids was replaced with their enantiomer. Replacing each L-amino acid for the D-amino acid resulted in a ~10 to >300 fold reduction in binding affinity to the BIR3 domain of XIAP.[59] From the compilation of such information at the atomic level, many researchers have used this knowledge as the basis for the rational design of both peptide based and non-peptide based Smac mimetics.

1.6.3 Design of Monovalent Smac Mimetic peptides and peptidomimetics

After the importance of the AVPI sequence was recognized (Section 1.5.2), a variety of research laboratories commenced publishing papers and patents covering a variety of peptides and peptidomimetics based off of this sequence. A majority of the first patents which were published focused primarily on extensive modifications done to the AVPI motif. Through previous studies it was made clear that AVPI could antagonize XIAP with a binding affinity of ~ 0.5 μM against its BIR3 domain,[60] and could also bind with high affinity to the BIR3 domain of cIAP-1 and -2, as well as the single BIR domain of ML-IAP. With this knowledge a large number of groups began to publish patents that disclosed specific amino-acid sequences derived from the amino terminus of Smac, caspase-9 or any of the drosophila IAP-binding proteins. However, the use of these peptide based compounds remained limited due to their lack of proteolytic stability, and cell permeability.

In order to improve the AVPI tetra-peptide motif into a potential drug candidate for use in clinical trials, many alterations to the AVPI motif have emerged over the past

several years. In the beginning, the first modified Smac mimetics easily targeted the IAP proteins but lacked the favourable physiochemical properties such as molecular weight, logP, and the number of hydrogen bond donors and acceptors required to develop a therapeutic compound.[61]Through an evolutionary process of a systematic examination of the tolerance to substitution at each of the amino acids of the AVPI motif, as described above, a large number of peptide and non-peptidic compounds have been synthesized and patented (Figure 1.12).

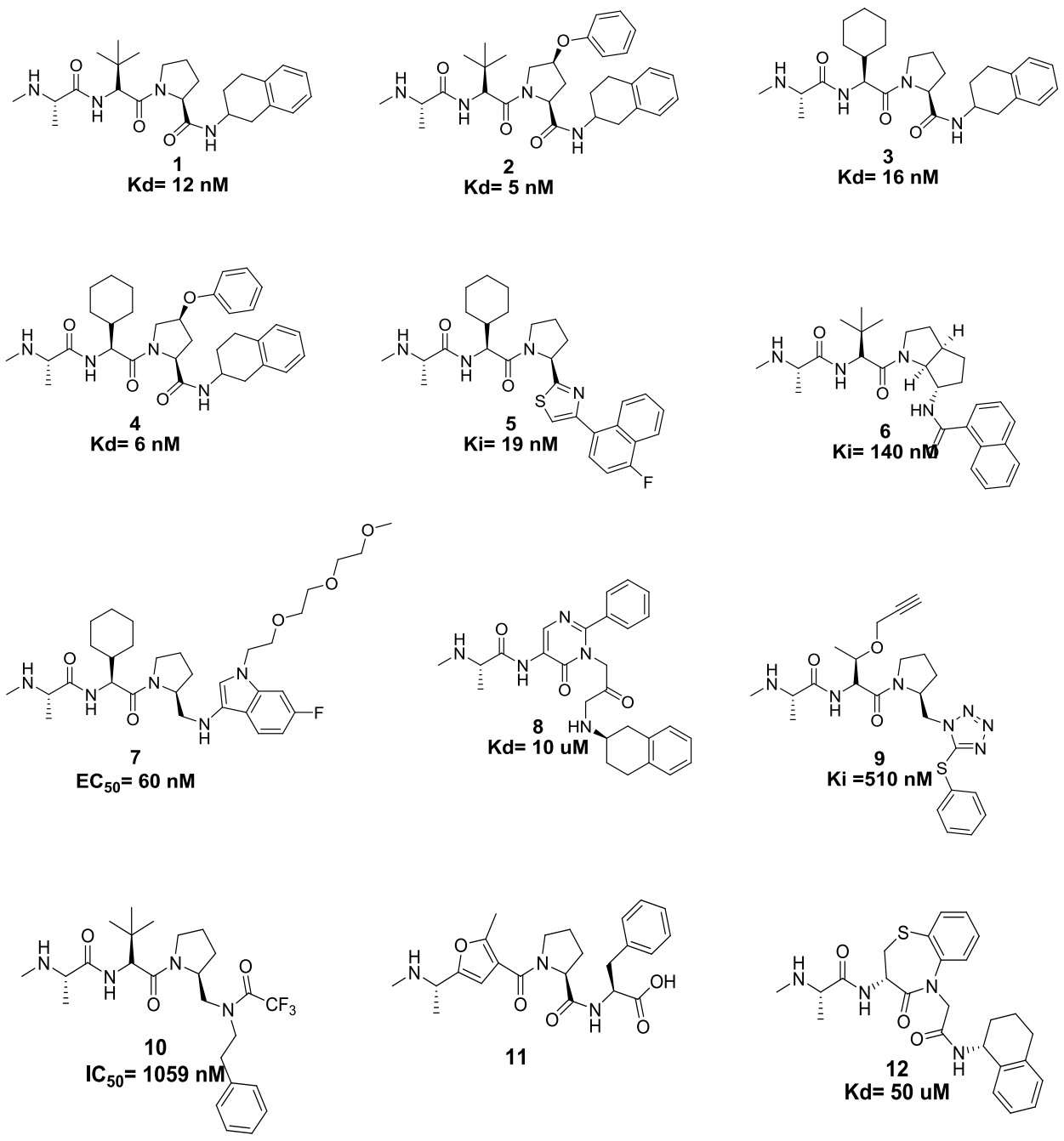

Figure 1.12 Representation of a few potent monomer Smac mimetics synthesized by different laboratories

One of the first few synthesizes of potent Smac mimetic monomers was conducted by

Oost and colleagues at Abbott Laboratories. Oost et al. synthesized a series of potent

Smac peptidomimetics **1**, **2**, **3**, and **4** which had the following binding affinities to the BIR3 domain of XIAP, with Kd values of 12, 5, 16, and 6 nM respectively.[62] These compounds were also all able to induce the activation of caspase-3 in the MDA-MB-231 human breast cancer cell line. Of these four compounds, compounds **1** and **3** were shown to inhibit cell growth with IC_{50} values of 68 and 13 nM respectively.

Since it is known that the P4 position of the tetra-peptide can tolerate significant structural variations which can increase the ability of such compound binding, many derivatives have been synthesized which vary at this position. A diverse range of substituent's at P4 is shown in Figure 1.12, represented by compounds **5**, **6**, **7**, **8**, **9**, **10** and **12**. In February 2010 Frederick Cohen et al. [63], at Genentech Pharmaceuticals, synthesized a library of thiazole amide isosters which were able to bind to XIAP-BIR3 and ML-IAP BIR of which compound **5** being the most active. Using a fluorescence polarization assay they were able to determine that compound **5** was able to bind to XIAP-BIR3 and ML-XBIR3SG with a Ki of 19 nM and 68 nM respectively. Their series of compounds focused on extending the P4 group to a napthyl substituent which dramatically increased the binding affinity of the analogs for both BIR domains. Through small modifications in substituent's to the napthylene ring, they discovered that adding a small electron-withdrawing group at position four on the ring also increased the binding affinity.[64] In the previous year Cohen and colleagues had synthesized an orally bioavailable antagonist built on an azabicyclooctane scaffold.[65] These azabicyclooctane mimetics, in particular compound **6**, were described as having an affinity for XIAP-BIR3 and ML-XBIR3SG with a Ki of 0.140 μM and 0.046 μM respectively. Compound **7**, synthesized with an indole at P4 with a polyethylene glycol

substituent on the indole nitrogen by Tetralogic Pharmaceuticals was shown to have a half maximal effective concentration (EC_{50}) of 60 nM when tested in a cytotoxicity assay using an SK-OV-3 ovarian cancer cell line.[66]

In view of the fact that the side chain at P2 does not play any significant role on the binding affinity of the tetra-peptide, presumably because the side chain of this residue is void of contact with the BIR protein and instead extends into the cytosol, many strategies have been pursued to modify this region. Between 2006 and 2007 Novartis Pharmaceuticals, in an aggressive hunt for a new lead, published several patent applications which revealed a succession of heterocyclic rings positioned at P2. From the series published by Novartis only compound **8** was synthesized on a large scale fashion, which displayed binding affinity of < 10 μM to XIAP-BIR3 and contained a hydropyrimidine at P2.[67] As well in 2007 compound **12** was developed by Aegera Pharmaceuticals which filed a patent on four novel Smac mimetic monomers which utilized a 7-membered ring at P2. Aegera reported these compounds to have binding affinities of < 50 μM for the XIAP-BIR3 domain.[68] In 2003 researchers from Princeton University disclosed a patent which revealed the use of an oxazole ring in replacement of the valine side chain; compound **11**. Through their investigation it was shown that these oxazole replacements actually caused a 10-fold increase in binding to the BIR3 of XIAP, when compared to the native AVPI tetra-peptide sequence.[69]

In 2004, at the University of Texas South-western Medical Center, through the use of a computer aided docking program based on a co-crystal arrangement of a structural variant of Smac in complex with the XIAP-BIR3 domain, Harran and colleagues were able to synthesize and evaluate compound **9**. The tetrapeptide used

for the study was comprised of an Alanine-Valine-Proline-Phenylalanine (AVPF) sequence, which had been shown to outperform the native AVPI motif as a Smac mimetic. Compound **9**, a tetrazoyl thioether, when used alone gave a Ki = 0.51 μM and moderate cell death when used in conjunction with tumour necrosis factor related apoptosis inducing ligand (TRAIL) at 50 ng/mL.[70] The region of Smac that binds to the XIAP-BIR3 domain is structurally similar to the amino tetra-peptide in caspase-9 comprised of Alanine-Threonine-Proline-Phenylalanine (ATPF). Based on this ATPF motif, Aegera Therapeutics published an article describing a highly active compound (**10)**, which displayed 1059 nM activity against the XIAP-BIR3 domain and higher activity against the BIR3 domains of cIAP-1 and -2[71]. However, when compound **10** was tested against several cell lines, other than human MDA-MB-231 breast cancer, none of the cell lines showed reduced viability even at high compound concentrations.

Although monovalent forms of novel Smac mimetics have shown promise and aided in the further development of other peptide and non-peptide based mimetics, in particular bivalent Smac mimetics, their use has shown very little success at compound concentrations lower than 1 μM.

1.6.4 Design of Bivalent Smac Mimetic peptides and peptidomimetics

It has been established that natural Smac, when released from the mitochondria actually forms a homodimer and binds to XIAP protein constructs containing both BIR2 and BIR3 domains with a much superior affinity than the monomer form of Smac (Figure

1.13).[72] Although binding of the Smac protein does occur to both BIR2 and -3 domains, the binding affinity is much higher for BIR3.

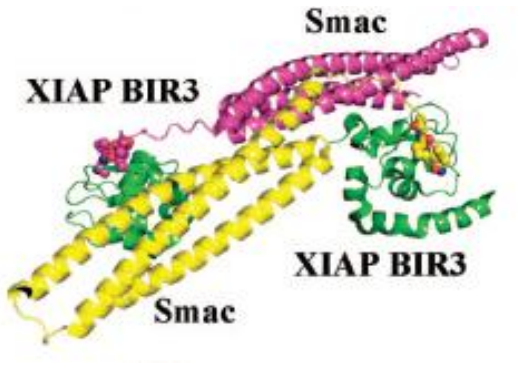

Figure1.13 Formation of Smac homodimer when complexed with BIR3 domain of XIAP[60]

Based on these findings it is much more desirable to design Smac mimetics which have at least two tetra-peptide binding motifis. This in turn would then mimic the mode of action of Smac protein to target XIAP and consequently be capable of achieving much larger binding affinities. On the foundation of these results, over the course of the past 12 years, many groups have synthesized bivalent Smac mimetics (Figure 1.14), some of which have shown great promise in inducing apoptosis in a variety of cancer cell lines and even a small quantity of which are currently in preclinical trials.

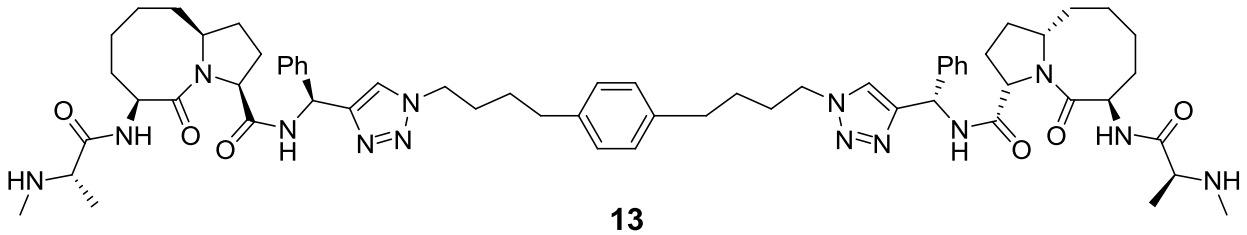

13
IC_{50}= 1.39 nM

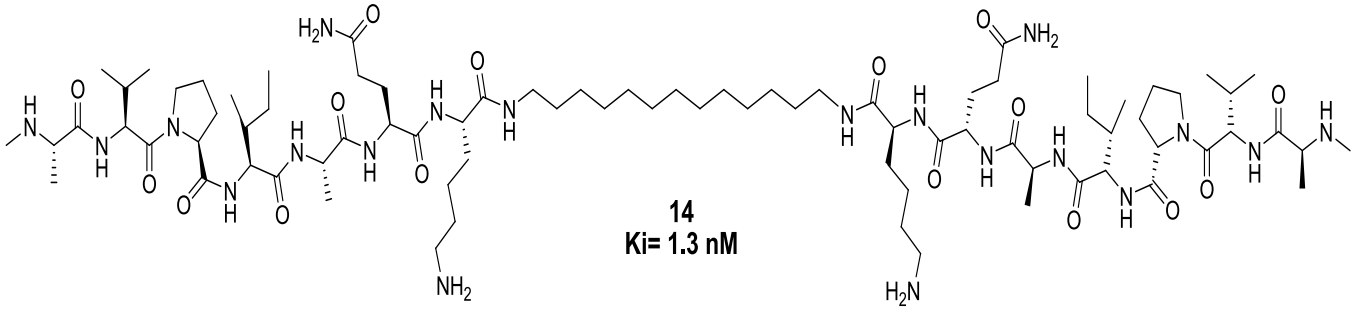

14
Ki= 1.3 nM

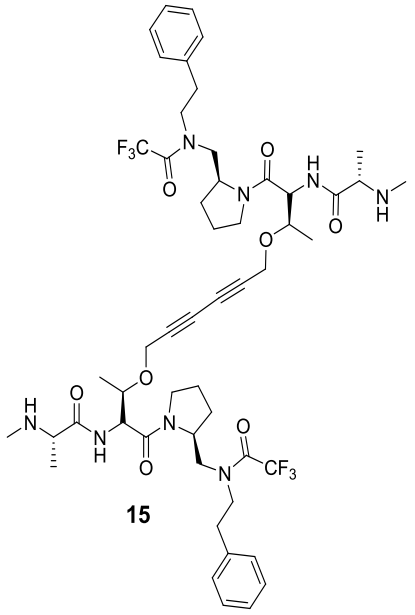

15

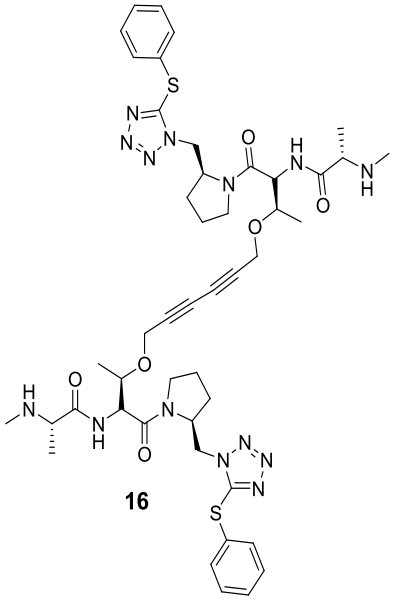

16

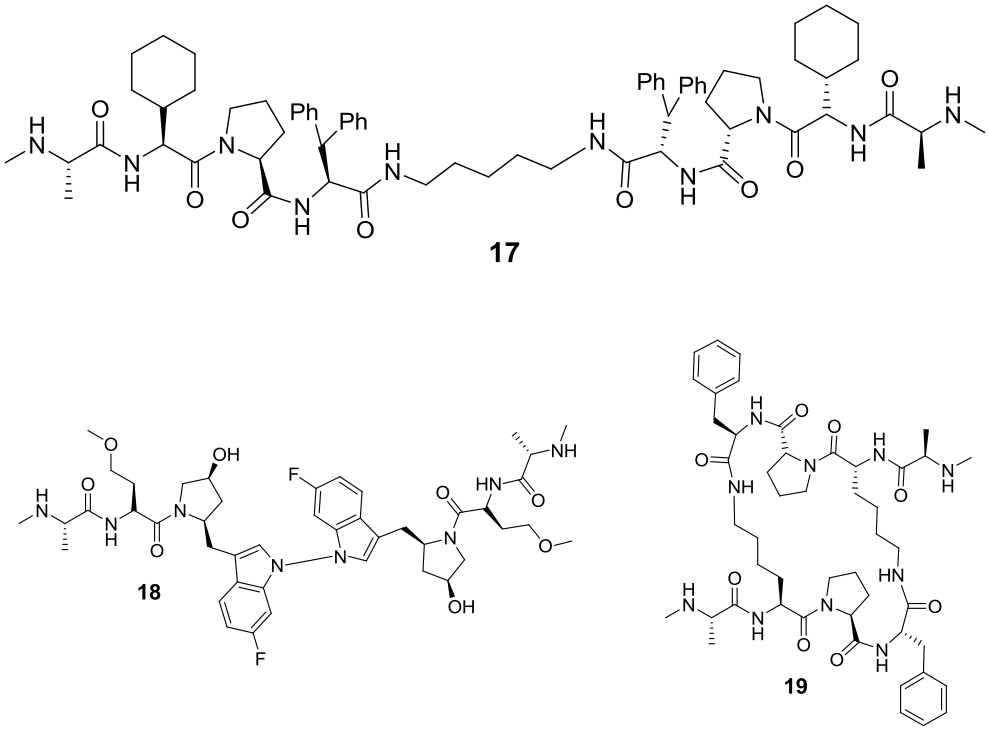

Figure 1.14. Representations of a few potent bivalent Smac mimetics

After the initial discovery of compound **9**, the Wang and Harran laboratories shifted their focus and efforts towards improving the oxazoline mimetic. [73] Through several attempts at a manipulation of the alkyne, off the threonine at P2, they discovered a by-product which was characterized as a C_2-symmetric diyne **16**, which was realized to be the endpoint of the oxidative homodimerization known as Glaser coupling. When the dimer (**16**) and the corresponding monovalent compound (**9**) were tested, they displayed similar binding affinity for the BIR3 domain in XIAP. However, compound **16** was found to be significantly more potent at activating caspase-3 in cellular extracts[74] further strengthening the hypothesis that bivalent Smac mimetics interact simultaneously with BIR2 and BIR3 domains in XIAP. Aegera Therapeutics

reported a cell permeable bivalent Smac mimetic which could bind to XIAP-BIR3 protein with an IC_{50} value of 100 nM[75], shown above as compound **15**. This bivalent Smac mimetic, compound **15**, when compared against its monovalent counterpart, compound **10**, displayed a 10 fold increase in affinity to the BIR3 domain in XIAP. Testing compound **15** for binding affinity to the BIR3 domain in cIAP1 and cIAP2 gave IC_{50} values of 17 and 34 nM respectively. Several cancer cell lines were then screened against monomer compound **10** and divalent compound **15**, some cell lines underwent rapid apoptosis after exposure **15** (e.g. MDA-MB-231, SKOV3) while others showed no reduction in viability, even after 72 hours of exposure.[76] From the cell lines that responding to **15**, the IC_{50} value was observed to be at a concentration of ~5 nM.

In 2007 the Wang Laboratory at the University of Michigan reported the design of a cell permeable, conformationally constrained, monovalent Smac mimetic known as SM-122. The compound consisted of a [8.5] bicyclic ring system (Figure 1.15), and was shown to have an IC_{50} value of 91 nM in a binding assay to the XIAP-BIR3.[77]

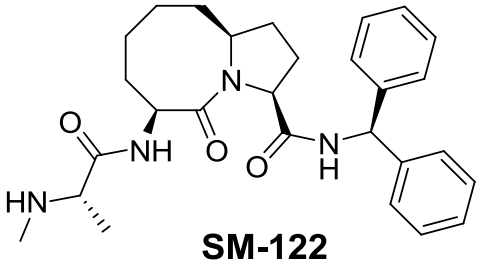

SM-122

Figure 1.15. Conformationally constrained, monovalent Smac mimetic SM-122 which shows an IC50 value of 91 nM to BIR3 in XIAP

Using SM-122 as a promising monovalent Smac mimetic template for the design of bivalent Smac mimetics, Wang et al. next focused on suitable sites to create

chemical tethers. Using computational modeling to predict binding of SM-122 to the BIR2 and BIR3 domain in XIAP, they were able to determine that one of the phenyl groups at P4 did not insert into the binding domain and made this a suitable anchoring site. Additionally they were able to determine that replacement of the non-binding phenyl ring with other aromatic rings did not compromise any binding. Thus in doing so were able to design and synthesize divalent compound **13** in which one of the phenyl groups was replaced by a triazole via "click chemistry", a highly efficient coupling method.[78] Using a fluorescence polarization based assay where **13** was fluorescently tagged, they were able to determine that compound **13** could induce cell death by binding to the XIAP-BIR domains with an IC_{50} value of 1.39 nM.[79]

In 2007 Jian and colleagues from the Memorial Sloan-Kettering Cancer Center published an article in which divalent compound **14** was made known. They demonstrated that the binding of compound **14** with the XIAP-BIR2 domain could effectively antagonize inhibition of the downstream effector caspase, caspase-3. In conducting caspase-3 recovery experiments they were able to determine that compound **14** could reactivate 50% of the caspase-3 activity at a concentration of 50 nM, while the monomer required > 1 uM concentrations.[80] Compound **17**, designed by Varfolomeev and colleagues at Genentech, was initially proposed in order to investigate the mechanism of action of divalent Smac mimetics involved in the induction of apoptosis. This compound was determined to bind to XIAP containing both BIR2 and BIR3 domains with a Ki value of 1.30 nm.[81]

One of the most potent compounds ever tested to date, in an ovarian cancer cell line SK-OV-3 and developed by Tetralogic Pharmaceuticals, has been compound **18**. A

patent filed by the company contained 163 different examples of compounds, all of which were attached at the P4 position.[82] The tether between the two monomer units is via the same indole nitrogen that was used to attach the polyethylene glycol chain on the monomer version, compound **7**.

In 2008 Nikolovska-Coleska and colleagues reported the synthesis and evaluation of compound **19**, a bivalent Smac mimetic that was cyclic in nature. They showed that compound **19** could bind to BIR2 and BIR3 in XIAP using a biphasic dose-response curve, giving them insight into two binding sites and the ability to determine IC_{50} values of 0.5 and 406 nM respectively. Testing compound **19** on XIAP constructs containing only BIR3 or BIR2 domains gave Ki values of 4 nm and 4.4 μM, respectively. Through a series of additional tests, Nikolovska-Coleska and her colleagues were able to determine that compound **19** could efficiently antagonize inhibiton of XIAP in a cell-free functional assay and that **19** was 200 times more potent than its monomer counterpart.[83]

1.6.5 Monovalent and Divalent Smac Mimetics bind to XIAP, cIAP-1/-2 and ML-IAP

Over the course of the past 12 years the primary focus has been on designing Smac mimetics which can interact with the BIR domains in XIAP. However, since Smac can also bind to the BIR domain(s) in cIAP-1 and -2 and ML-IAP,[84] it is not surprising that monovalent and divalent Smac mimetics can also target other IAP proteins.

For monovalent Smac mimetics, compounds **5** to **12** all have exhibited the ability to bind to cIAP1, cIAP2, or ML-IAP with a diverse range in Ki values. Compound **5**

binds to ML-XBIR3SG with a Ki value of 68 nM while compound **6** binds to ML-XBIR3SG with a Ki value of 0.046 μM. Also compound **10** binds to cIAP1 and cIAP2 with Ki values of 49 and 86 nM respectively.[85]

For divalent Smac mimetics, compound **13** was determined to bind to the BIR2 and BIR3 domains in cIAP1 with a Ki value of 0.3 nM, and to the BIR3 domain of cIAP2 with a Ki value of 1.1 nM.[86] Compound **15** was shown to bind to the BIR3 domain in both cIAP1 and cIAP2 with Ki values of 17 and 34 nM, respectively.[87] Compound **17** binds to both BIR2 and BIR3 in cIAP1 with a Kd value of 0.46 nM[88], and it has been indicated that compound **18** has been binds to cIAP1 with picomolar affinity but no precise values have been reported.[89]

Overall, the biochemical data obtained over the years by many groups has given a clear insight indicating that monovalent and bivalent Smac mimetics not only bind to XIAP with high affinity but they can also bind with other IAP proteins, in particular cIAP1 and cIAP2.

1.7 Smac Mimetics as New Cancer Therapeutics

Apoptosis has been accepted as a fundamental component in the pathogenesis of cancer. It is known that dysfunction of the apoptotic pathway and deregulated cellular proliferation will ultimately lead to carcinogenesis and tumour progression.[90] Many different apoptosis regulators have been documented in rendering tumour cells resistant to apoptosis both in vivo and in vitro, in particular a family of proteins known as the inhibitors of apoptosis proteins (IAPs). Increased expression in cancer tissues,

together with functional significance in tumour maintenance and therapeutic resistance, makes the family of IAP proteins attractive targets for anticancer therapeutic intervention. To date the most effective strategy has involved mimics of the amino terminus of the endogenous IAP protein antagonist Smac. These constructs interfere with the critical IAP-caspase and IAP- Smac interactions.[91]

It is evident, as seen from the examples above, that Smac mimetics have been able to stimulate cell death and sensitize a number of tumour cell lines to apoptosis. What is even more impressive is the reported success in treating malignant glioma, breast cancer, non-small cell lung cancer, and multiple myeloma models in vivo with Smac mimetics.[92,93,94] To date, only a hand full of laboratories have been able to design and synthesise Smac mimetics which can bind to the BIR domains of XIAP, cIAP1, cIAP2, and ML-IAP and antagonize their interactions with proapoptotic proteins such as caspase-3,-7, and -9 and progress into phase 1 clinical trials. An alternative anti-IAP therapeutic strategy has been to block the action of IAP proteins by the use of antisense oligonucleotides that down-regulate IAP protein levels by targeting native mRNAs[95]. Although this method has shown significant effects on the viability of tumour cells, most preclinical studies have focused in on XIAP since it seems to be the strongest anti-apoptotic family member.[96]

With the increased probability of targeting IAP proteins to disrupt their interactions with pro-apoptotic proteins such as caspases and Smac, and the overall ability of IAP proteins to act as inhibitors of apoptosis, together with their prominent expression in human malignancies, makes them attractive targets for new therapeutic interventions.

References:

[1] La Casse, EC., Mahoney, DJ., Cheung, HH., Plenchette, S., Baird, S., Korneluk, RG. *Nature (Oncogene*) **2008,** 27, 6252–6275

[2] Alberts, B., Johnson, A., Lewis, J., Raff, M., Roberts, K., Walter, P. **Molecular Biology of the cell**. New York and London: Garland Science; c2002

[3] Alberts, B., Johnson, A., Lewis, J., Raff, M., Roberts, K., Walter, P. **Molecular Biology of the cell**. New York and London: Garland Science; c2002

[4] Alberts, B., Johnson, A., Lewis, J., Raff, M., Roberts, K., Walter, P. **Molecular Biology of the cell**. New York and London: Garland Science; c2002

[5] La Casse, EC., Mahoney, DJ., Cheung, HH., Plenchette, S., Baird, S., Korneluk, RG. *Nature (Oncogene*) **2008,** 27, 6252–6275

[6] Alberts, B., Johnson, A., Lewis, J., Raff, M., Roberts, K., Walter, P. **Molecular Biology of the cell**. New York and London: Garland Science; c2002

[7] Kufe, Donald W.; Pollock, Raphael E.; Weichselbaum, Ralph R.; Bast, Robert C., Jr.; Gansler, Ted S.; Holland, James F.; Frei III, Emil. **Cancer in Medicine**. Hamilton (Canada): BC Decker inc.; c2003

[8] Alberts, B., Johnson, A., Lewis, J., Raff, M., Roberts, K., Walter, P. **Molecular Biology of the cell**. New York and London: Garland Science; c2002

[9] Kufe, Donald W.; Pollock, Raphael E.; Weichselbaum, Ralph R.; Bast, Robert C., Jr.; Gansler, Ted S.; Holland, James F.; Frei III, Emil. **Cancer in Medicine**. Hamilton (Canada): BC Decker inc.; c2003

[10] Algeciras-Schimnich, A., Barnhart, B.; Peter, M.. **Madame Curie Bioscience Database – Apoptosis.** Chapters taken from the Madame Curie Bioscience Database: Eurekah.com and Landes Bioscience and Springer Science+Business Media; c2009

[11] Algeciras-Schimnich, A., Barnhart, B.; Peter, M.. **Madame Curie Bioscience Database – Apoptosis.** Chapters taken from the Madame Curie Bioscience Database: Eurekah.com and Landes Bioscience and Springer Science+Business Media; c2009

[12] Algeciras-Schimnich, A., Barnhart, B.; Peter, M.. **Madame Curie Bioscience Database – Apoptosis.** Chapters taken from the Madame Curie Bioscience Database: Eurekah.com and Landes Bioscience and Springer Science+Business Media; c2009

[13] Kufe, Donald W.; Pollock, Raphael E.; Weichselbaum, Ralph R.; Bast, Robert C., Jr.; Gansler, Ted S.; Holland, James F.; Frei III, Emil. **Cancer in Medicine**. Hamilton (Canada): BC Decker inc.; c2003

[14] Kufe, Donald W.; Pollock, Raphael E.; Weichselbaum, Ralph R.; Bast, Robert C., Jr.; Gansler, Ted S.; Holland, James F.; Frei III, Emil. **Cancer in Medicine**. Hamilton (Canada): BC Decker inc.; c2003

[15] Kufe, Donald W.; Pollock, Raphael E.; Weichselbaum, Ralph R.; Bast, Robert C., Jr.; Gansler, Ted S.; Holland, James F.; Frei III, Emil. **Cancer in Medicine**. Hamilton (Canada): BC Decker inc.; c2003

[16] Strachan, Tom and Read, Andrew P. **Human Molecular Genetics 2.** New York and London: Garland Science; c1999

[17] Strachan, Tom and Read, Andrew P. **Human Molecular Genetics 2.** New York and London: Garland Science; c1999

[18] Alberts, B., Johnson, A., Lewis, J., Raff, M., Roberts, K., Walter, P. **Molecular Biology of the cell**. New York and London: Garland Science; c2002

[19] Alberts, B., Johnson, A., Lewis, J., Raff, M., Roberts, K., Walter, P. **Molecular Biology of the cell**. New York and London: Garland Science; c2002

[20] Raymond, RW. **Cancer in Medicine-Biochemistry of cancer.** Hamilton (Canada): BC Decker inc.; c2003

[21] Alberts, B., Johnson, A., Lewis, J., Raff, M., Roberts, K., Walter, P. **Molecular Biology of the cell**. New York and London: Garland Science; c2002

[22] Alberts, B., Johnson, A., Lewis, J., Raff, M., Roberts, K., Walter, P. **Molecular Biology of the cell**. New York and London: Garland Science; c2002

[23] Alberts, B., Johnson, A., Lewis, J., Raff, M., Roberts, K., Walter, P. **Molecular Biology of the cell**. New York and London: Garland Science; c2002

[24] Alberts, B., Johnson, A., Lewis, J., Raff, M., Roberts, K., Walter, P. **Molecular Biology of the cell**. New York and London: Garland Science; c2002

[25] Kufe, Donald W.; Pollock, Raphael E.; Weichselbaum, Ralph R.; Bast, Robert C., Jr.; Gansler, Ted S.; Holland, James F.; Frei III, Emil. **Cancer in Medicine**. Hamilton (Canada): BC Decker inc.; c2003

[26] Kufe, Donald W.; Pollock, Raphael E.; Weichselbaum, Ralph R.; Bast, Robert C., Jr.; Gansler, Ted S.; Holland, James F.; Frei III, Emil. **Cancer in Medicine**. Hamilton (Canada): BC Decker inc.; c2003

[27] Petronelli, A., Riccioni, R., Pasquini, L., Petrucci, E., Testa, U. Drugs Fut. **2005**, 30(7): 707

[28] Flygare, J.; Fairbrother, W.; Expert Opin. Ther. Patents **2010,** 20,(2):251-267

[29] Kufe, Donald W.; Pollock, Raphael E.; Weichselbaum, Ralph R.; Bast, Robert C., Jr.; Gansler, Ted S.; Holland, James F.; Frei III, Emil. **Cancer in Medicine**. Hamilton (Canada): BC Decker inc.; c2003

[30] Michalke, M.; Stepczynska, A.; Bui, TN.; Loser, K.; Krzemieniecki, K.; Los, Marek. M**adame Curie Bioscience Database – Caspases as Targets for drug development.** Chapters taken from the Madame Curie Bioscience Database: Eurekah.com and Landes Bioscience and Springer Science+Business Media; c2009

[31] Rohrmann, GF.; **Baculovirs molecular biology- Baculovirs infection: the cell cycle and apoptosis.** Bethesda (MD): National Library of Medicine (US), NCBI; 2008

[32] Rohrmann, GF.; **Baculovirs molecular biology- Baculovirs infection: the cell cycle and apoptosis.** Bethesda (MD): National Library of Medicine (US), NCBI; 2008

[33] Kufe, Donald W.; Pollock, Raphael E.; Weichselbaum, Ralph R.; Bast, Robert C., Jr.; Gansler, Ted S.; Holland, James F.; Frei III, Emil. **Cancer in Medicine-Protein domains involved in apoptosis regulation**. Hamilton (Canada): BC Decker inc.;c2003

[34] Silke, J.; Hawkins, CJ.; Ekert, P, et al. J Cell Biol. **2002,** 157, 115-124

[35] Kufe, Donald W.; Pollock, Raphael E.; Weichselbaum, Ralph R.; Bast, Robert C., Jr.; Gansler, Ted S.; Holland, James F.; Frei III, Emil. **Cancer in Medicine-Protein domains involved in apoptosis regulation**. Hamilton (Canada): BC Decker inc.;c2003

[36] Sun, H.; Stuckey, J.; Nikolovska-Coleska, Z.; Quin, D.; Meagher, J.; Qiu, S.; Lu, J.; Yang, CY.; Saito, NG.; Wang, S. J. Med. Chem., **2008**, 51 (22), 7169–7180

[37] Huang, J.W.; Zhang,Z.; Wu, B.; Cellitti, J.; Dahl, R.; Shiau, C.; Weslh, K.; Emdadi, A.; Stebbins, J.; Reed, J.; Pellecchia, M.; J. Med. Chem. **2008**, 51, 7111-7118

[38] Wu, G.; Chai, J.; Suber, TL, et al. Nature, **2000**, 408:1004-1008

[39] Kufe, Donald W.; Pollock, Raphael E.; Weichselbaum, Ralph R.; Bast, Robert C., Jr.; Gansler, Ted S.; Holland, James F.; Frei III, Emil. **Cancer in Medicine**. Hamilton (Canada): BC Decker inc.; c2003

[40] Liu, Z.; Sun, C.; Olejniczak, E.; Meadows, R.; Betz, S.; Oost, T.; Herrmann, J.; Wu, J.; Fesik, S. *Nature*, **2000,** 408, 1004-1008

[41] Michalke, M.; Stepczynska, A.; Bui, TN.; Loser, K.; Krzemieniecki, K.; Los, Marek. M**adame Curie Bioscience Database – Caspases as Targets for drug development.** Chapters taken from the Madame Curie Bioscience Database: Eurekah.com and Landes Bioscience and Springer Science+Business Media; c2009

[42] Shi, Y. Molecular Cell,**2002** Vol. **9**, 459–470,

[43] Yang, L.; Sun, M.; Sun, XM.; Cheng, G.; Nicosia, S.; Cheng, J. The journal of biological chemistry, **2007**, 282 , 15, 10981–10987

[44] Yang, L.; Sun, M.; Sun, XM.; Cheng, G.; Nicosia, S.; Cheng, J. The journal of biological chemistry, **2007**, 282 , 15, 10981–10987

[45] Lin, M.; Beal, MB. *Nature* **443**, 787-795 (19 October 2006)

[46] Yang, L.; Sun, M.; Sun, XM.; Cheng, G.; Nicosia, S.; Cheng, J. The journal of biological chemistry, **2007**, 282 , 15, 10981–10987

[47] Wu, G.; Chai, J.W.; Kyin, S.; Wang, X.; Shi, Y.; Nature **2000**, 408, 1008-1012

[48] Liu, Z.; Sun, C.; Olejniczak, E.; Meadows, R.; Betz, S.; Oost, T.; Herrmann, J.; Wu, J.; Fesik, S. *Nature*, **2000,** 408, 1004-1008

[49] Flygare, J.A.; Fairbrother, W.J.;. Expert. Opin. Ther. Patents **2010,** 20,(2): 251-267

[50] Flygare, J.A.; Fairbrother, W.J.;. Expert. Opin. Ther. Patents **2010,** 20,(2): 251-267

[51] Sun, H.; Nikolovska-Coleska, Z.; Yang, C-Y.; Qian, D.; Lu, J.; Qiu, S.; Bai, L.; Peng, Y.; Cai, Q.; Wang, S.; Accounts of Chemical Research **2008**, 41(10) : 1264:1277

[52] Kipp, R.A.; Case,M.A.; Wist, A.D.; Cresson, C.M.; Carrell, M.; Griner, E.; Wiita, A.; Albiniak, P.A.; Chai, J.; Shi, Y.; Semmelhack, M.F.; McLendon, G.L. Biochemistry **2002**, 41, 7344-7349

[53] Sun, H.; Nikolovska-Coleska, Z.; Yang, C-Y.; Qian, D.; Lu, J.; Qiu, S.; Bai, L.; Peng, Y.; Cai, Q.; Wang, S.; Accounts of Chemical Research **2008**, 41(10) : 1264:1277

[54] Sun, H.; Nikolovska-Coleska, Z.; Yang, C-Y.; Xu, L.; Liu, M.; Tomita, Y.; Pan, H.; Yoshioka, Y.; Krajewski, K.; Roller, P.P.; Wang, S.; . Am. Chem. Soc. **2004,** 126: 16686-16687

[55] Sun, H.; Nikolovska-Coleska, Z.; Yang, C-Y.; Xu, L.; Liu, M.; Tomita, Y.; Pan, H.; Yoshioka, Y.; Krajewski, K.; Roller, P.P.; Wang, S.; . Am. Chem. Soc. **2004,** 126: 16686-16687

[56] Sun, H.; Nikolovska-Coleska, Z.; Yang, C-Y.; Qian, D.; Lu, J.; Qiu, S.; Bai, L.; Peng, Y.; Cai, Q.; Wang, S.; Accounts of Chemical Research **2008**, 41(10) : 1264:1277

[57] Sun, H.; Nikolovska-Coleska, Z.; Yang, C-Y.; Qian, D.; Lu, J.; Qiu, S.; Bai, L.; Peng, Y.; Cai, Q.; Wang, S.; Accounts of Chemical Research **2008**, 41(10) : 1264:1277

[58] Oost, TK.; Sun, C.; Armstrong, RC.; J. Med. Chem. **2004,** 47:4417-4426

[59] Oost, TK.; Sun, C.; Armstrong, RC.; J. Med. Chem. **2004,** 47:4417-4426

[60] Wu, G.; Chai, J.; Suber, TL.; et al. Nature **408**:1004-1008

[61] Flygare, J.A.; Fairbrother, W.J.;. Expert. Opin. Ther. Patents **20**(2): 251-267

[62] Oost, TK.; Sun, C.; Armstrong, RC.; J. Med. Chem. **2004,** 47:4417-4426

[63] Genentech, Inc. Pyrrolidine inhibitors of IAP. WO2006069063A1; 2005

[64] Genentech, Inc. Pyrrolidine inhibitors of IAP. WO2006069063A1; 2005

[65] Cohen, F; Alicke, B.; Elliott, L.O.; et al. J. Med. Chem. **2009**, 52: 1723-1730

[66] Tetralogic Pharmaceuticals Corporation, IAP binding compounds. US7456209B2; 2005

[67] Novartis AG. Organic compounds. WO2006133147A2; 2006

[68] Aegera Therapeutics, Inc. BIR domain binding compounds. WO2007101347A1; 2007

[69] The Trustees of Princeton University. IAP binding compounds. WO2004007529A3; 2003

[70] Li, L.; Thomas, R.M.; Suzuki, H.; De Brabander, J.K.; Wang, X.; Harran, P.; Science **2004**, 305: 1471-1474

[71] Bertrand, M. J.; milutinovic, S.; Dickson, K.M.; Ho, W.C.; Boudreault, A.; Durkin, J.; Gillard, J. W.; Jaquith, J. B.; Morris, S. J.; Barker, P. A.; Mol. Cell, **2008**, 30,689-700

[72] Sun, H.; Nikolovska-Coleska, Z.; Yang, C-Y.; Qian, D.; Lu, J.; Qiu, S.; Bai, L.; Peng, Y.; Cai, Q.; Wang, S.; Accounts of Chemical Research **2008**, 41(10) : 1264:1277

[73] Li, L.; Thomas, R.M.; Suzuki, H.; De Brabander, J.K.; Wang, X.; Harran, P.; Science **2004**, 305: 1471-1474

[74] Li, L.; Thomas, R.M.; Suzuki, H.; De Brabander, J.K.; Wang, X.; Harran, P.; Science **2004**, 305: 1471-1474

[75] Bertrand, M. J.; milutinovic, S.; Dickson, K.M.; Ho, W.C.; Boudreault, A.; Durkin, J.; Gillard, J. W.; Jaquith, J. B.; Morris, S. J.; Barker, P. A.; Mol. Cell, **2008**, 30,689-700

[76] Bertrand, M. J.; milutinovic, S.; Dickson, K.M.; Ho, W.C.; Boudreault, A.; Durkin, J.; Gillard, J. W.; Jaquith, J. B.; Morris, S. J.; Barker, P. A.; Mol. Cell, **2008**, 30,689-700

[77] Sun, H.; Nikolovska-Coleska, Z.; Lu, J.; Meagher, J. L.; Yang, C.Y.; Qiu, S.; Tomita, Y.; Ueda, Y.; Jiang, S.; Krajewski, K.; Roller, P.P.; Stuckey, J.A.; Wang, S.; J. Am. Chem. Soc. **2007,** 129,:15279-15294

[78] Rostovtsev, V. V.; Green, L. G.; Fokin, V. V.; Sharpless, K. B.; Angew. Chem., Int. Ed. **2002**, 41(14), 2596-2599

[79] Sun, H.; Nikolovska-Coleska, Z.; Lu, J.; Meagher, J. L.; Yang, C.Y.; Qiu, S.; Tomita, Y.; Ueda, Y.; Jiang, S.; Krajewski, K.; Roller, P.P.; Stuckey, J.A.; Wang, S.; J. Am. Chem. Soc. **2007,** 129,:15279-15294

[80] Gao, Z.; Tian, Y.; Wang, J.; Yin, Q.; Wu, H.; Li, Y. M.; Jiang, X.; J. Biol. Chem. **2007,** 282, 30718-30727

[81] Varfolomeev, E.; Blankenship, J. W.; Wayson, S. M.; Fedorova, A. V.; Kayagaki, N.;Garg, P.; Zobel, K.; Dynek, J. N.; Elliott, L. O.; Wallweber, H. J.; Flygare, J. A.;Fairbrother, W. J.; Deshayes, K.; Dixit, V. M.; Vucic, D. Cell, **2007,** 131**,** 669–681.

[82] Tetralogic Pharmaceuticals Corporation. Dimeric IAP inhibitors. US7517906B2; 2006

[83] Nikolovska-Coleska, Z.; Meagher, J. L.; Jiang, S.; Yang, C.-Y.; Qiu, S.; Roller, P. P.; Stuckey, J. A.; Wang, S.; (. *Biochemistry **2008,** 47*, 9811–9824.

[84] Sun, H.; Nikolovska-Coleska, Z.; Yang, C-Y.; Qian, D.; Lu, J.; Qiu, S.; Bai, L.; Peng, Y.; Cai, Q.; Wang, S.; Accounts of Chemical Research **2008**, 41(10) : 1264:1277

[85] Bertrand, M. J.; milutinovic, S.; Dickson, K.M.; Ho, W.C.; Boudreault, A.; Durkin, J.; Gillard, J. W.; Jaquith, J. B.; Morris, S. J.; Barker, P. A.; Mol. Cell, **2008**, 30,689-700

[86] Lu, J.; Bai, L.; Sun, H.; Nikolovska-Coleska, Z.; McEachern, D.; Qiu, S.; Miller, R. S.; Yi, H.; Shangary, S.; Sun, Y.; Meagher, J. L.; Stuckey, J. A.; Wang, S. *Cancer Res. **2008***, 68(22):9384-9393

[87] Bertrand, M. J.; milutinovic, S.; Dickson, K.M.; Ho, W.C.; Boudreault, A.; Durkin, J.; Gillard, J. W.; Jaquith, J. B.; Morris, S. J.; Barker, P. A.; Mol. Cell, **2008**, 30,689-700

[88] Varfolomeev, E.; Blankenship, J. W.; Wayson, S. M.; Fedorova, A. V.; Kayagaki, N.;Garg, P.; Zobel, K.; Dynek, J. N.; Elliott, L. O.; Wallweber, H. J.; Flygare, J. A.;Fairbrother, W. J.; Deshayes, K.; Dixit, V. M.; Vucic, D. Cell, **2007**, 131**,** 669–681.

[89] Vince, J. E.; Wong, W. W.; Khan, N.; Feltham, R.; Chau, D.; Ahmed, A. U.; Benetatos, C. A.; Chunduru, S. K.; Condon, S. M.; McKinlay, M.; Brink, R.; Leverkus, M.; Tergaonkar, V.; Schneider, P.; Callus, B. A.; Koentgen, F.; Vaux, D. L.; Silke, J.. *Cell*, ***2007**,131*, 682–693.

[90] Nachmias, B.; Ashhab, Y.; Ben-Yehuda, D. Semin Cancer Biol**,2004,** 14: 231−243

[91] Schimmer, AD. Cancer Res. **2004**, 64: 7183-7190

[92] Fulda, S.; Wick, W.; Weller, M.; Bebatin, K.M.; Nat. Med. **2002**, 8:808-815

[93] Oost, T.K.; Sun, C.; Armstrong, R.C. et al. J. Med. Chem.**2004,** 47: 4417-4426

[94] Chauhan, D.; Neri, P.; Velankar, M. et al. Blood. **2007**, 109**:** 1220-1227

[95] Cao, C.; Mu, Y.; Hallanhan, D.E.; Lu, B.; Oncogene **2004,** 203: 7047-7052

[96] Sile, J.; Vaux, D.L., J. Cell Sci. **2001**, 114: 1821-1827

Chapter 2: Goals and Objectives

2.1 Factors Responsible for the Initiation of Apoptosis in Cancer Cells

The proper regulation of apoptosis is vital for the normal development and homeostasis of living organisms. Many disease states result from over-sensitivity or resistance to apoptotic stimuli.[1] Resistance to apoptosis in many forms of cancer has become an area of special interest, since a lack of death response often allows these cancers to tolerate medical and chemotherapy treatments.[2] The key component in such cancer cell lines, which allows them to avoid cell death, is thought to occur between baculoviral IAP repeat (BIR) domains, as described in Sections 1.4.1 and 1.4.2, and initiation and effector caspases-3,-7, and -9.[3] Over-expression of IAP proteins in many human cancers has shown to suppress apoptosis and in particular over-expression of XIAP, a potent inhibitor of caspase and one of the most studied, has lead to the resistance of many cancer cell lines to chemotherapeutic agents.[4,5,6,7] As described in Section 1.6.0, the discovery of short peptides that disrupt the interaction of the IAPs with caspase[8] have lead to multiple efforts into the development of Smac mimetics with reduced peptide character, increased affinity for BIR domains, higher permeability, and pharmacokinetic properties in hopes of one day being useful new anticancer therapeutic agents.[9,10]

Given the importance of Smac mimetics, our laboratory began to focus on SAR work in designing and synthesizing peptide and non-peptide based compounds. The research focused on designing monovalent and divalent forms which would then be able to induce apoptosis in human breast cancer cell line. As seen in Sections 1.6.2

and 1.6.3, structural variations at the valine (P2) and isoleucine (P4) residues on the native AVPI Smac sequence has provided numerous compounds (Figure 1.12) in which binding affinity to the BIR domains of IAPs has increased significantly; giving nanomolar IC_{50} values.[11,12, 13,14,15,16] Based on the above findings, our goal was to synthesise compounds which could induce apoptosis by modifying the tetrapeptide sequence in three following ways: (1) varying the flexibility of the tether linking the divalent mimetcs, (2) altering the sequence of the amino acids in the native AVPI protein, by synthesizing divalent mimetics containing MeAVPI-linker-IPVMeA (forward-reverse) and MeAVPI-linker-MeAVPI (forward-forward) sequence to observe its effect on binding affinity, (3) and synthesizing a library of monovalent Smac mimetics modified at the second (P2) and fourth (P4) residue through incorporation of a propargyl-glycine at P2 and various hydrophobic moieties at P4. These modifications are based on the SAR results obtained by Aegera on compounds **10** and **15** (Sections 1.6.3 and 1.6.4).

2.1.1 Objective 1: Probing the Effect of Divalent Smac Mimetics Synthesized in a MeAVPI-linker-IPVMeA (forward-reverse) and MeAVPI-linker-MeAVPI (forward-forward) sequence and their ability to Induce apoptosis.

As described in Section 1.6.4, when natural Smac is released from the mitochondria it forms a homodimer, which then binds to the BIR domains in XIAP with a superior affinity than its monovalent form.[17] The better binding ability of divalent tetrapeptides has been validated by many research groups.[18,19,20,21] However, the exact cause for the increased effectiveness of divalent Smac mimetics remains unclear. It

has been suggested that increased activity of divalent peptides could be attributed to the simultaneous binding of the divalent Smac mimetic to both BIR2 and BIR3 domains[22,23] in a similar fashion as predicted for native Smac.[24] This suggestion has been refuted by Splan *et al.* [25] who further explored the basis for enhanced dimer effectiveness. From their investigation they were able to conclude that simultaneous interaction of the divalent tetrapeptide with both BIR domains was not likely. In 1951, Pauling and colleagues[26] were able determine the length of various polypeptides in Angstrom units through the determination of crystal structures of amino acids, peptides, and other simple substances related to proteins; generating information about inter-atomic distances. Using this knowledge one could reliably predict the configuration of various polypeptide chains (Figure 2.1). Using the Angstrom data, Splan *et al.* calculated that it would take more than 20 amino acids to span a distance of ≥ 45 Å; correlating to the space between the BIR2 and BIR3 domains.

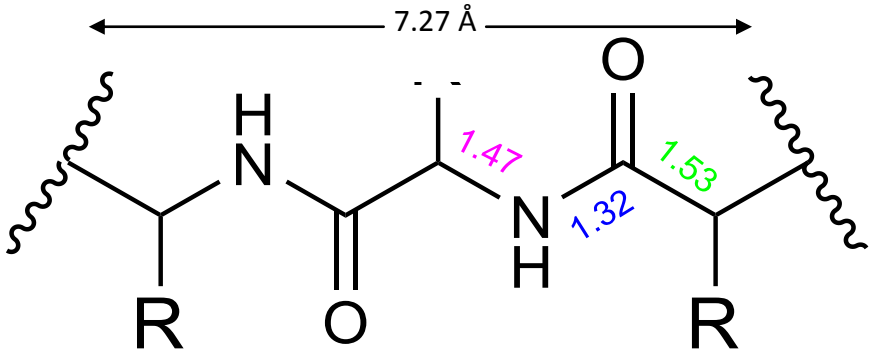

Figure 2.1 Dimensions of a polypeptide. Bond lengths are shown in Å[26]

Previously our group had synthesized compounds **20** and **21** which displayed moderate apoptotic activity when tested in-vitro; yielding EC_{50} values of 500 μM and 100 μM respectively. The two divalent mimetics studied contained a structural variation

at the free amine on alanine, Figure 2.2.

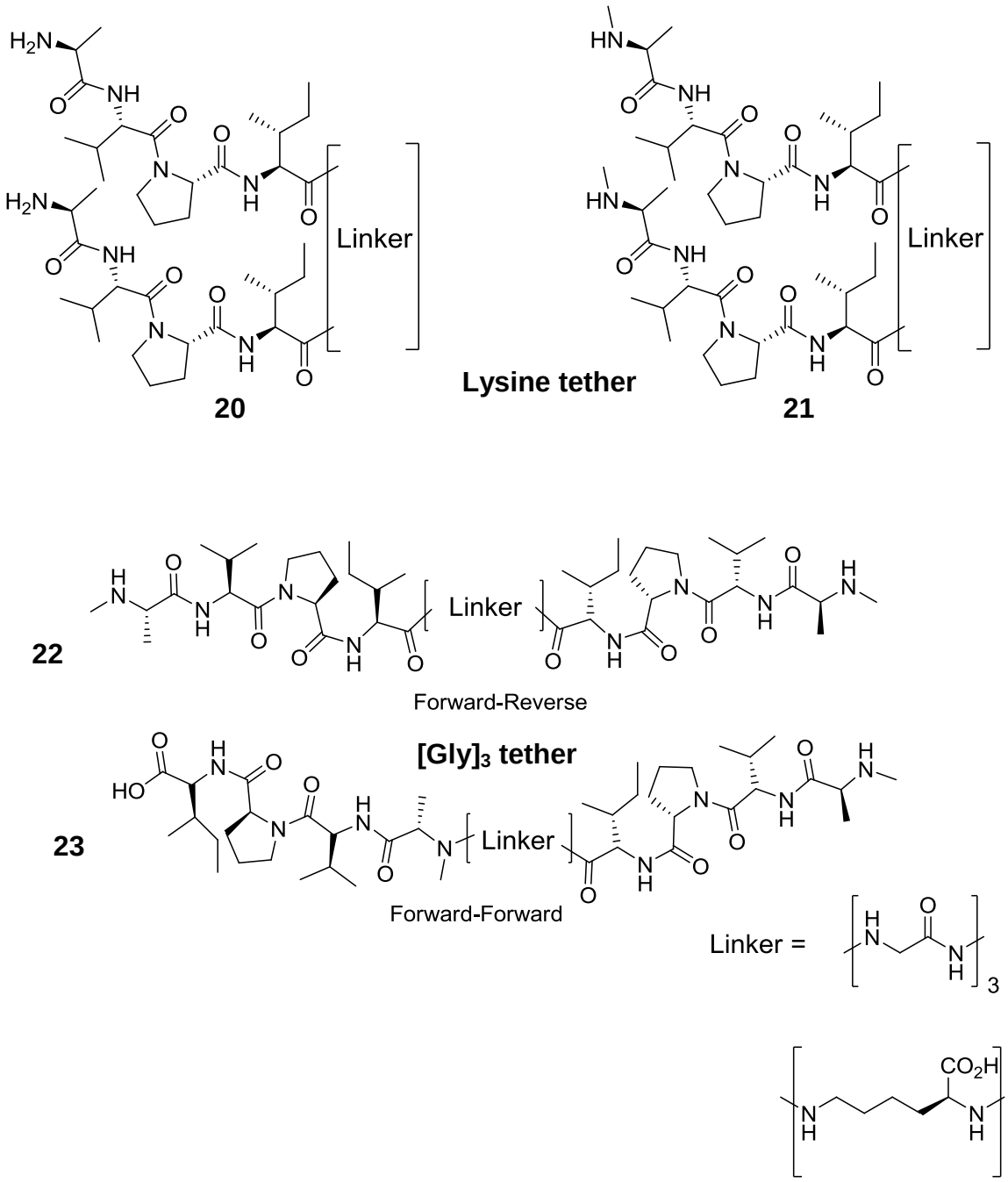

Figure 2.2 Homodimers built on a lysine tether containing an AVPI-lysine-IPVA (**20**) and a MeAVPI-lysine-IPVMeA (**21**); Also a triglycine tether built in a MeAVPI-Gly_3-IPVMeA (**22**) (forward-reverse), and MeAVPI-Gly_3-MeAVPI (**23**) (forward-forward)

The significance of this addition of a methyl substituent demonstrates how the subtle change in the structure of a Smac mimetic is able to affect the apoptotic activity of these proteins. Thus, to investigate how changes along the Smac mimetic peptide could affect apoptotic activity in the cancer cell line, we synthesized compounds **22** and **23**. Assessing the apoptotic activity of these divalent mimetics will allow us to use this information as a peptide screening parameter to rationally design potent divalent Smac mimetics rapidly.

To validate the work done by the Wang group and Splan *et al*. we have chosen to synthesize a library of simple divalent tetrapeptide compounds comprising of 9 to 11 amino acid sequences, designed to mimic the native AVPI homodimer (Figure 2.2). We also propose to synthesize a series of analogues of compound **23,** which will be modified with other amino acids at the valine and isoleucine residues. Screening these new divalent mimetics for apoptotic activity will enable a tool allowing the optimal amino acid sequence into the synthetic Smac mimetics for potent apoptotic activity, as well support research conducted by Wang or Splan.

2.1.2 Objective 2: Determination of The Effect of Substituent Variations at the fourth residue on Smac mimetics Containing L-Propargyl Glycine, Inspired by**15**, on Apoptotic acivity

One of the most common tendencies in Smac mimetics that have been synthesized involves the variation at the second and fourth residues of the native AVPI peptide. [27],[28],[29],[30],[31] The most potent monovalent and divalent Smac mimetics to have

been synthesised, at the time of writing this thesis, were those developed by Aegera Therapeutics;[32] Figure 2.3.

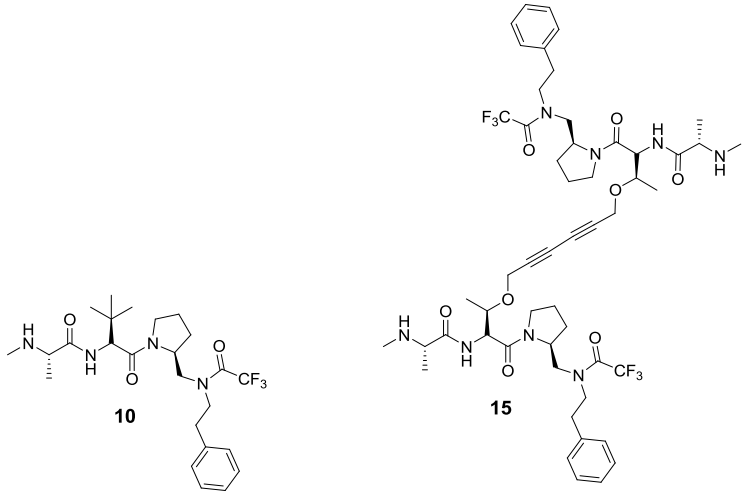

Figure 2.3 Monomer (**10**) and Divalent (**15**) potent Smac mimetics synthesized by Aegera Therapeutics.[32]

In the case of both compounds **10** and **15,** an increase in the hydrophobic moiety at the fourth residue (P4) and variation at the second residue (P2) had an increase effect on inducing apoptosis.[33] In all cases of divalent Smac mimetics an increase in apoptotic activity has been observed; Section 1.6.4 (Figure 1.14).

The relationship that an increase in the hydrophobic nature of the substituent at P4, and a size increase in the substituent at P2 was proportional to increased apoptotic activity, led to the initial hypothesis that a bulky substituent at P2 and a hydrophobic moiety at P4 would allow the peptide to orient itself within the binding pocket and create the favoured interactions to induce apoptotic activity. Since one of our goals is to synthesize potent Smac mimetics, we believed that this could be done by using a propargyl glycine at P2 and hydrophobic aromatic at P4. As a result, in doing so

compound **43** was synthesized as well as a diverse library of compounds which varied at P4; Figure 2.4.

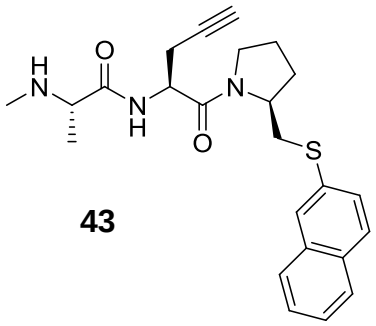

43

Figure 2.4 Lead compound **43** built with a naphthalenethiol at the fourth residue (P4)

In addition to the monomers synthesized, we sought to investigate the increased activity of the divalent counterparts. As seen in Section 1.6.4, divalent forms of Smac mimetics display higher affinity for BIR domains than their monomer counterparts. Inspired by work by Aegera Therapeutics,[34] we envisioned the synthesis of the divalent Smac mimetic via a Glaser coupling of the terminal alkynes in **43**, producing the bis-acetylene bridged derivative **60**; Figure 2.5.

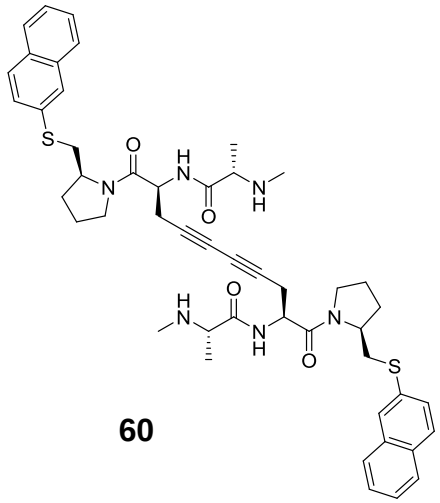

60

Figure 6.5 A potent divalent naphthalenethiol Smac mimetic synthesized via Glaser coupling, 60

2.2 Summary of Goals and Objectives:

i. To determine if homodivalent Smac mimetics induce apoptosis by either binding to BIR2 and BIR3 simultaneously or bind solely to BIR3.

ii. Comparisons will be made by synthesizing MeAVPI-tether-IPVMeA (forward-reverse) and MeAVPI-tether-MeAVPI (forward-forward) to determine if direction of synthesis has any effect on the ability to induce apoptosis.

iii. To probe the effect of increasing hydrophobic substituent's at P4 and to find the most effective substituent at the fourth residue. As well, through the inspiration of compound **15** replacing the substituted threonine for a propargyl-glycine. In doing so will allow SAR work to focus on position four, and should increase the chances in obtaining an effective compound through a reduced number of synthetic steps.

References:

[1] Thompson, C. B.; *Science* **1995**, 267, 1456–1462.

[2] Salvesen, G. S., and Dixit, V. M.; *Cell* **1997**, 91, 443–446.

[3] Salvesen, G. S., and Duckett, C. S.; *Nat. Rev. Mol. Cell. Biol*. **2002**, 3, 401–410.

[4] Stennicke, H. R., Ryan, C. A., and Salvesen, G. S.;. *Trends Biochem. Sci***. 2002**, 27, 94–101.

[5] Li, J., Feng, Q., Kim, J. M., Schneiderman, D., Liston, P., Li, M., Vanderhyden, B., Faught, W., Fung, M. F., Senterman, M., Korneluk, R. G., and Tsang, B. K.; *Endocrinology* **2001**, 142, 370–380.

[6] Fong, W. G., Liston, P., Rajcan-Separovic, E., St Jean, M., Craig, C., and Korneluk, R. G.; *Genomics* **2000**, 70, 113–122.

[7] Cummins, J. M., Kohli, M., Rago, C., Kinzler, K. W., Vogelstein, B., and Bunz, F.; Cancer Res**. 2004**, 64, 3006–3008.

[8] Kipp, R. A.; Case, M. A.; Wist, A. D.; Cresson, C. M.; Carrell, M.; Griner, E.; Wiita, A.; Albiniak, P. A.; Chai, J.; Shi, Y.; Semmelhack, M. F.; McLendon, G. L.; *Biochemistry***, 2002**, 41, 7344.

[9] Li, L.; Thomas, R. M.; Suzuki, H.; De Brabander, J. K.; Wang, X.; Harran, P. G.; *Science***, 2004**, 305, 1471.

[10] Zobel, K.; Wang, L.; Varfolomeev, E.; Franklin, M. C.; Elliott, L. O.; Wallweber, H.; J. A.; Okawa, D. C.; Flygare, J. A.; Vucic, D.; Fairbrother, W. J.; Deshayes, K.; *Chem. Biol*. **2006**, 1**,** 525.

[11]Sun, H.; Nikolovska-Coleska, Z.; Yang, C-Y.; Qian, D.; Lu, J.; Qiu, S.; Bai, L.; Peng, Y.; Cai, Q.; Wang, S.; *Accounts of Chemical Research* **2008**, 41(10) : 1264:1277

[12] Sun, H.; Nikolovska-Coleska, Z.; Yang, C-Y.; Qian, D.; Lu, J.; Qiu, S.; Bai, L.; Peng, Y.; Cai, Q.; Wang, S.; *Accounts of Chemical Research* **2008**, 41(10) : 1264:1277

[13] Oost, TK.; Sun, C.; Armstrong, RC.; *J. Med. Chem*. **2004**, 47:4417-4426

[14] Flygare, J.A.; Fairbrother, W.J.; *Expert. Opin. Ther. Patents* **2010**, 20(2): 251-267

[15] Oost, T.K.; Sun, C.; Armstrong, R.C.; Al-assaad, A.S.; Bentz, S.F.; Deckwerth, T.L.; Ding, H.; Elmore, S. W.; Meadowns, R. P.; Olejniczak, E. T.; Oleksijew, A.; Oltersadorf, T.; Rosenberg, S.H.; Shoemaker, A. R.; Tomaselli, K. J.; Zou, H.; Fesik, S. W.; *J. Med. Chem*. **2004**, 47: 4417-4426

[16] Genentech, Inc. Pyrrolidine inhibitors of IAP. WO2006069063A1; **2005**

[17] Sun, H.; Nikolovska-Coleska, Z.; Yang, C-Y.; Qian, D.; Lu, J.; Qiu, S.; Bai, L.; Peng, Y.; Cai, Q.; Wang, S.; *Accounts of Chemical Research* **2008**, 41(10) : 1264:1277

[18] Li, L.; Thomas, R. M.; Suzuki, H.; De Brabander, J. K.; Wang, X.; Harran, P. G.; *Science***, 2004**, 305, 1471.

[19] Bertrand, M. J.; milutinovic, S.; Dickson, K.M.; Ho, W.C.; Boudreault, A.; Durkin, J.; Gillard, J. W.; Jaquith, J. B.; Morris, S. J.; Barker, P. A.; *Mol. Cell*, **2008**, 30, 689-700

[20] Sun, H.; Nikolovska-Coleska, Z.; Lu, J.; Meagher, J. L.; Yang, C.Y.; Qiu, S.; Tomita, Y.; Ueda, Y.; Jiang, S.; Krajewski, K.; Roller, P.P.; Stuckey, J.A.; Wang, S.; *J. Am. Chem. Soc*. **2007**, 129:15279-15294

[21] Tetralogic Pharmaceuticals Corporation. Dimeric IAP inhibitors. US7517906B2; **2006**

[22] Sun, H.; Nikolovska-Coleska, Z.; Lu, J.; Meagher, J. L.; Yang, C.Y.; Qiu, S.; Tomita, Y.; Ueda, Y.; Jiang, S.; Krajewski, K.; Roller, P.P.; Stuckey, J.A.; Wang, S*.; J. Am. Chem. Soc*. **2007**, 129:15279-15294

[23] Li, L.; Thomas, R. M.; Suzuki, H.; De Brabander, J. K.; Wang, X.; Harran, P. G.; *Science***, 2004**, 305, 1471.

[24] Huang, Y., Rich, R. L., Myszka, D. G., and Wu, H.; *J. Biol. Chem*. **2003**, 278, 49517-49522.

[25] Splan, K.E.; Allen, J.E.; McLendon, G.L.; *Biochemistry*, **2007**, 46, 11938-11944

[26] Pauling, L.; Corey, R.B.; Branson, H.R.; *PNAS*, **1951,** 37, 205-212

[27] Oost, T.K.; Sun, C.; Armstrong, R.C.; Al-assaad, A.S.; Bentz, S.F.; Deckwerth, T.L.; Ding, H.; Elmore, S. W.; Meadowns, R. P.; Olejniczak, E. T.; Oleksijew, A.; Oltersadorf, T.; Rosenberg, S.H.; Shoemaker, A. R.; Tomaselli, K. J.; Zou, H.; Fesik, S. W.; *J. Med. Chem*. **2004**, 47: 4417-4426

[28] Genentech, Inc. Pyrrolidine inhibitors of IAP. WO2006069063A1; **2005**

[29] Cohen, F; Alicke, B.; Elliott, L.O.; et al.; *J. Med. Chem*. **2009**, 52: 1723-1730

[30] Tetralogic Pharmaceuticals Corporation, IAP binding compounds. US7456209B2; **2005**

[31] Novartis AG. Organic compounds. WO2006133147A2; **2006**

[32] Bertrand, M. J.; milutinovic, S.; Dickson, K.M.; Ho, W.C.; Boudreault, A.; Durkin, J.; Gillard, J. W.; Jaquith, J. B.; Morris, S. J.; Barker, P. A.; *Mol. Cell*, **2008**, 30, 689-700

[33] Bertrand, M. J.; milutinovic, S.; Dickson, K.M.; Ho, W.C.; Boudreault, A.; Durkin, J.; Gillard, J. W.; Jaquith, J. B.; Morris, S. J.; Barker, P. A.; *Mol. Cell*, **2008**, 30, 689-700

[34] Bertrand, M. J.; milutinovic, S.; Dickson, K.M.; Ho, W.C.; Boudreault, A.; Durkin, J.; Gillard, J. W.; Jaquith, J. B.; Morris, S. J.; Barker, P. A.; *Mol. Cell*, **2008**, 30, 689-700

Chapter 3: Determination of the binding domain for Smac mimetics leads to the investigation of linker flexibility in divalent Smac mimetics

3.1 Introduction to caspase inhibition by XIAP-BIR domains

Research over the past several years has provided great insight into the mechanisms that regulate apoptosis.[1,2,3] As described in Section 1.4.2, a major point of regulation occurs at the initiator and effector caspases, procaspases-2,-8,-9, and -10 and procaspase-3,-6, and -7, respectively.[4] Caspase are initially synthesized as zymogens that have little or no enzymatic activity. However, once this pro-caspase is cleaved by an upstream protease the result leads to producing an active protein.[5] If this activated protein is not inhibited, other proteolytic cascades can be activated in a hierarchal fashion which ultimately induces apoptosis. Although the first level of caspase regulation occurs by controlling zymogen activation, the second and equally important level involves direct inhibition of active caspases, which is achieved by the inhibitor of apoptosis protein XIAP.[6]

In 1999 Deveraux et al.[7] demonstrated through structure-function analysis that two distinct domains, BIR2 and BIR3, in XIAP have the capability to suppress caspase activity. They established that the BIR3 domain, which binds directly to the carboxy-terminal of caspase-9 was responsible for this ability. In addition, subsequent studies showed that the second domain, BIR2, could also suppress the activity of caspase-3 and -7.[8,9,10] The BIR2 domain was shown to function by reversible and high-affinity binding to caspase-3 and caspase-7, with Ki values of 7×10^{-10} M and 2×10^{-10} M[11]

respectively. The consequence of this shielding, of the caspase surface, also prevents additional interaction with other caspase substrates; Figure 3.1.[12]

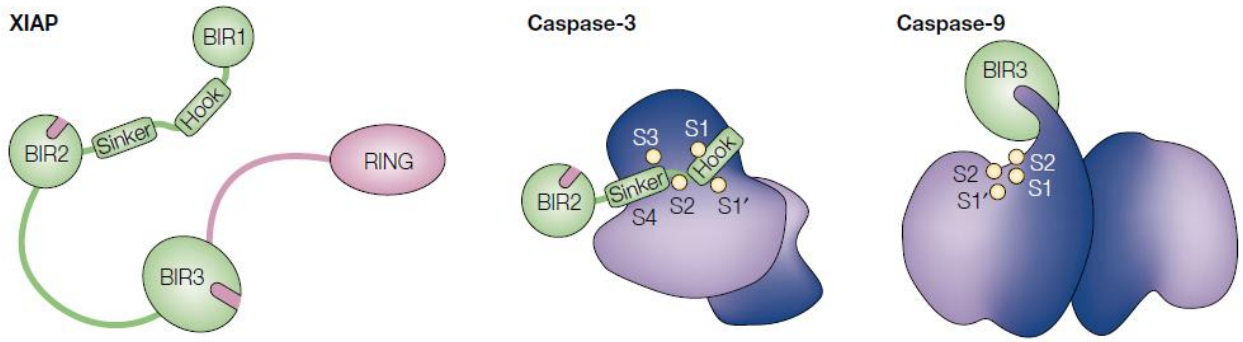

Figure 3.1. BIR2 and BIR3 domain of (a) XIAP, and its interaction with (b) caspase-3 (blue) and (c) caspase-9 (blue).[12]

3.2 Known inhibitors of apoptosis protein binding motifs

In humans, the response to apoptotic stimuli is the release of an IAP-interacting protein known as the second mitochondria-derived activator of caspase (Smac) along with Cytochrome-C from the inter-membrane space of the mitochondria, as previously described in Section 1.5.2.[13] Smac is thought to act as a negative regulator of IAPs, given that it can displace bound caspase's from the BIR domains in XIAP. Structural studies have provided significant insight into the mechanism by which Smac regulates IAP functionality.[14,15] These studies have indicated that Smac can bind two distinct regions of XIAP through an exposed amino-terminal motif that is homologous to that used by caspase-9, which binds to BIR3, thereby displacing bound caspase-9 from the

formed complex.[16] The significant similarity in the binding motifs of caspase-9 and Smac to XIAP is not limited to these two proteins alone, as shown in Figure 3.2. [17]

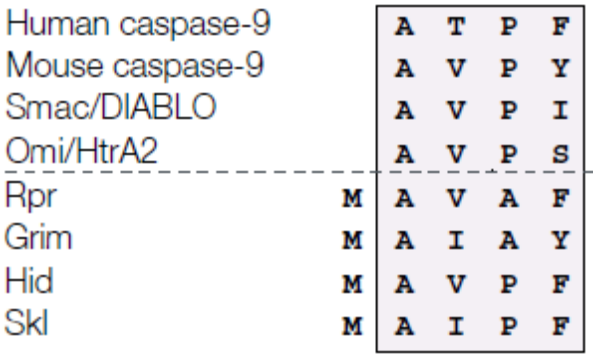

Figure 3.2 Other IAP-binding motifs with structural similarity to Smac.[19]

However, the exact means by which Smac binds to the BIR2 domain of XIAP is not completely understood. Salvasen and co-workers have revealed that a divalent Smac molecule is required to bind to BIR2, in order to inhibit XIAP.[18]

The studies described above demonstrate that although it is known that Smac binds to XIAP, further studies are required in order to develop much more effective mimetics. Undertaking such work could have considerable ramifications in the design of novel monovalent and divalent Smac mimetics, leading possibly to a cure for breast cancer.

3.3 Assessing the Smac-XIAP interaction

The ambiguity[19,20,21,22] as to how Smac is capable of inhibiting IAPs has caused much confusion over the past several years over the ideal target in XIAP. Data suggests, as described in Section 3.1, that both BIR2 and BIR3 domains do indeed bind to and sequester both initiator and effector caspases. Therefore, designing Smac mimetics which could interrupt these BIR-caspase interactions may perhaps allow such molecules to aid in the cure of breast cancer.

Over the past several years many groups[23,24,25] have developed their own theories as to whether binding occurs to BIR3 alone or to both BIR2 and BIR3 simultaneously. Considerable disagreement over this issue along with experimental evidence has lead to support both theories. However, majority of publications have strengthened the hypothesis that binding occurs solely to BIR3.

3.3.1 Evidence Supporting Simultaneous binding to BIR2 and BIR3 by Smac

In 2004 Li et al.[26] described the synthesis and properties of a small molecule Smac mimetic which had the ability to bind not only both BIR2 and BIR3 domains simultaneously, but as well the cellular inhibitors of apoptosis proteins 1 and 2 (cIAP-1 and -2) when used in conjunction with TNF-related apoptosis inducing ligand (TRAIL).

It is known that synthetic Smac peptides fused to cell-permeable peptides are capable of bypassing mitochondrial regulation and can make human cancer cells sensitive in culture, as well as tumour xenographs in mice.[27,28] Using cell permeable TRAIL with their Smac mimetics Li et al. were able to use this method as a synergistic

way to increase caspase activation, and thus induce apoptosis. Additionally, previous crystal structure work done with the Smac-BIR3 complex[29] has shown that the native tetrapeptide motif (AVPI) of Smac directly interacts BIR3, by contacting an existent three-stranded anti-parallel β-sheet. Using computer-simulated conformations and the knowledge gained from structure work by Wu et al., they designed and synthesized a library of non-peptidyl substituents for the C-terminus of the tetrapeptide. From this library, their oxazoline derivative (**24**) displayed the highest potency (Figure 3.3).

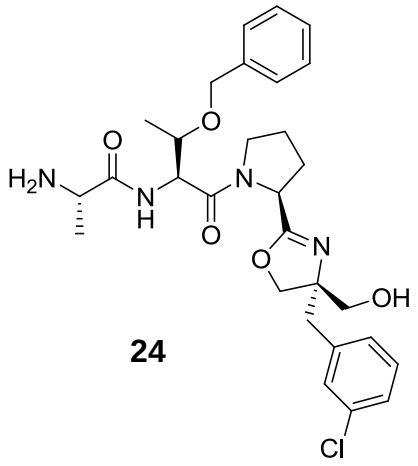

24

Figure 3.3 First active compound synthesized after use of computer simulation, oxazoline derivative.[30]

Although compound **24** did exhibit high potency it did not display higher activity than Alanine-Valine-Proline-Phenylalanine (AVPF), a tetrapeptide considered more active than native AVPI sequence for in-vitro studies.[31] In an effort to obtain a compound with even greater bioactivity, numerous structural modifications were performed on **24**. In the end compounds **9** and **16** (Figure 3.4) displayed the greatest activity.[32]

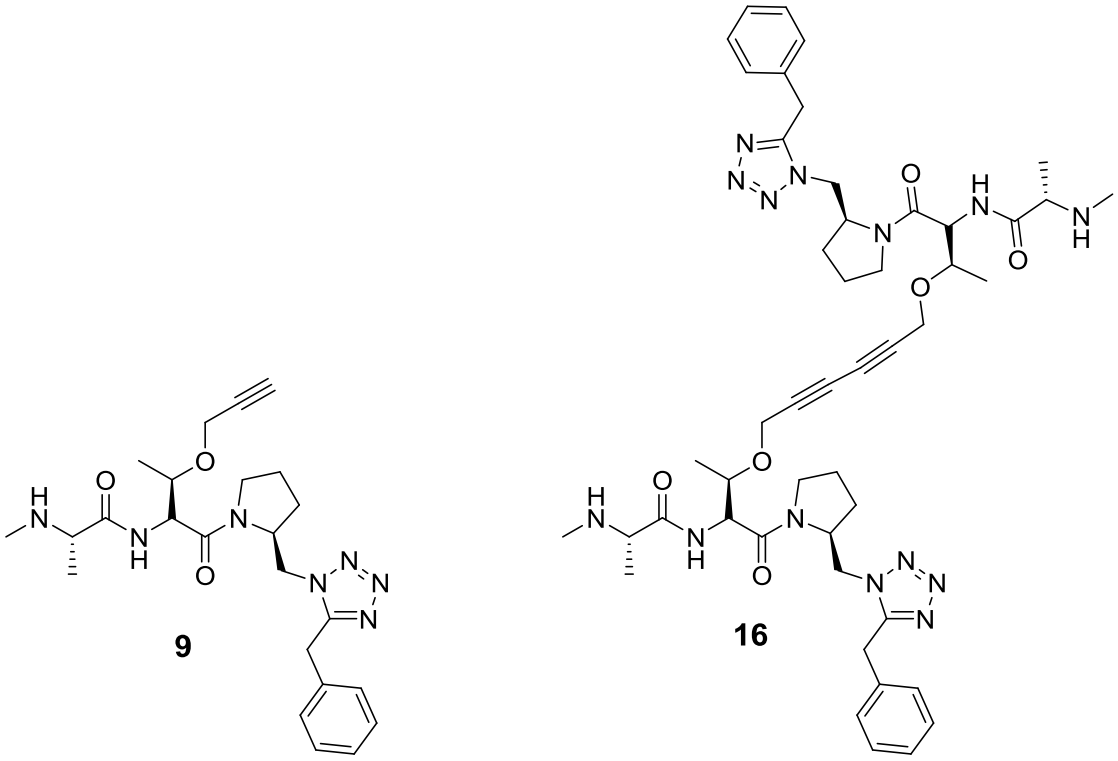

Figure 3.4 Potent tetrazoyl threonine-ethers synthesized numerous structural modifications were performed on **24**. [34]

Upon conducting a fluorescence polarization assay and polyacrylamide gel electrophoresis, the authors established that both compounds **9** and **16** had comparable binding affinities to the BIR3 domain. However, in a caspase-3 activation assay they determined that the divalent tetrazoyl threonie-ether mimetic **16** was significantly more active (Figure 3.5a and b). They attributed the increased bioactivity of **16** to the fact it was divalent and proposed it was able to interact with both BIR domains.[33]

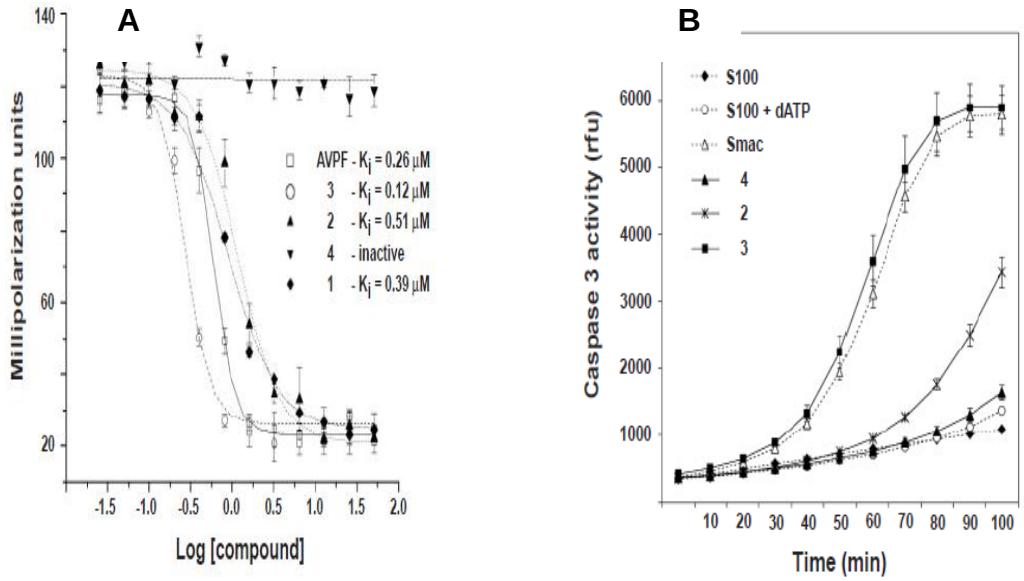

Figure 3.5. A) Fluorescence polarization assay for the interaction of Smac mimetic and BIR3. **B**) Time course comparison of caspase 3 activation by recombinant Smac.[35]

Additional testing of compound **16** against a Smac-XIAP complex was shown to disrupt the complex with a reported K_d value of ~300 pM. In contrast, compound **9** even in a fivefold excess gave no indication of disrupting the Smac-XIAP complex. Although Li et al. were able to conduct several experiments to strengthen their argument that divalent mimetics bind to both BIR domains, it is not clear as to whether the increased apoptotic activity observed was due to the enhancing effect of TRAIL on caspase-8. A control experiment was also conducted in the presence of TRAIL alone without compound **16** and no caspase-8 activity was noticed. However, the absence of active caspase-8 does not necessarily corroborate their idea that divalent Smac mimetics bind to both BIR domains and cause the induction of apoptosis.

In 2008 Nikolovska-Coleska et al.[34] published an article in which they had designed and synthesized a divalent Smac-based ligand **Smac-1** and its fluorescent labelled analogue **Smac-1F** (Figure 3.6). Both compounds **Smac-1** and **Smac-1F** were characterized for their interactions with different XIAP constructs.

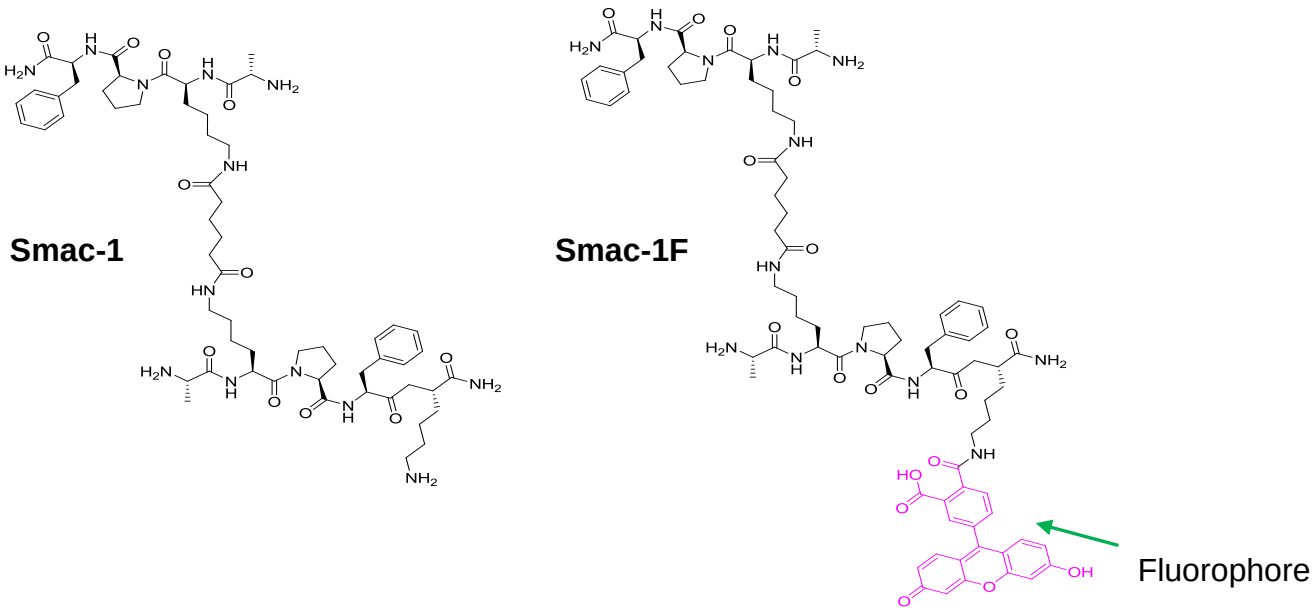

Figure 3.6. Smac-1 and **Smac-1F** as synthesized to determine BIR2-BIR3 binding.[34]

Using fluorescence polarization assays and gel filtration experiments they were able to investigate the interaction of the bivalent Smac mimetics, using the monvalent counterparts as controls.

The design of **Smac-1** and **Smac-1F** mimetics were based on previously known structural modifications[35,36] that enhanced binding affinity, which were then used to synthesize an AKPF-NH2 monomer and the subsequent dimer. Although a three-dimensional structure of XIAP containing both BIR2 and BIR3 domains has never been reported, Nikolovska-Coleska et al. predicted that the linker region between BIR2 and

BIR3 consisting of approximately 25 residues in length, was not well-defined for its secondary structure and should be quite flexible.[37] They hypothesised that their divalent mimetics, tethered via adipic acid therefore should be sufficient in length and flexibility to concurrently bind to both BIR domains simultaneously, and in the same XIAP molecule. Using a fluorescence polarization assay, to determine the binding affinities of **Smac-1F** to several different XIAP-constructs (BIR3, BIR2, and BIR2-BIR3), they were able to generate K_d values of each **Smac1F-XIAP** construct (Figure 3.7).

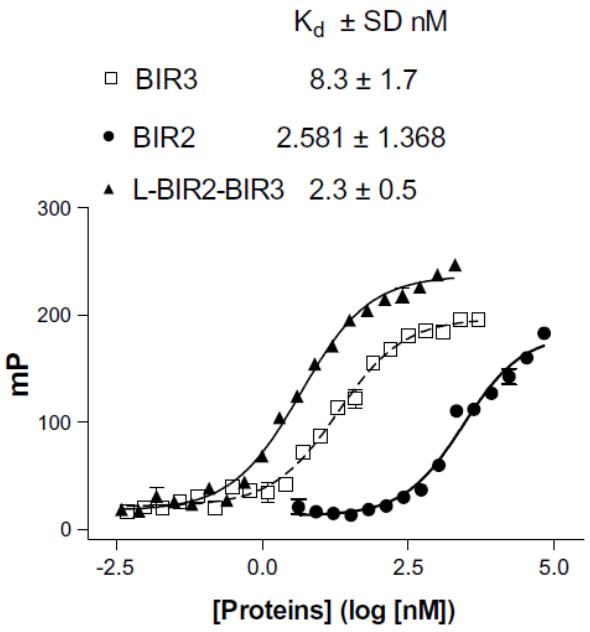

Figure 3.7. K_d values determined from saturation curves of three different XIAP-Smac1F complexes.[39]

From Figure 3.7 they concluded, based on the similarity of binding of **Smac-1F** to the three different BIR domains that **Smac-1F** may bind to both BIR2 and BIR3 domains using a similar binding mode.[38] The authors concluded that **Smac-1F** interacts concurrently with both the BIR domain in XIAP.

3.3.2 Evidence Supporting non-Simultaneous binding to BIR2 and BIR3 by Smac

In 2007 Splan et al.[39] published an article which refuted the idea that Smac mimetics could bind to both BIR2-BIR3 domains simultaneously, as published by Li et al.[40] In this work they compared the peptide binding site on the BIR3 domain and a truncated construct which included both BIR2 and BIR3 domains.

Using a fluorescent probe, they explored the hydrophobic nature of the binding site using compounds **25** and **26**, Figure 3.8. Their studies revealed that a significant change in the BIR3 binding site occurs when it is in close proximity to BIR2.

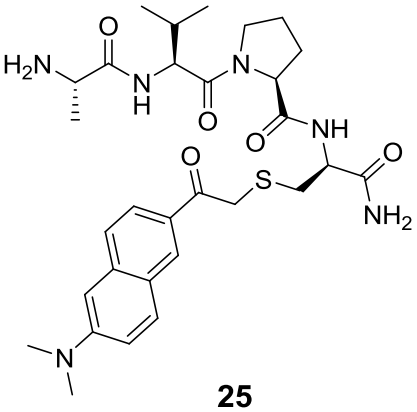

25

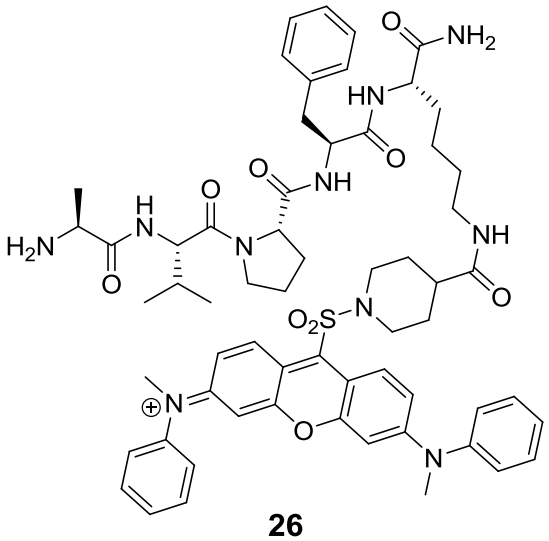

26

Figure 3.8. AVPC-badan (**25**) used in an earlier study to reflect the local polarity and rigidity of the binding site and AVPFK-QSY (**26**) used in 2007 study to help determine the distance between BIR2 and BIR3 through FRET measurements. [41]

Previous work done by the McLendon laboratory demonstrated that when **25** was bound to the BIR3 domain, the compound generated a fluorescence emission spectrum which reflected the local polarity and rigidity of the binding site.[42] While earlier studies have indicated that BIR3 is a more favourable binding site for Smac peptide mimetics relative to BIR2,[43] they hypothesized that the observed spectral difference could be a reflection of a binding distribution between both BIR2 and BIR3 sites. Consequently, they created a modified BIR2-BIR3 construct that contained a mutated BIR2 binding pocket in which the free cysteine residues were replaced by alanine and glycine.[44] When compound **25** was tested, a fluorescence spectrum equivalent to that of the un-mutated BIR2-BIR3 was observed, suggesting that BIR2 is not directly involved in binding.

While both BIR2 and BIR3 domains of XIAP have been isolated and characterized, their relative orientation to each other is unknown. To shed light onto this issue, fluorescent resonance energy transfer (FRET) measurements were employed to elucidate the distance between the binding pockets. Using a triple mutant construct[45] of BIR2-BIR3, where the BIR2 binding groove was labelled with a thiol specific fluorescent derivative and the BIR3 binding groove was labelled using the acceptor chromophore for fluorescence, they were able to synthesize compound **26.**[46] Upon conducting FRET measurements, the efficiency of energy transfer and the donor-acceptor distance yielded a site to site distance of 45 Å.[47] Molecular modeling of compound **20 (**Section 2.1.1), on the basis of the crystal structure of AVPI bound to BIR3,[48] revealed a distance of 26 Å[49] between the terminal alanine residues when in its extended conformation. Therefore the results presented by Splan et al. suggest that the distance between the

two sites, found to be 45 Å, is too far of a distance for a nine amino acid sequence to span, and the probability of a divalent mimetic binding to both BIR2 and BIR3 domains simultaneously is not likely. Thus, together with the fact that the mutant BIR2 of the BIR2-BIR3 mutant construct had similar binding affinities to native BIR2-BIR3 suggest that the BIR3 domain is the sole target of Smac based divalent mimetics.

Rationalization for increased binding affinity of the divalent mimetics has been attributed to the extended BIR2-BIR3 construct, which may provide some additional hydrophobic surface area. Thus, allowing greater interaction with additionally available hydrophobic residues on the dimer. This hypothesis is in agreement with previous observations that, although both divalent AVPI and AVPF mimetics have greater affinity than their monomeric counterparts, divalent AVPF binds more strongly than divalent AVPI.[50]

3.4 Investigation into Enhanced binding of Divalent Smac mimetics

Due to the controversy between whether divalent Smac peptides bind to BIR2-BIR3 or just BIR3 alone, we decided to investigate this issue further. Our first task was to synthesize the established binding sequence (MeAVPI) and compare our assay data with that reported in literature. Consequently, compounds **20** and **21** (Section 2.1.1) were synthesized by our laboratory as described in Scheme 3.1, and tested at the apoptosis center at the Children's Hospital of Eastern Ontario (CHEO) against a human MDA-MB-231 breast cancer cell line, Figure 3.9.

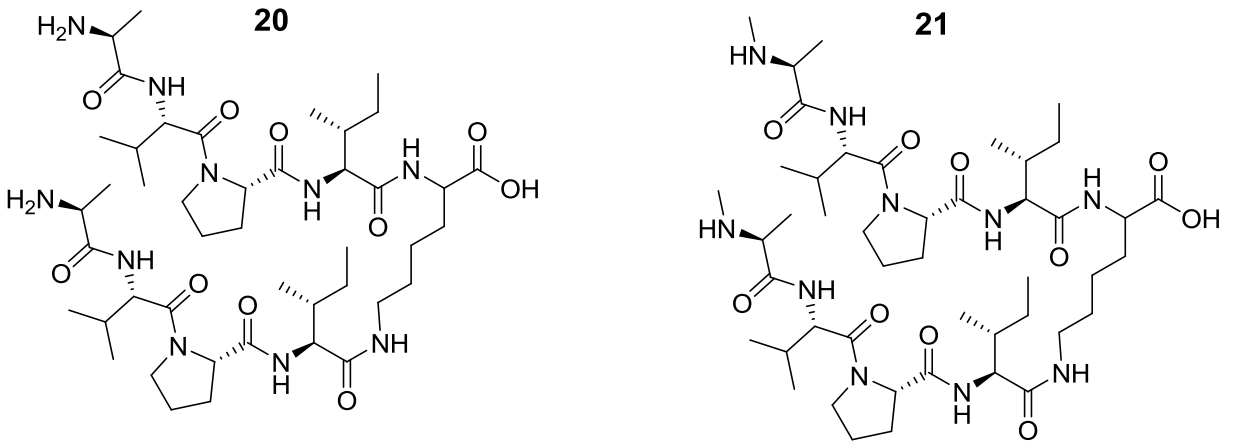

Figure 3.9. Synthesis of divalent AVPI (**20**) and MeAVPI (**21**) Smac mimetics built on a lysine linker.

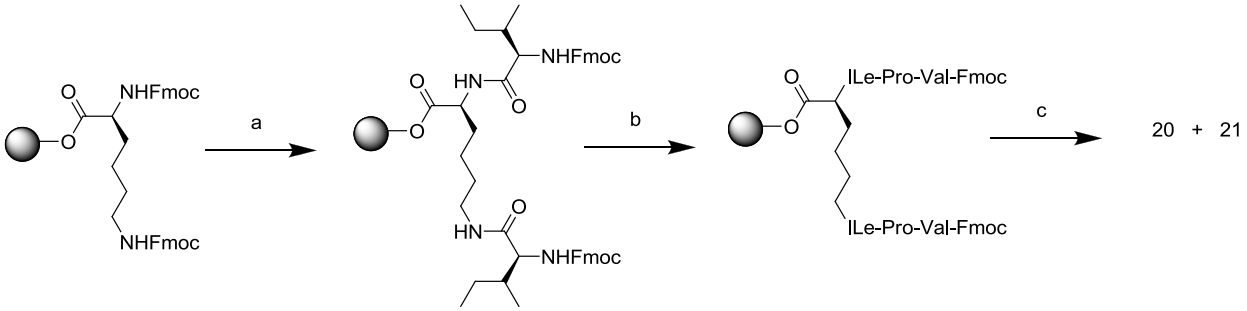

Scheme 3.1 Synthesis compounds **20** and **21** Reagents and conditions: (A) (a)(i) 20% piperidien in DMF, (ii) 1 cycle of Fmoc SPPS with HCTU/HOBT/DIPEA, (b)(i) 20% piperidien in DMF, (ii) 3 cycles of Fmoc SPPS with HCTU/HOBT/DIPEA, (c))(i) 20% piperidien in DMF, (ii) 1 cycle of Fmoc SPPS with HCTU/HOBT/DIPEA, and MeAlanine or Alanine

The compounds were then tested in conjunction with death ligands TRAIL and tumour necrosis factor alpha (TNF-α) (Figure 3.10) and against Aegera Therapeutics divalent AEG40730,[51] (**15**); Table 3.1.

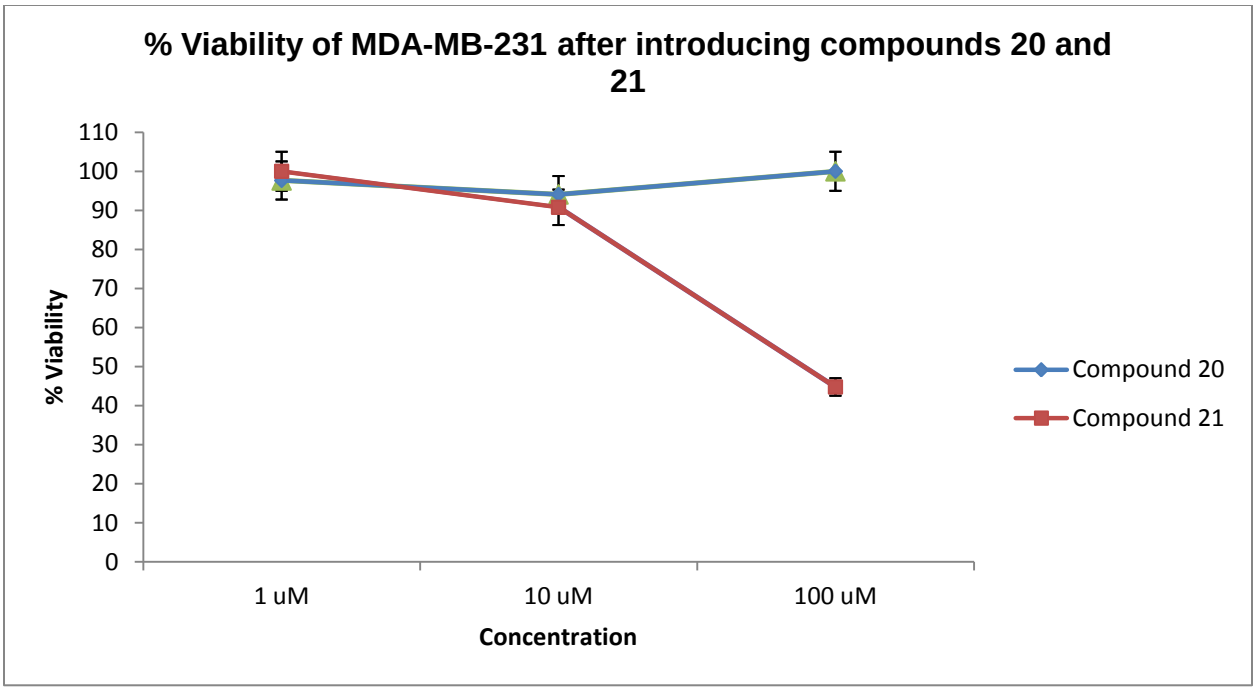

Figure 3.10 Viability of $(AVPI)_2K$ and $(MeAVPI)_2K$ when tested against human MDA-MB-2311 cancer cell line determined by Alamar blue assay.

The results from testing compounds **20** and **21** generated the expected difference in EC_{50} values. Compound **21**yielded an EC_{50} value of 90 μM while compound **21**, even at 100 μM, was unable to induce apoptosis. This further verifies previous studies of enhanced binding affinity when alanine is methylated.[52] Compound **21** was then further tested with death ligands TRAIL and TNF, Figure 3.10.

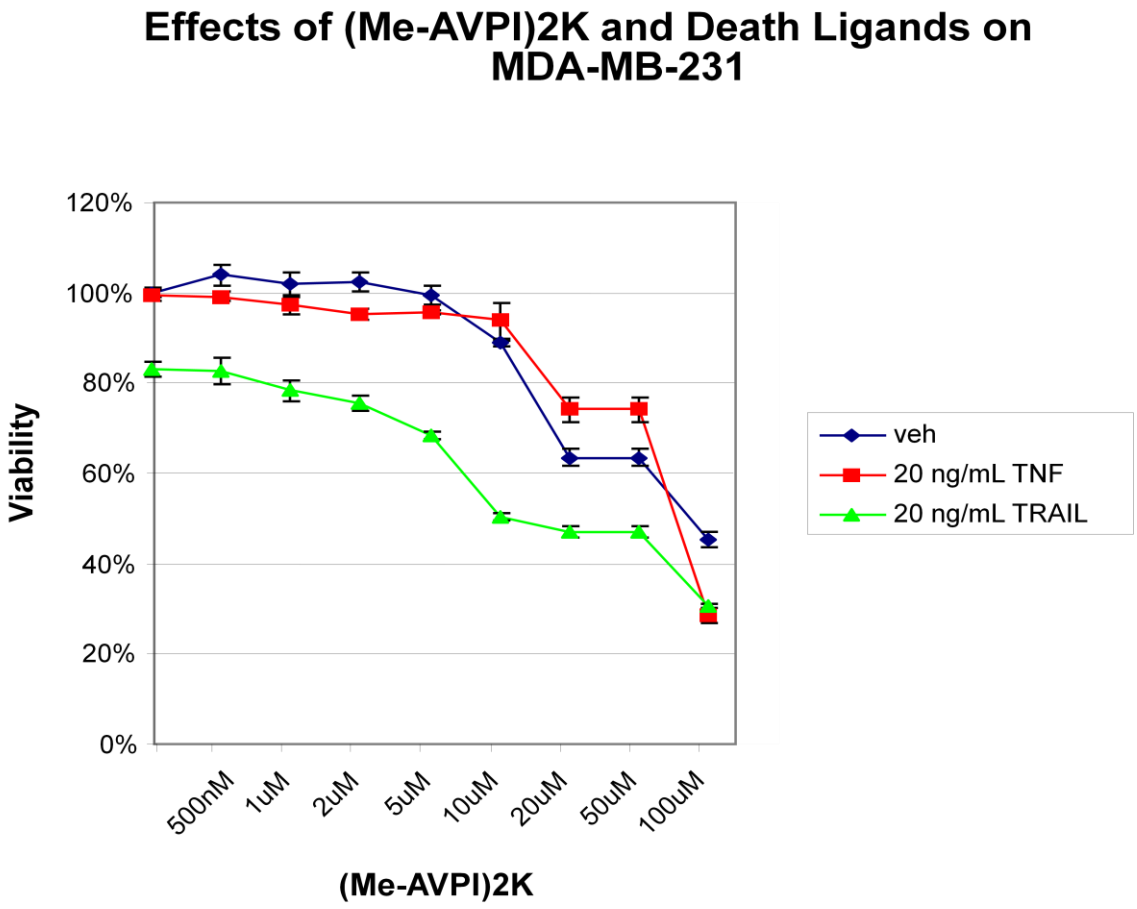

Figure 3.11. The effects of compound 21 and death ligands TRAIL and TNF on MDA-MB-231, vehicle (veh) used DMSO.

As described in Section 1.2.2, activation of the death machinery can occur via two pathways, the intrinsic and extrinsic pathways. The extrinsic pathway is initiated by ligation of transmembrane death receptors (Fas, TNF receptor, and TRAIL receptor) with their respective ligands (FasL, TNF, and TRAIL) to activate membrane-proximal caspases (caspase-8 and –10), which in turn cleave and activate effector caspases such as caspase-3 and –7.[53] Procaspase-8 is then recruited by its death effector domains (DED) to form what is known as the death-inducing signalling complex (DISC), which ultimately leads to cell death (Figure 3.11).

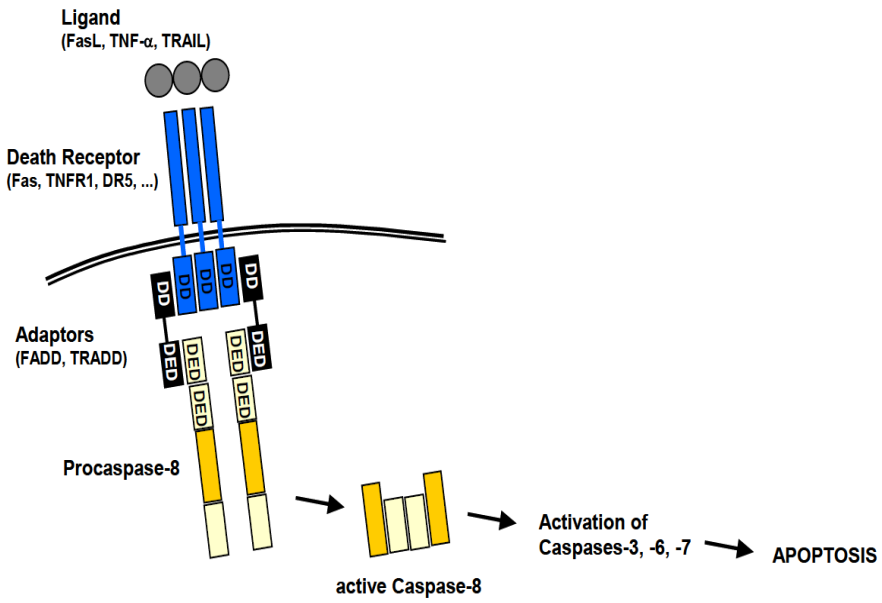

Figure 3.12. Receptor-mediated caspase-8 activation of DISC.[54]

To determine how effective compounds **20** and **21** were in-vitro for inducing apoptosis, the compounds were tested against compound **15;** known to have an IC_{50} value less than 10 nM[55] Table 3.1.

Table 3.1 Comparison in apoptotic activity of divalent Smac mimetics (**20, 21, 15**), in MDA-MB-231 cell line. Apoptotic activity is described as EC_{50} values determined by graph data extrapolation, and by cell morphology. Pink colour shows the non-methylated alanine; Green highlights Methylated-alanine.

Divalent Smac Mimetic	**IC_{50} Value (nM)**	**Representation of dead cells after 24 hours of compound introduction**
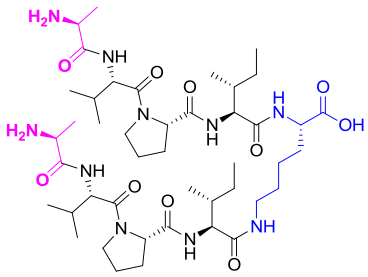 **20**	>1000	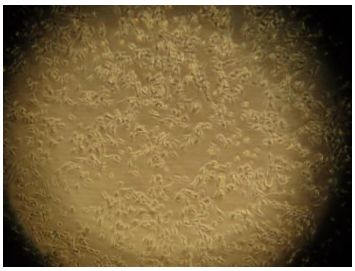
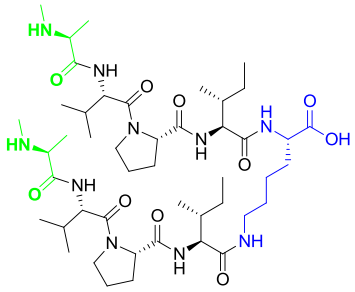 **21**	800	
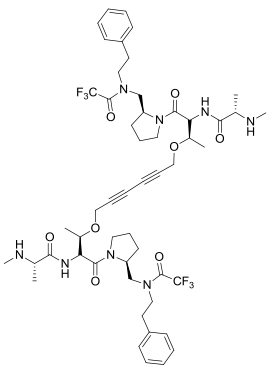 **15**	< 10	

Table 3.1 shows that we have been able to reproduce the apoptosis assay, and compared synthesized divalent peptides (**20, 21**) with the widely accepted apoptosis inducer, **15**.

3.4.1 Evaluating the Directional Nature of the Tetrapeptide Motifs in the Design of Divalent Smac Mimetics.

After verifying we could synthesize compounds to induce apoptosis we began to focus on tackling the issues in Section 3.3, whether binding occurred to both BIR2-BIR3 or alone to BIR3. We hypothesized that if we built two divalent mimetics containing the same tetrapeptide motif but had one of the motifs "reversed" (i.e. IPV(Me)A), the divalent mimetic with the reversed motif would have substantially less binding affinity for the BIR domains and decreased apoptotic activity. To test this theory, compounds **22** and **23** were synthesized by solid phase peptide synthesis, employing a MeAVPI-G-G-G-IPVAMe (forward-reverse) and a MeAVPI-G-G-G-MeAVPI (forward-forward) sequence (Figure 3.12).

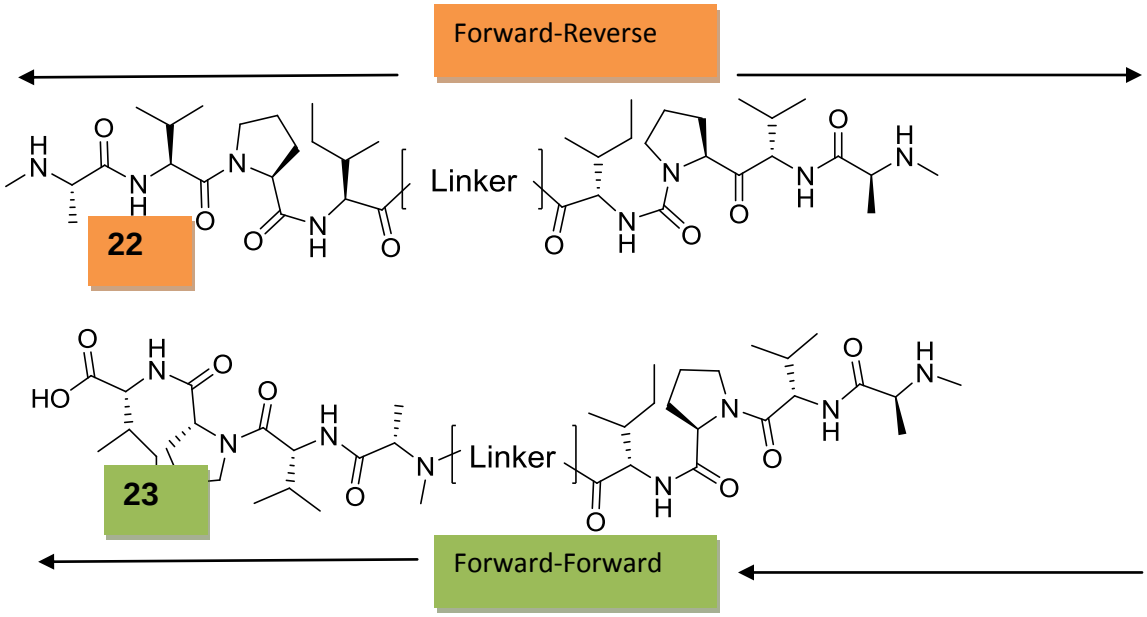

Figure 3.13 Divalent Smac mimetics built on a triglycine linker (linker = GGG) to help determine BIR domain binding targets. Compound **22** was synthesized in a forward-reverse sequence and compound **23** was synthesized in a forward-forward sequence.

Both compounds (**22**-**23)** were tested in-vitro on a human MDA-MB-231 breast cancer cell line, at the Children's Hospital of Eastern Ontario (CHEO) by Dr. Herman Cheung.

Surprisingly, Smac mimetics possessing the triglycine linker failed to exhibit any apoptotic activity independent of the nature or "direction" of the two AVPI sequences (Figure 3.13). This was unexpected as it had been previously reported that the nature of the tetrapeptide alone had a direct effect on apoptotic activity (Section 1.6.4). Based on this result we hypothesized that the reason for the lack of activity likely could be due to the rigid linker joining the two tetrapetide motifs, which might be hindering the peptides ability to "fit" into the binding pocket. To determine if the rigid triglycine linker was the reason for decreased apoptotic activity, we synthesized a library of analogues that possessed flexible linkers between the two tetrapeptide binding motifs. The flexible linkers chosen were gamma-Aminobutyric acid and L-Ornithine, done so to simplify

synthesis and allow equal distance between the two tetrapeptides. In some these analogues, amino acids at P2 and P4 were changed to ascertain how modifications to the native sequence affected binding and subsequent activity; as previously described in Section 1.6.2).

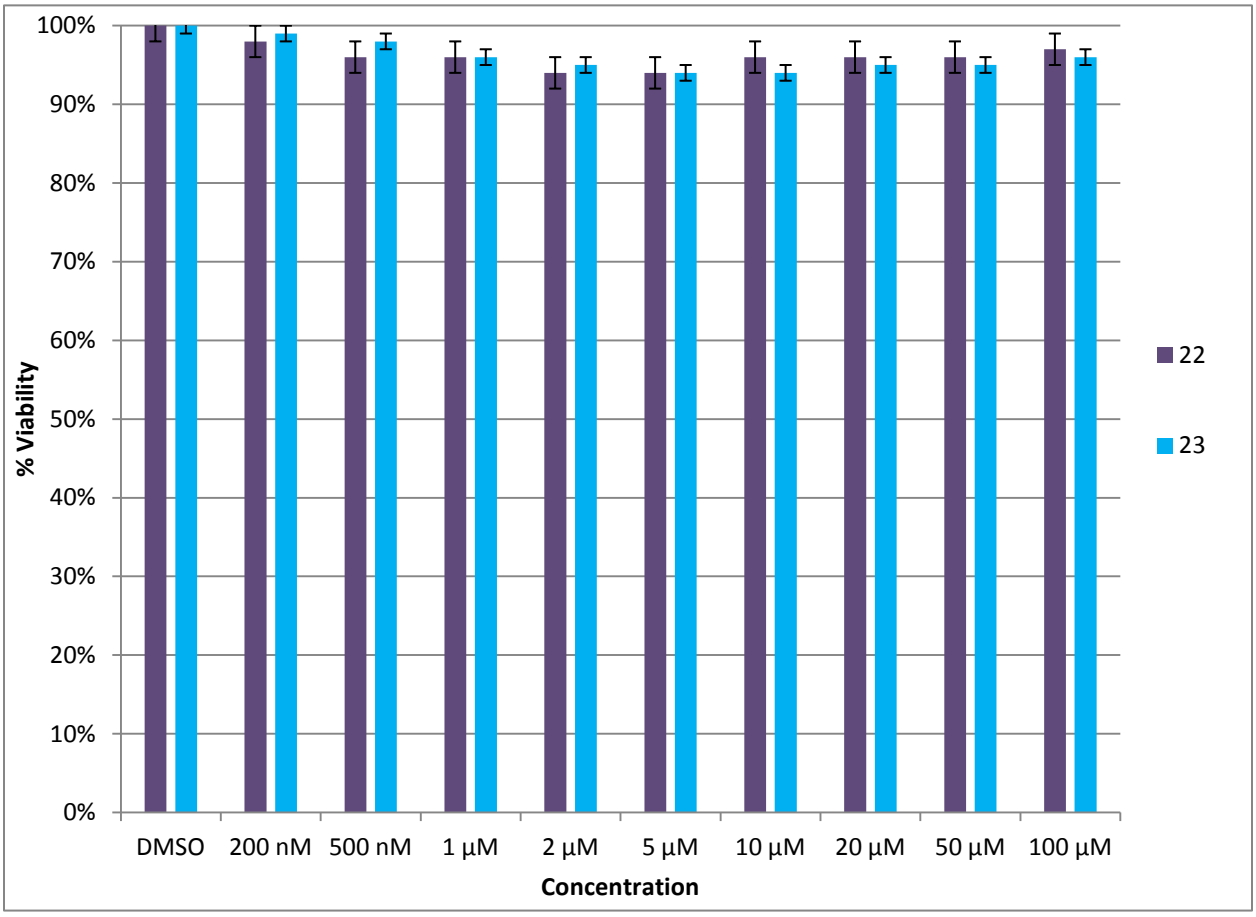

Figure 3.14. Triglycine linked divalent Smac mimetics show no ability to induce apoptosis at all ranges of compound concentrations (≥100 uM).

3.4.2 Synthesis of Ornithine and GABA tethered divalent mimetics

Synthesis of compound **20** was first prepared by Splan et al[56] and re-synthesized by our laboratories as shown above; as well as its N-terminus methylated version compound **21**. Before starting the synthesis of compounds **31** – **38,** both tethers had to be appropriately protected for synthesis on solid phase resin. The Fmoc-Orn(Boc)-OH linker had to be Boc deprotected using a 1:1 mitxure of TFA:DCM and re-protected with a Fmoc protecting group using 10% Na_2CO_3 and Fmoc-OSu;[57] (**27);** Scheme 3.1 (A). The free amine terminus on GABA was protected using 10% Na_2CO_3 and Fmoc-OSu (**28)**, with an overall yield of 84.71%; Scheme 3.2 (B).

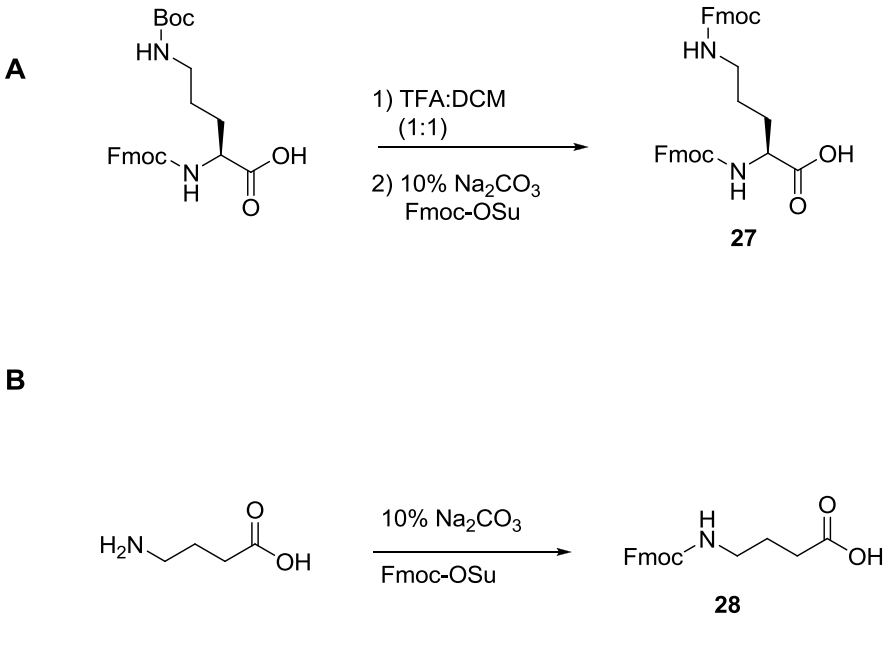

Scheme 3.2 Chemical modifications done to tethers used in synthesizing divalent Smac mimetics. (A)(i) 50% TFA in DCM, 15 min; (ii) 10% Na_2CO_3, 10 min; (iii) Fmoc-OSu, 30 min. (B) (i)10% Na_2CO_3, 10 min; (ii) Fmoc-OSu, 30 min.

The synthesis of compounds **31** to **38** were all conducted on an Apex 396 automated solid phase peptide synthesizer (SPPS) under inert argon atmosphere and in a 40-well Teflon reaction block; Scheme 3.3.

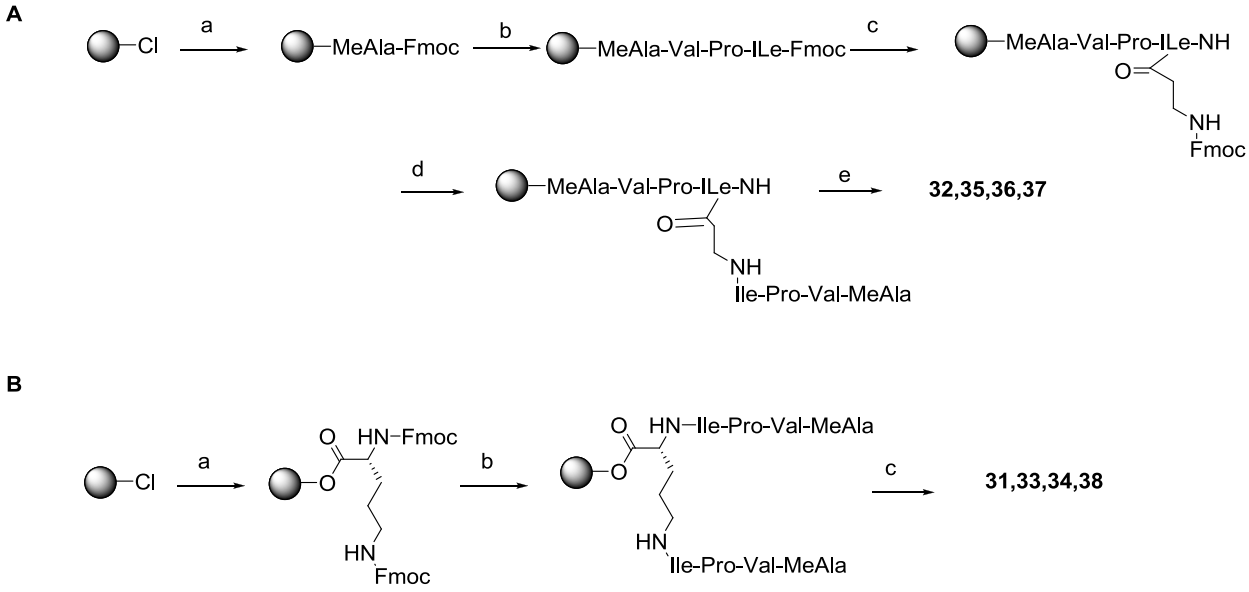

Scheme 3.3. Synthesis of divalent Smac mimetics **31** to **38**. Reagents and conditions: (A) (a)(i)HCTU/HOBT in DMF, (ii) DIPEA in DMF, 3 cycles, (b)(i) 20% piperidien in DMF, (ii) 3 cycles of Fmoc SPPS with HCTU/HOBT/DIPEA, (c) GABA, DIPEA, (d)(i) 20% piperidine in DMF, (ii) 4 cycles of Fmoc SPPS with HCTU/HOBT/DIPEA, (e) 95% TFA, 2.5% TIS, 2.5% H_2O. (B) (a)(i) DIPEA in DMF, 3 cycles, (b) (i) 20% Piperidine in DMF, (ii) 8 cycles of HCTU/HOBT/DIPEA in DMF, (c) 95% TFA, 2.5% TIS, 2.5% H_2O.

In order to build the methylated version of alanine, commercially available N-Boc-alanien was cyclised to furnish oxazolidinone (**29**), which was then reduced using TFA:DCM and triethylsilane affording N-methylalanine[58] (**30**) (Scheme 3.4).

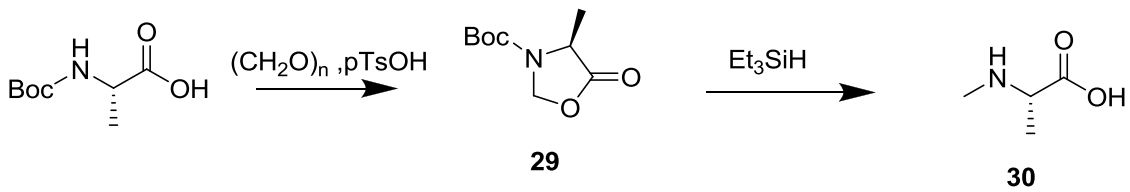

29 **30**

Scheme 3.4. Synthesis of N-methylalanie through the reduction of oxazolidinone.

3.4.3 Probing the Effects of Linker Rigidity

Given the precedent that divalent Smac mimetics have been documented to elicit an apoptotic response, we questioned the choice of the triglycine linker. The results suggested that the nature of the linker joining the tetra-peptide units had to have flexibility, in order for the divalent mimetics to bind with both BIR domains simultaneously in XIAP. In order to test this hypothesis, we substituted the triglycine linker with two flexible and freely rotatable alkyl linkers (Figure 3.14 **65** and **66**).

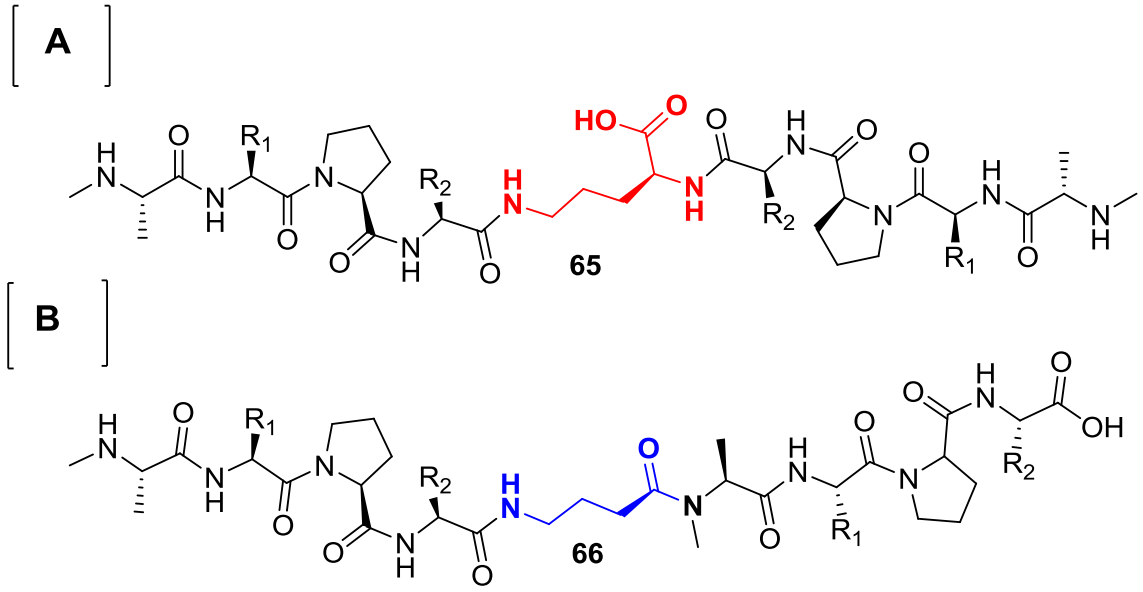

Figure 3.15. Representation of forward-reverse (**65**) sequence built on an Ornithine linker shown in red. Also a forward-forward sequence (**66**) built on a gamma-amino butyric acid (GABA) linker shown in blue. Sequences were built with variations at P2 and P4 (MeAXPX).

This hypothesis was confirmed when the triglycine linker was replaced with a more flexible one such as GABA or Ornithine, which resulted in EC_{50} values of 10 µM and 5 µM for compounds **31** and **35**, respectively (Figure 3.15). The SMAC mimetics in this study employed either a MeAVPI-linker-IPVAMe (forward-reverse) or MeAVPI-

linker-MeAVPI (forward-forward) sequence that possessed flexible linkers. Further modifications were then performed at P2 and P4 creating MeAXPX-linker-XPXAMe and MeAXPX-linker-MeAXPX divalent mimetics, where X represents another amino acid. Ornithine and GABA were utilized as linkers with more flexibility than the triglycine linker previously used.

Table 3.2 Structure of divalent Smac analogues **31-38** synthesized through solid phase peptide synthesis on either a GABA or Ornithine linker. The valine residue at P2 and isoleucine residue at P4 were substituted with a series of different amino acids.

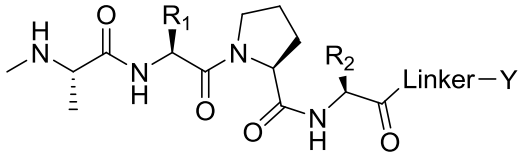

Compound	R1	R2	Linker	Y
31	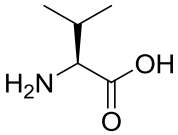	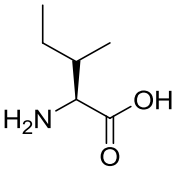	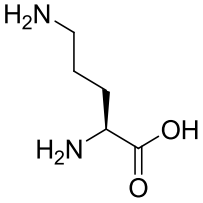	IPVA(Me)
32	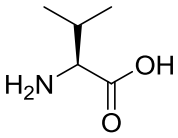	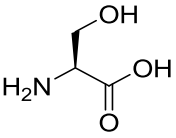	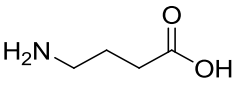	MeAVPS
33	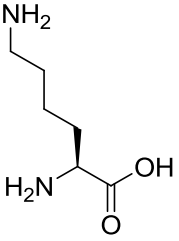	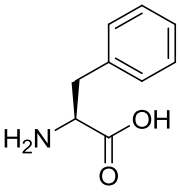	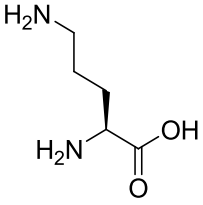	FPKA(Me)

34	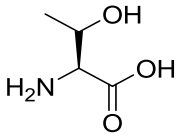	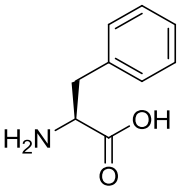	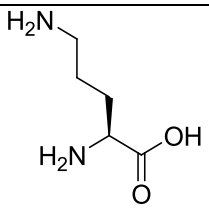	FPTA(Me)
35	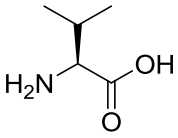	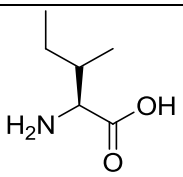	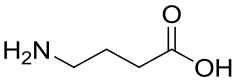	MeAVPI
36	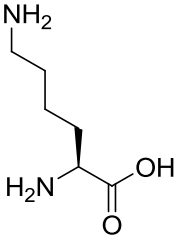	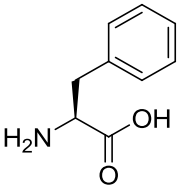	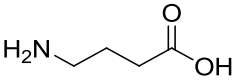	MeAKPF
37	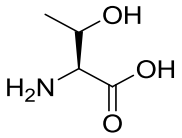	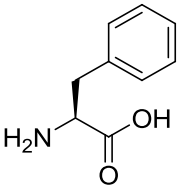	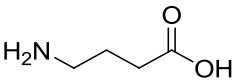	MeATPF
38	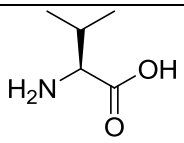	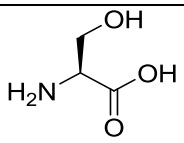	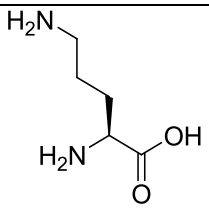	SPVA(Me)

All Smac mimetics were designed based upon the N-methyl-L-alanine (MeAla) residue at P1 which has been shown to be an essential structural feature.[59] This was achieved by coupling MeAla to four commercially available amino acids (lysine, serine, phenylalanine, and threonine) in positions two and four. Variations at P2 and P4 were chosen based on several known IAP-binding motifs hCasp9-p12, xCasp9-p12, and HtrA2.[60] Since these IAP-binding motifs are known to complex with BIR domains, which are stabilized by electrostatic interactions, the focus could then be on the linkers and not on whether the sequence was able to bind to the surface of the BIR domains. All eight divalent mimetics were designed to contain the same length carbon chain tether with four carbons via a GABA or Ornithine linkage. Previous literature reports have suggested that the structure and flexibility of linker was not essential as long as the tether was long enough to permit simultaneous binding to both BIR2 and BIR3 domains.[61] Our results demonstrate that the divalent Smac mimetics, linked either via ornithine or gamma-amino butyric acid (GABA) (**31** to **38**), had increased activity against cell proliferation relative to our first generation analogues **22** and **23**. We hypothesized that this is a result of these constructs not containing the ridged triglycine linker, which contains four amide linkages. Since a single amide bond provides a barrier to rotation that is ~23 kcal/mol[62] and greater than 65 kJ/mol for a Gly-Gly dipeptide, with a free energy difference between the *cis* and *trans* isomers of ΔG^{o}= 11.4 kJ/mol,[63] this ensures the linker is more “linear” than the other two linkers used.

As well, surprisingly all compounds (**31-38**) were able to induce apoptosis to some extent, indicating that the “direction” of synthesis of the divalent tetrapeptides does not seem to make a difference in overall activity.

To ensure that binding was indeed occurring to the BIR domain(s), we obtained the EC_{50} data generated by the monomeric tetrapeptide Smac mimetic **67** which was initially synthesized and tested by our group in 2008; Figure 3.16. Compound **67** displayed an EC_{50} value of 460 μM.

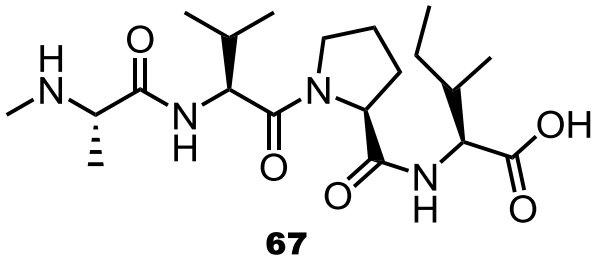

67

Figure 3.16. Compound **67**, synthesized in 2008, gave an EC_{50} value of 460μM.

3.4.4 Assessment of apoptotic activity of compounds **31** to **38**

The eight compounds were then tested in an MDA-MB-231 cell line either alone or with the addition of death ligand FasL, since FasL alone can initiate apoptosis and necrosis,[64] and the EC_{50} was determined by extrapolation of graph values after plotting from data generated through the Alamar Blue assay,[65] Figure 3.15 and Table 3.3. Using FasL alone at 10ng/ml resulted in 44% cell viability. Finally, the viability of the cell line was determined against each of the eight compounds using a serial dilution of the eight SMAC mimetics

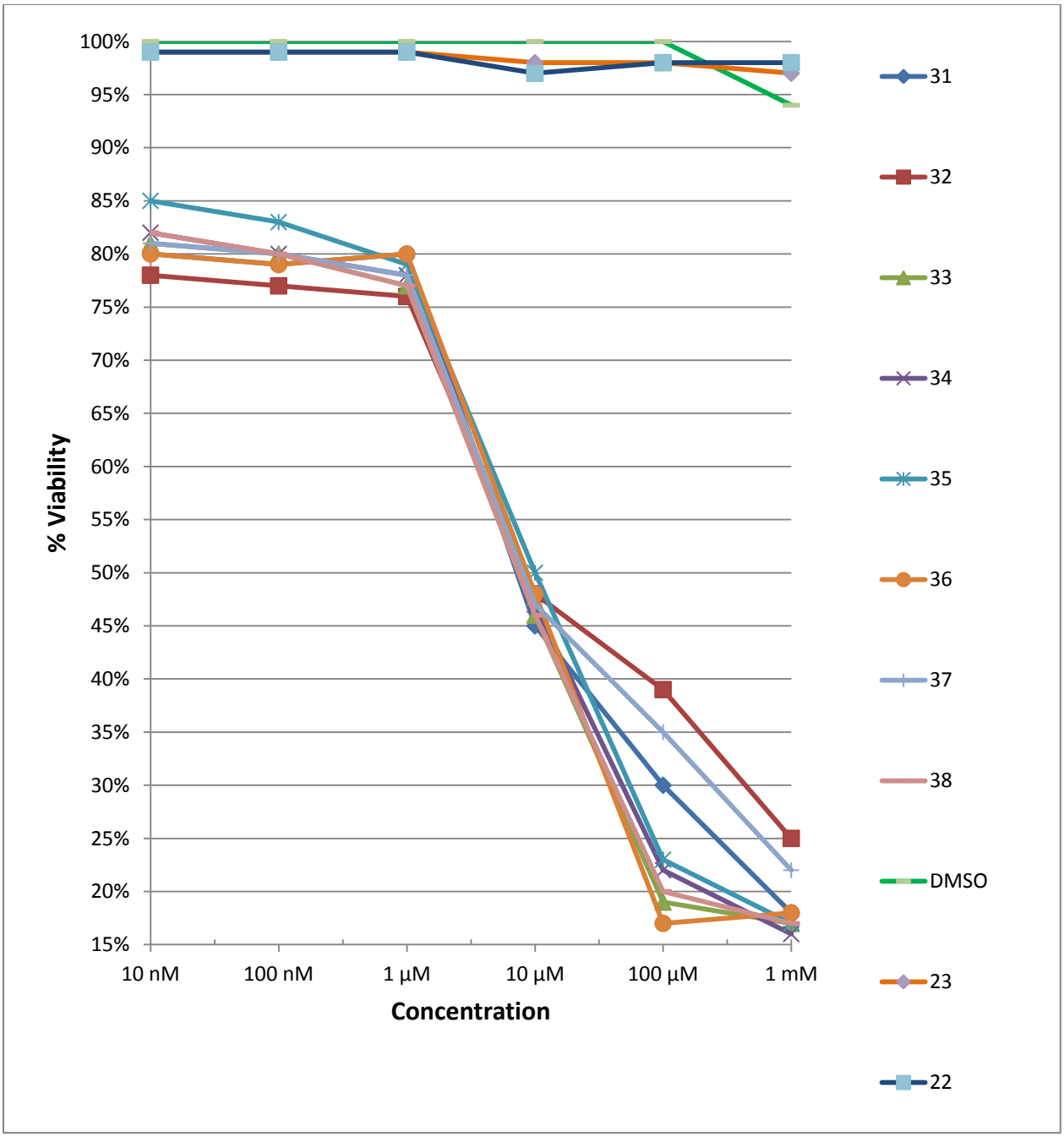

Figure 3.17. Determination of cell viability using divalent Smac mimetics synthesized on an Ornithine or GABA linker. Compounds were synthesized in either a forward-reverse or forward-forward sequence. An EC_{50} value for each compound was extrapolated from the graph above.

Table 3.3: EC_{50} values of **31-38** divalent Smac mimetics used with or without FasL death ligand. FasL alone gave 44% cell viability when used at 10ng/ml. Divalent mimetics built on triglycine linker shown below for comparison.

Compound	**Without Fas**	**With Fas 10ng/ml**
31	10 µM	80 nM
32	7 µM	85 nM
33	8 µM	100 nM
34	7 µM	100 nM
35	5 µM	100 nM
36	6 µM	100 nM
37	5 µM	100 nM
38	7 µM	85 nM
FasL	N/A	10ng/ml
22	>1 mM	N/A
23	**>1 mM**	**N/A**
67	460 µM	N/A

Lowest inhibitory concentration was observed with compound **35** (MeAVPI) concluded from graphical extrapolation, a direct analogue of the AVPI sequence found in the mitochondria, with the exception of the modification to the first amino acid alanine. All eight compounds, to our surprise, showed good activity with EC_{50} ranging from 5 uM to 10 uM (Table 3.3). A range which is > 46 times more potent than our monomer **67**. Testing the divalent tetra peptide with the triglycine amino acid spacer, under the same testing conditions, was unable to induce any apoptosis even at saturated concentrations. It was the results from the triglycine linker study that fuelled the current

study and led us to believe that flexibility was a key requirement for binding to occur to the BIR domains.

3.4.5 Likely target is the BIR3 binding site for Smac peptides

Compounds **31-38** emphasize the importance of designing divalent Smac mimetics which possess linkers that allow for conformational flexibility in order for increased binding to the BIR domains to occur. Whether divalent Smac mimetics are binding to both BIR2-BIR3 or solely to BIR3 in XIAP still remains unknown. Previous studies by McLendon et al.[66] demonstrated that the binding of a Smac mimetic dimer (Figure 3.1.6) is solely to BIR3 since the distance between BIR2 and BIR3 is 45 Å, making the binding to both highly unlikely.

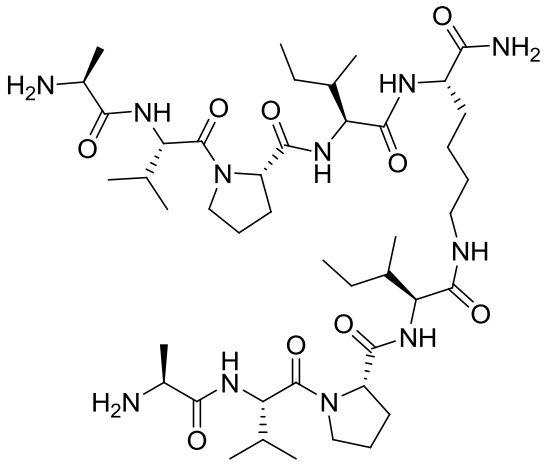

Figure 3.18 AVPI dimer built on a lysine backbone with a measured distance of 26 Å between terminal alanine residues when in an extended conformation and bound to BIR3.[66]

Smac mimetics **31 - 38** exhibit the same degree of activity in-vitro, and this is independent of the "direction" of the two AXPX sequences. This result suggests that

these analogues are not binding to both BIR2 and BIR3 of XIAP simultaneously in an intra-molecular fashion. The likely target is then BIR3, as proposed by McLendon. [67] The observation that a ridged linker is inactive could suggest that these molecules could bind to BIR3 domains of 2 different XIAP. Further studies are ongoing.

3.5 Chapter Summary

In review, this chapter has illustrated two key points. First the importance of linker structure in divalent Smac mimetics. Specifically, the linker must be flexible in nature to allow for binding between the divalent mimetics and BIR domains to occur. Based upon the in-vitro studies there is a fine balance between rigidity and flexibility.

Our initial investigation into Smac-BIR2/BIR3 and Smac-BIR3 binding had us hypothesizing that bivalent Smac mimetics synthesized in a forward-reverse sequence would provide the greatest binding affinity. Based on the result obtained from compounds **22** and **23** we conducted several new experiments. One new study focused on the flexibility of the linker as a key requirement for binding. Through the course of our investigation our hypothesis on this matter was proven correct.

Secondly, the initial investigation into the specificity of the "direction" of synthesis of the divalent tetrapetptides was proven incorrect. These results suggest that these analogues are likely not binding to both BIR2 and BIR3 of XIAP simultaneously in an intra-molecular fashion. The likely target is then BIR3, as proposed by McLendon. [68] The distance of 45 Å[69] between BIR2 and BIR3 is too great of distance for any divalent mimetic synthesized, which is less than 20 amino acid sequences in length.

References:

[1] Sun, H. S., J.A.; Nikolovska-Coleska, Z.; C-Y.; Xu, L.; Llu, M.; Tomita, Y.; Pan, H; Yoshioka, Y.; Krajewski, K.; Roller, P. P; Wang, S.; *J. Am. Chem. Soc.* **2004**, 126: 16686-16687.

[2] Oost, T. K. e. a. F., S. W.; *J. Med. Chem*. **2004**, 47: 4417-4426.

[3] Kipp RA, C. M., Wist AD, Cresson CM, Carrell M, Griner E, Wiita A, Albiniak PA, Chai J, ShiY, Semmelhack MF, McLendon GL.; *Biochemistry* **2002**, 41: 7344-7349.

[4] Michalke, M.; Stepczynska, A.; Bui, TN.; Loser, K.; Krzemieniecki, K.; Los, Marek. Madame Curie Bioscience Database – Caspases as Targets for drug development**.** Chapters taken from the Madame Curie Bioscience Database: Eurekah.com and Landes Bioscience and Springer Science+Business Media; **c2009**

[5] Nicholson, D. W.; *Cell Death Differ*. **1999**, 6, 1028–1042

[6] Liston, P. et al.; *Nature* **1996**, 379, 349–353

[7] Deveraux, Q. L. et al.; *EMBO* J. **1999**, 18, 5242–5251

[8] Huang, Y. et al.; *Cell* **2001**, 104, 781–790

[9] Riedl, S. J. et al.; *Cell* **2001**, 104, 791–800

[10] Chai, J. et al.; *Cell* **2001**, 104, 769–780

[11] Salvesen, G.S.; Duckett, C.S.; *Molecular Cell Bio*. **2002**, 3, 401-410

[12] Salvesen, G.S.; Duckett, C.S.; *Molecular Cell Bio*. **2002**, 3, 401-410

[13] Sun, H.; Stuckey, J.; Nikolovska-Coleska, Z.; Quin, D.; Meagher, J.; Qiu, S.; Lu, J.; Yang, CY.; Saito, NG.; Wang, S.; *J. Med. Chem*., **2008**, 51 (22), pp 7169–7180

[14] Chai, J. et al.; *Nature* **2000**, 406, 855–862

[15] Wu, G. et al.; *Nature* **2000**, 408, 1008–1012

[16] Salvesen, G.S.; Duckett, C.S.; *Molecular Cell Bio*. **2002**, 3, 401-410

[17] Salvesen, G.S.; Duckett, C.S.; *Molecular Cell Bio*. **2002**, 3, 401-410

[18] Salvesen, G.S.; Duckett, C.S.; *Molecular Cell Bio*. **2002**, 3, 401-410

[19] Sun, H. S., J.A.; Nikolovska-Coleska, Z.; C-Y.; Xu, L.; Llu, M.; Tomita, Y.; Pan, H; Yoshioka, Y.; Krajewski, K.; Roller, P. P; Wang, S.; *J. Am. Chem. Soc.* **2004**, 126: 16686-16687..

[20] Kipp RA, C. M., Wist AD, Cresson CM, Carrell M, Griner E, Wiita A, Albiniak PA, Chai J, ShiY, Semmelhack MF, McLendon GL.; *Biochemistry* **2002**, 41: 7344-7349.

[21] Riedl, S. J. et al.; *Cell* **2001**, 104, 791–800

[22] Li, L.; Thomas, R.M.; Suzuki, H.; De Brabander, J.K.; Wang, X.; Harran, P.; *Science* **2004**, 305: 1471-1474

[23] Li, L.; Thomas, R.M.; Suzuki, H.; De Brabander, J.K.; Wang, X.; Harran, P.; *Science* **2004**, 305: 1471-1474

[24] Li, L.; Thomas, R.M.; Suzuki, H.; De Brabander, J.K.; Wang, X.; Harran, P.; *Science* **2004**, 305: 1471-1474

[25] Liu, Z., Sun, C., Olejniczak, E. T., Meadows, R. P., Betz, S. F., Oost, T., Herrman, J., Wu, J. C., and Fesik, S. W.; *Nature* **2000**, 408, 1004-1008.

[26] Li, L.; Thomas, R.M.; Suzuki, H.; De Brabander, J.K.; Wang, X.; Harran, P.; *Science* **2004**, 305: 1471-1474

[27] Fulda, S.; Wick, W.; Weller, M.; Debatin, K.M.; *Nat. Med*. **2002**, 8, 808

[28] L. Yang *et al*.; *Cancer Res. **2003**,* 63, 831

[29] G. Wu et al., Nature **2000**, 408, 1008

[30] Li, L.; Thomas, R.M.; Suzuki, H.; De Brabander, J.K.; Wang, X.; Harran, P.; *Science* **2004**, 305: 1471-1474

[31] Z. Liu et al., Nature **408**, 1004 (2000)

[32] Li, L.; Thomas, R.M.; Suzuki, H.; De Brabander, J.K.; Wang, X.; Harran, P.; *Science* **2004**, 305: 1471-1474

[33] Li, L.; Thomas, R.M.; Suzuki, H.; De Brabander, J.K.; Wang, X.; Harran, P.; *Science* **2004**, 305: 1471-1474

[34] Z. Nikolovska-Coleska et al.; Anal. Biochem. **2008**, 374, 87-98

[35] Kipp RA, C. M., Wist AD, Cresson CM, Carrell M, Griner E, Wiita A, Albiniak PA, Chai J, ShiY, Semmelhack MF, McLendon GL.; *Biochemistry* **2002**, 41: 7344-7349.

[36] Wu, G.; Chai, J.; Suber, T.L.; Wu, J.W.; Du, C.; Wang, X.; Shi, Y.; *Nature* **2000**, 408 : 1008–1112.

[37] Z. Nikolovska-Coleska et al.; Anal. Biochem. **2008**, 374, 87-98

[38] Z. Nikolovska-Coleska et al.; Anal. Biochem. **2008**, 374, 87-98

[39] Splan, KE.; Allen, JE.; Mclendon, GL.; *Biochemistry*, **2007**, 46 11938-11944

[40] Li, L.; Thomas, R.M.; Suzuki, H.; De Brabander, J.K.; Wang, X.; Harran, P.; *Science* **2004**, 305: 1471-1474

[41] Splan, KE.; Allen, JE.; Mclendon, GL.; *Biochemistry*, **2007**, 46 11938-11944

[42] Kipp RA, C. M., Wist AD, Cresson CM, Carrell M, Griner E, Wiita A, Albiniak PA, Chai J, ShiY, Semmelhack MF, McLendon GL.; *Biochemistry* **2002**, 41: 7344-7349.

[43] Liu, Z., Sun, C., Olejniczak, E. T., Meadows, R. P., Betz, S. F., Oost, T., Herrman, J., Wu, J. C., and Fesik, S. W.; *Nature* **2000**, 408, 1004-1008.

[44] Wu, G.; Chai, J.; Suber, T.L.; Wu, J.W.; Du, C.; Wang, X.; Shi, Y.; *Nature* **2000**, 408 : 1008–1112.

[45] Sun, C., Cai, M., Gunasekera, A. H., Meadows, R. P., Waant, H., Chen, J., Zhang, H., Wu, W., Xu, N., ng, S. C., and Fesik, S. W.; *Nature* **1999,** 401, 818-822.

[46] Splan, KE.; Allen, JE.; Mclendon, GL.; *Biochemistry*, **2007**, 46 11938-11944

[47] Splan, KE.; Allen, JE.; Mclendon, GL.; *Biochemistry*, **2007**, 46 11938-11944

[48] Wu, G.; Chai, J.; Suber, T.L.; Wu, J.W.; Du, C.; Wang, X.; Shi, Y.; *Nature* **2000**, 408 : 1008–1112.

[49] Splan, KE.; Allen, JE.; Mclendon, GL.; *Biochemistry*, **2007**, 46 11938-11944

[50] Splan, KE.; Allen, JE.; Mclendon, GL.; *Biochemistry*, **2007**, 46 11938-11944

[51] Bertrand, M. J.; milutinovic, S.; Dickson, K.M.; Ho, W.C.; Boudreault, A.; Durkin, J.; Gillard, J. W.; Jaquith, J. B.; Morris, S. J.; Barker, P. A.; *Mol. Cell*, **2008**, 30, 689-700

[52] Flygare, J.A.; Fairbrother, W.J.; *Expert. Opin. Ther. Patents* **2010**, 20(2): 251-267

[53] Algeciras-Schimnich, A., Barnhart, B.; Peter, M.. **Madame Curie Bioscience Database – Apoptosis.** Chapters taken from the Madame Curie Bioscience Database: Eurekah.com and Landes Bioscience and Springer Science+Business Media; c2009

[54] Gewies, A.; (**2003**). Introduction to Apoptosis. Apo Review, Cell death

[55] Bertrand, M. J.; milutinovic, S.; Dickson, K.M.; Ho, W.C.; Boudreault, A.; Durkin, J.; Gillard, J. W.; Jaquith, J. B.; Morris, S. J.; Barker, P. A.; *Mol. Cell*, **2008**, 30, 689-700

[56] Splan, KE.; Allen, JE.; Mclendon, GL.; *Biochemistry*, **2007**, 46 11938-11944

[57] Reiriz, C.; Castedo, L.; Granja, J.; *J. Pept. Sci*. **2008**, 14 (2): 241-249

[58] Freidiner, R.; *J. Org. Chem*. **1983**, 48, 77

[59] Kipp RA, C. M., Wist AD, Cresson CM, Carrell M, Griner E, Wiita A, Albiniak PA, Chai J, ShiY, Semmelhack MF, McLendon GL.; *Biochemistry* **2002**, 41: 7344-7349.

[60] Flygare, J.A.; Fairbrother, W.J.; *Expert. Opin. Ther. Patents* **2010**, 20(2): 251-267

[61]Splan, KE.; Allen, JE.; Mclendon, GL.; *Biochemistry*, **2007**, 46 11938-11944

[62] Kang, Y.K.; Park, H.S.; *J. Molecular Structure* **2004**, 676: 171-176

[63] Scherer, G.; Kramer, M.L.; Schutowski, M.; Reimer, U.; Fischer, G.; *J. Am. Chem. Soc*.**1998**, 120: 5568-5574

[64] Matsumura, H.: Shimizu, Y.; Ohsawa, Y. et al.; *J Cell Biol*. **2000,** 151: 1247-1256

[65] Nakayama,GR.; Caton, MC.; Nova, MP.; Parandoosh,Z.; *J. Immunol Methods*. **1997**, 2 (204), 205-208

[66] Splan, KE.; Allen, JE.; Mclendon, GL.; *Biochemistry*, **2007**, 46 11938-11944

[67] Splan, KE.; Allen, JE.; Mclendon, GL.; *Biochemistry*, **2007**, 46 11938-11944

[68] Splan, KE.; Allen, JE.; Mclendon, GL.; *Biochemistry*, **2007**, 46 11938-11944

[69] Splan, KE.; Allen, JE.; Mclendon, GL.; *Biochemistry*, **2007**, 46 11938-11944

Chapter 4: Design, Synthesis and Evaluation of monovalent Smac mimetics-modified exclusively at P4

4.1 Structure Activity Relationship of Smac mimetics on Inducing Apoptosis when Modified at Residue 2 and 4

As seen in Section 1.6.2, modifications on the native Smac tetrapeptide motif at positions P2 and P4 significantly increases the apoptotic activity of the peptide.

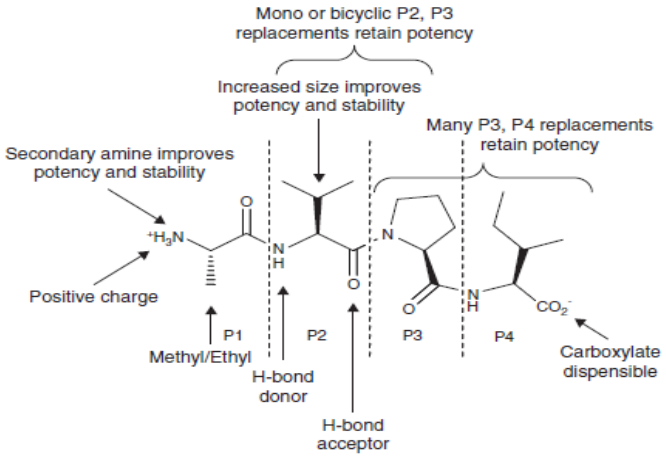

It has been shown by several laboratories that the side chain at P2 has no interactions with the BIR domains itself but is suspended in the cytosol,[1] and substantial structural modifications have been done at this position in order to improve potency. [2] Substitution of the isoleucine at P4 is also tolerated, provided hydrophobic moieties are utilized. [3]

In 2008 Bertrand et al. used the N-terminal tetrapeptide Ala-Thr-Pro-Phe (ATPF) motif found in caspase-9 as a template for the development of new XIAP antagonists.[4] It was discovered that the following structural modifications resulted in the

synthesis of compound **10,** which has high affinities to various BIR3 domains: (i) methylation of the N-terminal alanine, (ii) substitution of P2 with a bulky and hydrophobic non-natural amino acid, containing a tert-butyl side chain, and (iii) substitution of the P4 substituent with a tertiary amine. The binding affinities of compound towards BIR3 domains in XIAP, cIAP1 and cIAP2 gave EC_{50} values of 1059 nM, 49 nM, and 86 nM respectively.[5]

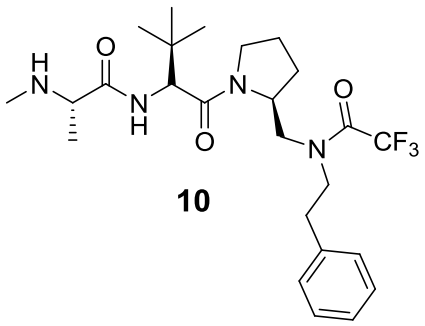

10

To further enhance the binding affinity of **10**, substitution at P2 with a propargyl-threonine and subsequently dimerization (**15)** resulted in increased binding affinities with EC_{50} values of 100 nM, 17 nM , 34 nM for XIAP, cIAP1 and cIAP2, respectively. In all cell lines reported[6] that responded to compound **15,** the half-maximal concentration for cell death was observed to be around 5 nM.

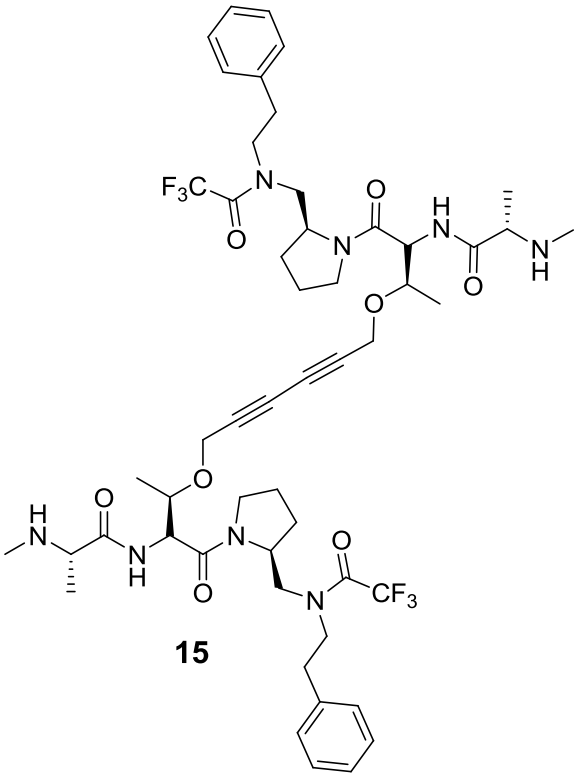

15

Despite the enhanced potencies observed in **10** and **15** compared to previous generations of Smac mimetics, we were interested in rationally designing, synthesizing, and testing novel monovalent Smac mimetics that had greater potency in bioactivity, as well simpler to synthesize in large scale. To address the latter issue, we decided upon the use of propargyl glycine (PAG) instead of the more sterically demanding propargyl threonine found at P2, in **15**. To simplify matters and synthesis, we decided to focus on first synthesizing the monovalent compounds.

As it has been shown previously, the bioactivity of Smac mimetics can decrease, increase, or stay the same based upon the structural modifications at the fourth residue (P4).[7] Since modifications at the fourth residue are well tolerated, we hypothesized that P4 would be the optimal position to modify and incorporate structural moieties that

possess unique properties known to enhance bioactivity.[8,9,10,11,12] Taking the above into consideration we were able to synthesize a library of novel Smac mimetics (Table 4.1).

Table 4.1. A diverse library of monovalent Smac mimetics synthesized based on structural modifications at P4.

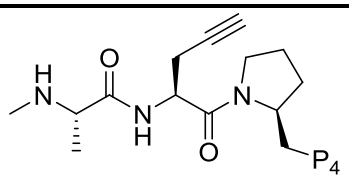

Compound	P4
39	**I**
40	**F**
41a	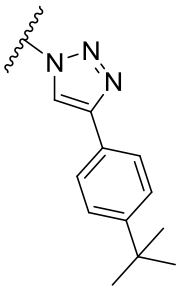
41b	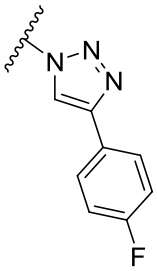
41c	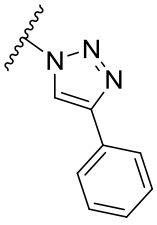

42	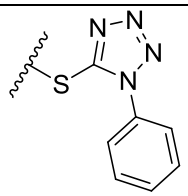
43	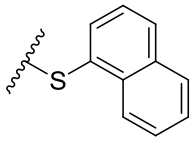
44	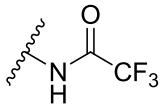
45	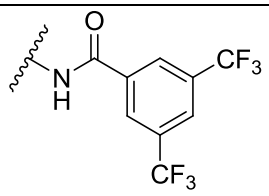

In an attempt to increase cell permeability of these analogues and therefore increase bioactivity, halogens were incorporated at P4 (**40** and **41b**). It has been shown that substitution of halogens generally increases cell permeability, decrease the H-bonding capabilities and polarity of the molecule, which then increases it lipophlicity.[13,14]

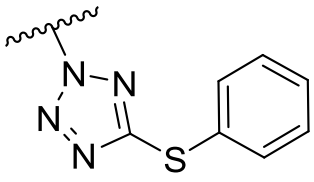

Figure 4.1. Tetrazoyl-thiophenyl moiety synthesized by Li et al. in the design of a potent Smac mimetic.[15]

Second, as shown in Section 3.3.1., previous work by Li et al.[15] demonstrated that a tetrazoyl thiophenyl moiety (Figure 4.1) exhibited potent activity when incorporated into Smac mimetics. However, the exact mechanism of action of these molecules is unclear. Therefore, we were interested in synthesizing and testing its derivatives (**41a-c**, **42**, Table 4.1).

An additional consideration, to enhance the overall bioactivity of Smac mimetics, was to decrease detection by proteases. Since protease enzymes cause proteolysis of peptide bonds that link amino acids together, the use of the napthanthiol moiety (**43)** would allow for the formation of a thioether which could "hide" the molecule from protease degradation.

Lastly, as the exact mechanism of action for potent analogues **10** and **15** was unclear, we were interested in investigating the role of the 2-phenylethylamine substituent of these compounds. This was achieved by the synthesis of compound **44**, which resembles **10** at P4, but lacked the phenylethyl component. In addition, we were also interested in designing a novel molecule that possessed both aromaticity and the trifluoromethyl substituents, which are present in both **10** and **15** at P4. In doing so led to the design and synthesis of compound **45**, which contained a 3,5-Bis(trifluoromethyl) benzoic acid component.[16]

4.2. Our Initial attempt at the Synthesis of compounds **39-45**

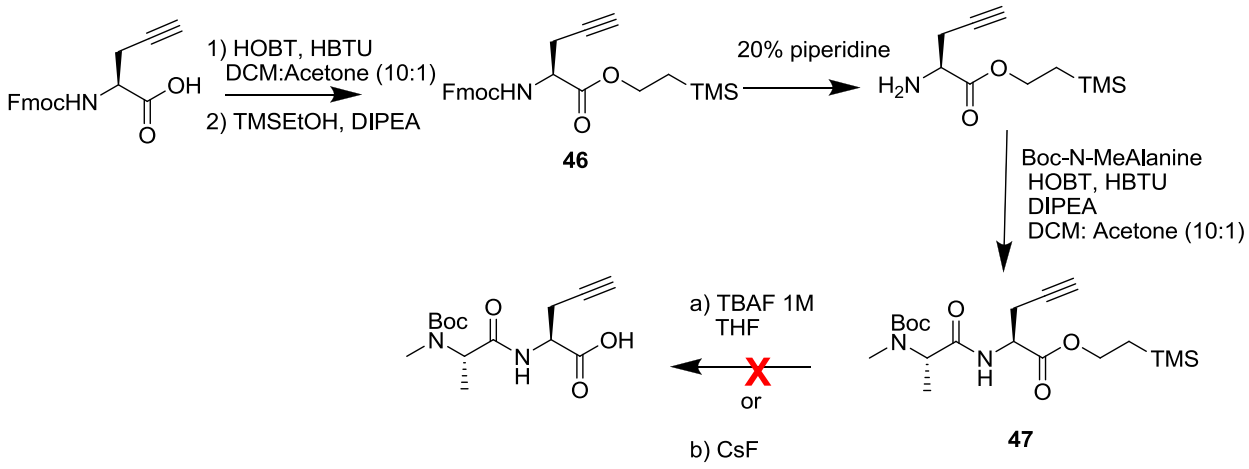

Scheme 4.1. Inital attempt at synthesizing compounds **40-45** through C-terminus protection (**46**) yielding dipeptide **47.**

Synthesis of compounds **39-45** was envisioned by the subsequent addition of residues to the N-terminus of the TMSEtOH protected amino acid through the use of solution phase chemistry. This approach was desired since the C-terminus (P4) is where all the various structural modifications were to occur on the peptide.

Initial synthesis of the library began by the protection of the C-terminus of commercially available Fmoc-Propargyl glycine, to afford **46** in 95% yield, Scheme 4.1. Deprotection of the Fmoc-group using 20% piperidine in dimethylformamide to yield the free amine, which was subsequently coupled to N-methyl-N-tertbutyloxycarbonyl-alanine (Boc-N(Me)Ala) to afford **47** in78% yield. Initial deprotection of the C-terminal protecting group in **47,** was attempted by treating **47** with 1M TBAF in THF. Unfortunately, after several attempts, the desired product was not observed. Also, the

use of cesium-fluoride (CsF) under refluxing conditions was also used, however this method was also unsuccessful.

4.2.1. Revised Synthesis of Compounds **39-45**

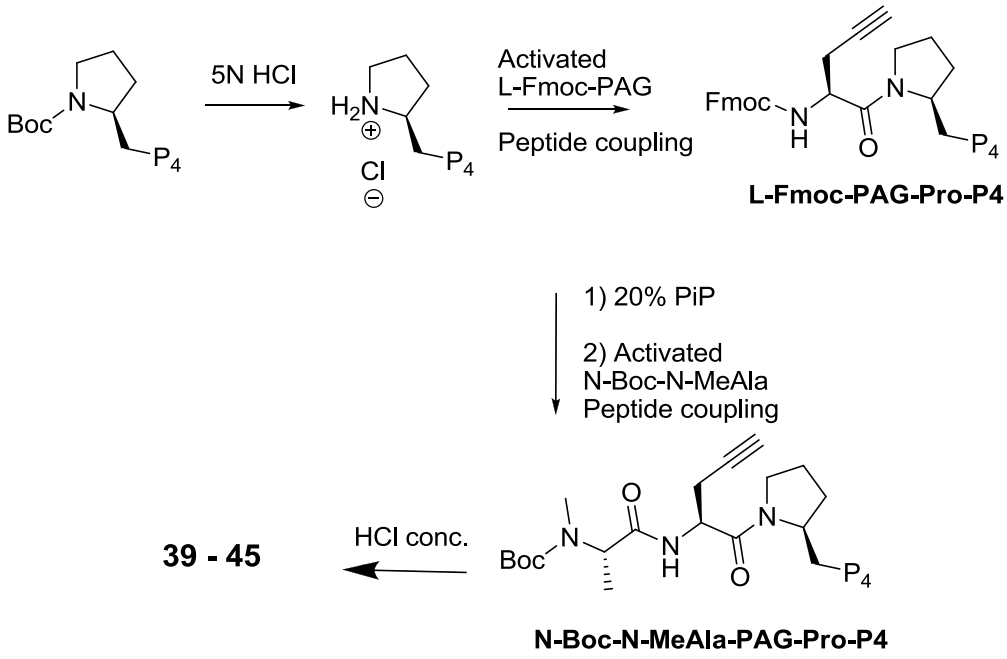

Scheme 4.2. Synthesis of compounds **39-45** starting with the P3-P4 dipeptide component.

Due to the lack of success in using TMSEtOH as a protecting group, we decided to perform the synthesis of these compounds by starting at the C-terminus (P4) and gradually adding residues via the N-terminus. In general, residues P3 and P4 were first coupled to form the corresponding Boc-protected proline dipeptide, followed by subsequent amino acids that were then conjugated using conventional solution phase peptide chemistry (Scheme 4.2).

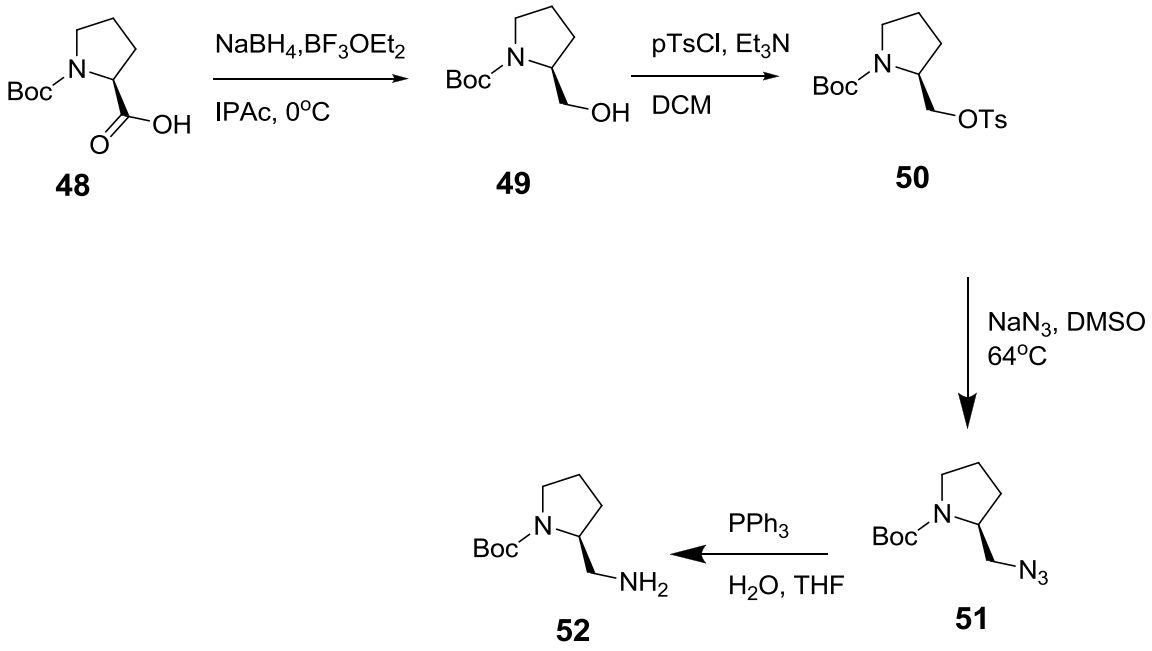

Scheme 4.3. Synthesis of compounds **49, 50**, **51**, and **52** starting from commercially available Boc-Proline.

In order to prepare unnatural amino acids (**53-59**), commercially available L-Boc-Pro-OH (**48**) was first reduced to the primary alcohol in 91% yield using sodium borohydrate ($NaBH_4$) and boron trifluoride diethyl etherate ($BF_3O(Et)_2$), in the presence of isopropyl acetate.[17] The alcohol was then converted into a leaving group by treatment with tosyl chloride[18] (Scheme 4.3), to generate a functional group that could then be used for subsequent functional group manipulations.

With compound **49** and **50** in hand, compounds **53** (via Mitsunobu reaction),[19] **54** (via Garegg-Samuelsson reaction),[20] **55** (via S_N2 displacement),[21] **56** (via "click chemistry"),[22] **57** (via S_N2 displacement),[23] and compounds **58** and **59** (via peptide coupling after formation of amine)[24] was achieved (Scheme 4.4 - 4.8).

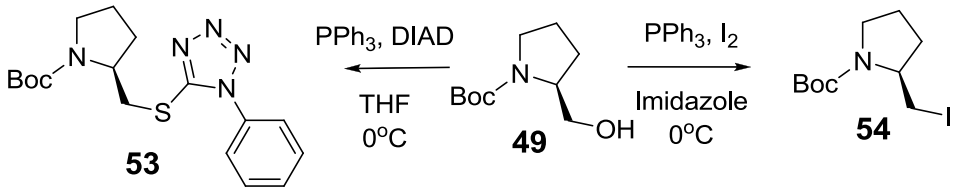

Scheme 4.4 Synthesis of unnatural dipeptides **53** and **54**

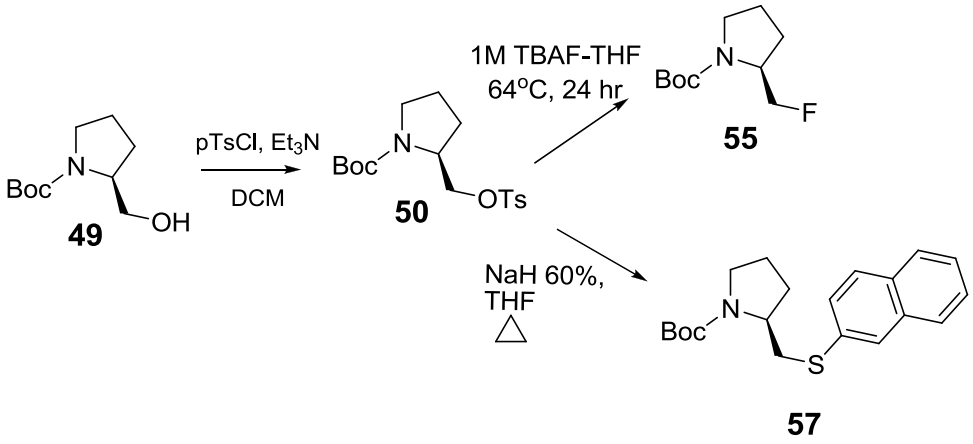

Scheme 4.5 Synthesis of unnatural dipeptides **55** and **57**

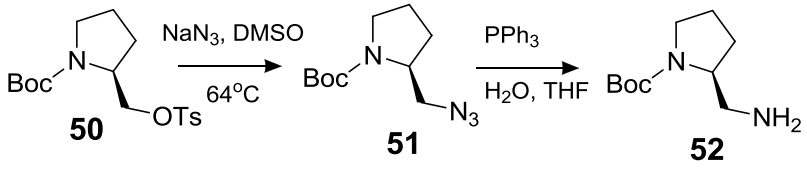

Scheme 4.6 Synthesis of precursor **55** and unnatural dipeptide **57**

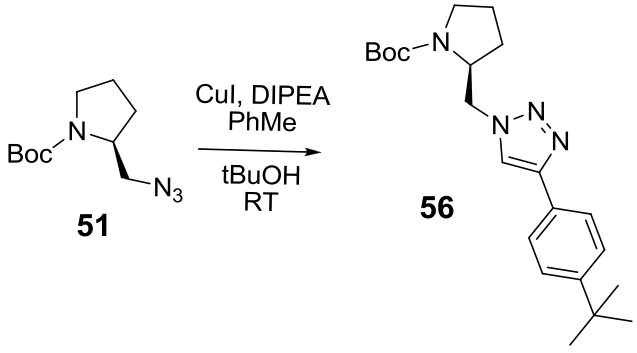

Scheme 4.7 Synthesis of unnatural dipeptide **56**

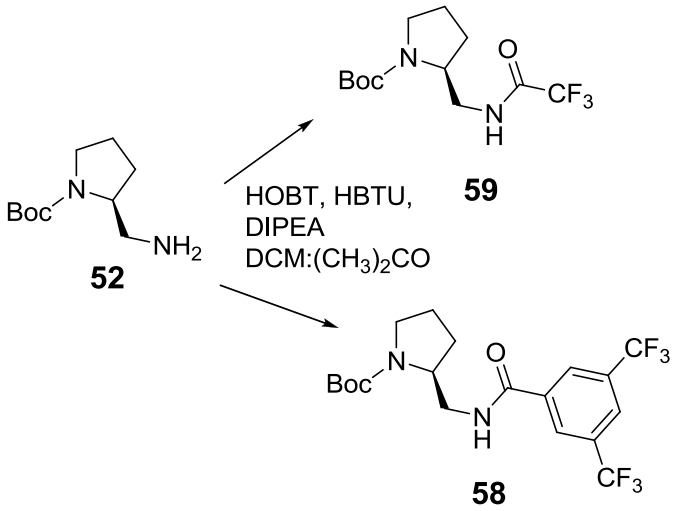

Scheme 4.8 Synthesis of unnatural dipeptides **58** and **59**

After deprotection of the Boc group from the P3-P4 dipeptide derivatives, using 5 N HCl in EtOH, the P3-P4 dipeptide was coupled to the activated L-Fmoc-PAG using standard peptide coupling conditions. Deprotection of the Fmoc group from the newly synthesised tetrapeptide, with 20% piperidine in DMF, allowed for the coupling to activated L-MeAla in the TFA salt form.

4.3 Evaluation of compounds **39-45** in MDA-MB-231 cancer cell line

The seven monovalent Smac mimetic compounds were evaluated by testing them in a human MDA-MB-231 breast cancer cell line without the addition of death ligands similar to that described in chapter 3. The cell line was cultured to confluence and then split into a 96 well plate with a cell concentration of 5,000 cells per well; determined through the use of a hemocytometer[25] (Figure 4.2).

[A]

[B]

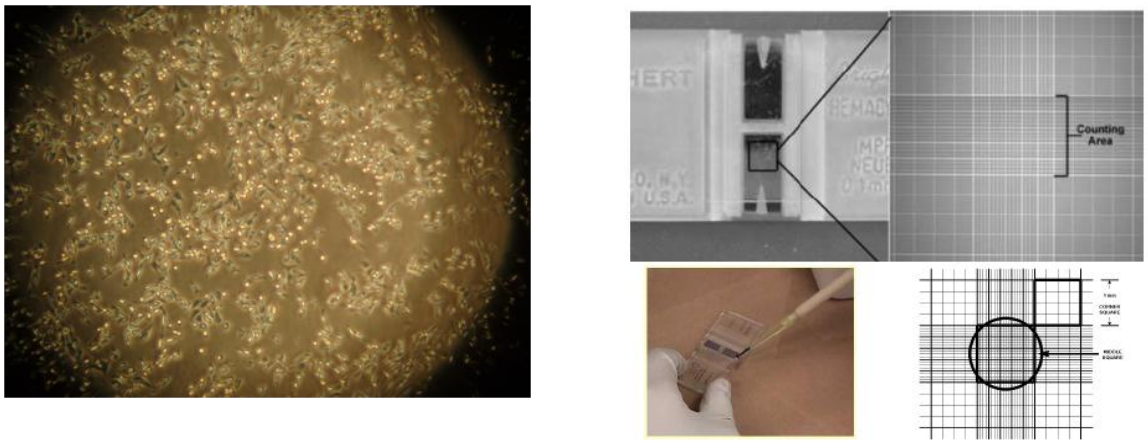

Figure 4.2 [A] MDA-MB-231 cell -line cultured to confluence before being split into a 96 well plate. **[B]** Hemocytometer used in establishing cell concentration.[25]

After 48 hours of cell proliferation in the 96 well plate, compounds were dissolved in a 0.1 M solution of DMSO in MEM and added to the cell line in a descending concentration range from 100 µM down to 1 nM; Figure 4.3.

[A]

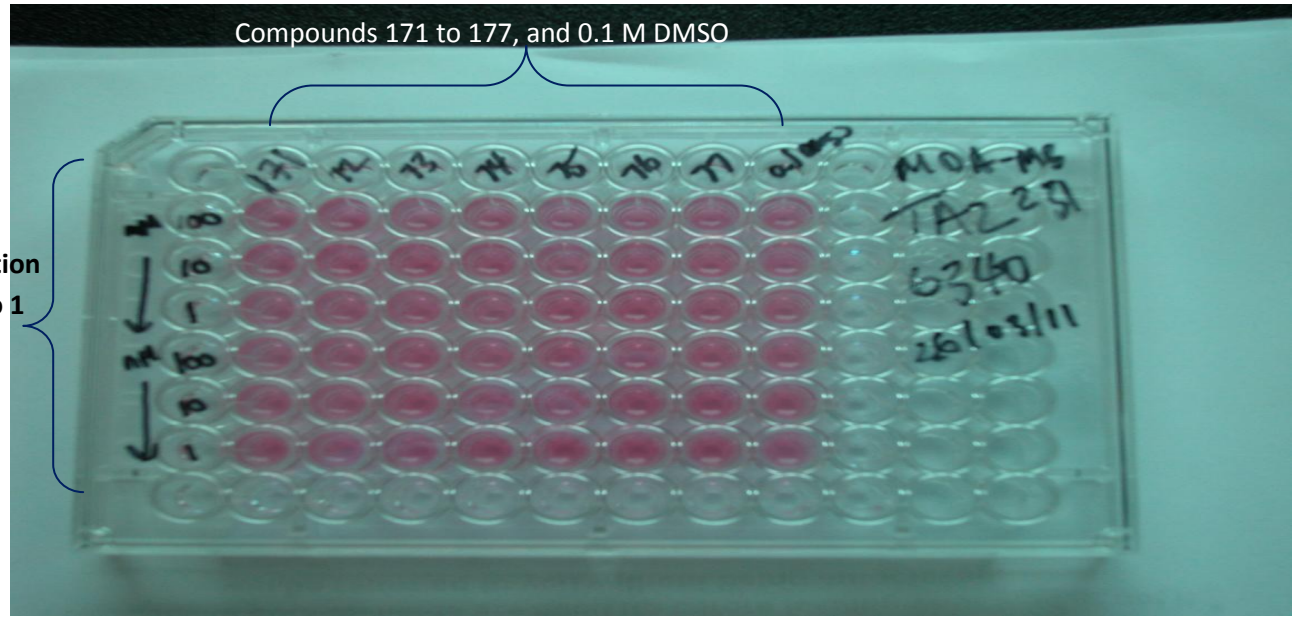

[B]

	2 39	3 40	4 41	5 42	6 43	7 44	8 45	9 0.1M DMSO
A –Blank								
B – 100 µM								
C – 10 µM								
D – 1 µM								
E – 100 nM								
F -10 nM								
G – 1 nM								

Figure 4.3 [A] Actual picture of plated cells at 5,000 count, with compounds dissolved in 0.1M DMSO at concentrations ranging from 100 µM down to 1 nM. **[B]** Schematic diagram of how cells and compounds were placed into the 96 well plate.

The effect of the compounds on the cell morphology, through a bright field microscope, was examined after 24 and 48 hours. Apoptotic activity of each compound was assessed via use of an Alamar Blue assay. The assay allows for indication on cell viability through natural reducing power of living cells, which convert blue resazurin to fluorescent resorufin. The results from the assay indicated that compound to **41a** enhanced apoptotic activity greater than the other compounds (Table 4.2).

Table 4.2 Selected pictures of MDA-MB-231 cells after exposure to compounds **39-45**, after 48 hours of in-vitro treatment. Picture 2 represents compound **41a** tested at a concentration of 10 mM.

Compound and Concentration used	Image of cells after treatment with compounds
40, 10 μM	1- 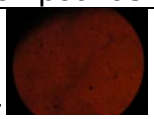
41a, 10 μM	2- 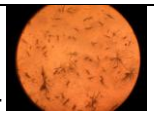
45, 1 μM	3- 
45, 100 nM	4- 

4.3.1 Quantifying data generated from Alamar Blue assay

To assess the effects of compounds **39-45** on their ability to induce apoptosis, a 0.01 % Alamar blue solution was added to each well and incubated at 37^{o} C for 48 hours.[26] After 48 hours a visual observation was conducted to see if a colour change had occurred (Figure 4.4.). Assessment of the assay[27] allowed for the quantification of the minimal inhibitory concentration (MIC) of each compound with the use of a UV-Vis spectroscopy.

[A]

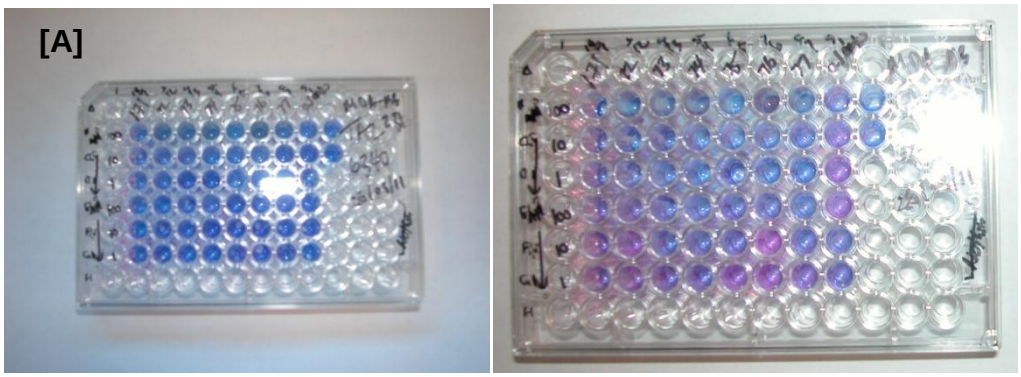

[B]

[C]

	2 39	3 40	4 41	5 42	6 43	7 44	8 45	9 0.1M DMSO	10 Blank
A –Blank									
B – 100 µM									
C – 10 µM									
D – 1 µM									
E – 100 nM									
F -10 nM									
G – 1 nM									

Figure 4.4 [A]. 96 well plate with the introduction of 0.01% Alamar Blue. [B] 48 hours after incubation with Alamar Blue to determine MIC. [C] Schematic diagram of how cells and compounds were placed into the 96 well plate.

Plotting the data generated from the assay, allowed for the extrapolation of EC_{50} values for each compound (Figure 4.5). Upon further analysis of the data we were surprised by the result and data obtained from compound **43**, the napthanthiol derivative. As seen from Figure 4.5, the EC_{50} appeared to be 10 nM which indicated potency of 100 times greater than Aegera's monovalent compound **10** and equally as potent as their divalent mimetic **15**.

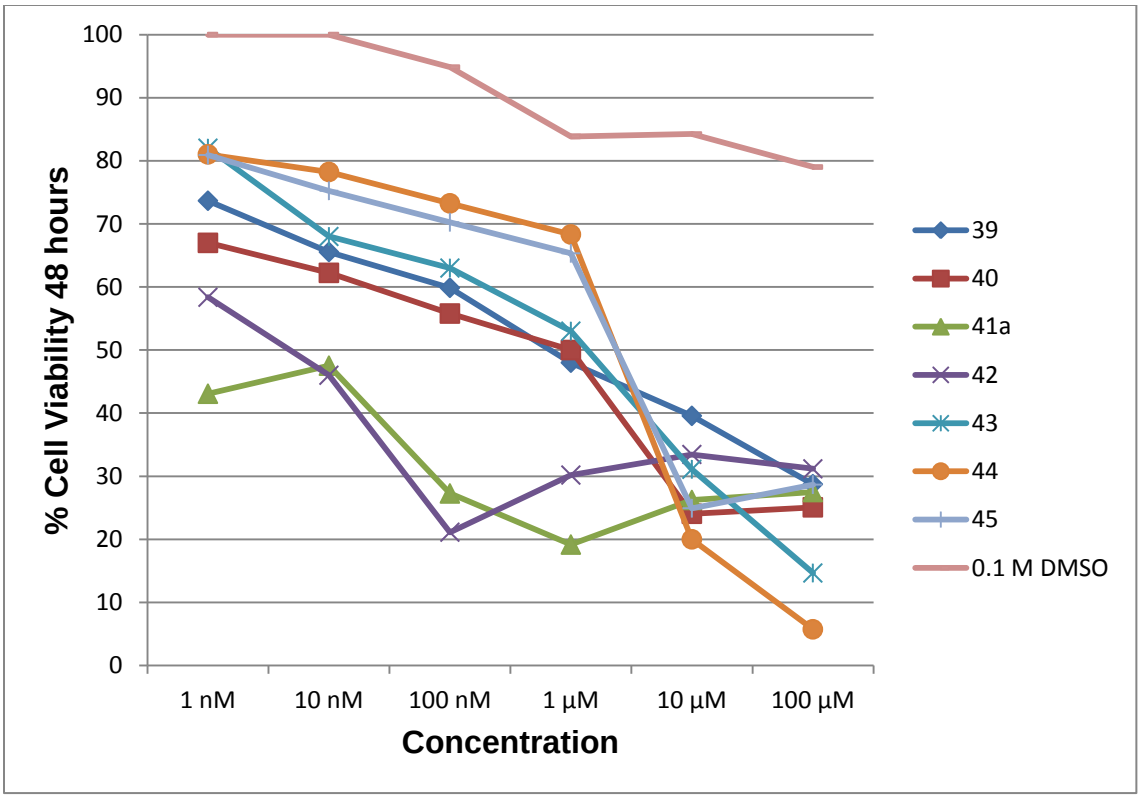

Figure 4.5 Determination of EC_{50} values through extrapolation of data from Assay results. Graph generated from data obtained through UV-Vis Spectroscopy.

Most compounds displayed a minimal inhibitory concentration greater than 1 µM, which was typical of most monovalent active mimetics. Upon assessing the results we decided to retest compound **43** due to its display in high potency. Compound **41a** was not considered, due to poor solubility it had crystallized out causing an inaccurate result. Most compounds synthesized and purified gave only enough material to run one test.

4.4 Synthesis of **43** and the synthesis of the a divalent compound **60**

To verify the results that we had obtained from our first trial, we set out to re-synthesize compound **43**. Cells were transferred to two 96 well plates with a cell concentration of 10,000 cells per well, calculated through the use a hemocytometer.[28] The cell line had been increased from the previous 5,000 cells since we believed that some wells may have actually had less than the 5,000 cells we were hoping for in the original trial, which may have lead to the obtained result (Figure 4.6).

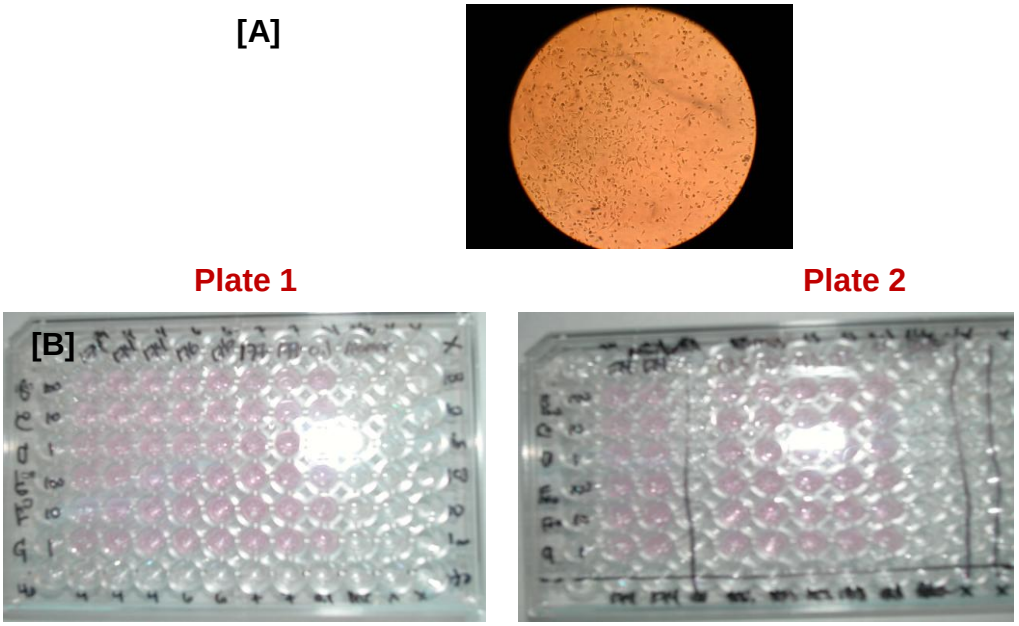

Figure 4.6 [A] Verification of cell culture confluence before transferring to 96 well plates. [B] Two 96 well plates with columns set for compounds **43**, **44**, **45**,and **60**, and 0.1 M DMSO. Four columns were set for each compound.

The synthesis of **43** began with compound **57** which was treated with 10 N HCl to deprotect the Boc protecting group, producing the hydrochloric salt. Using standard peptide coupling compound **61** was synthesized after addition of Fmoc-PAG-OH. To make purification simpler the Fmoc group was removed from **61** and the free amine was

re-protected with Boc anhydride, forming the tert-Butyl carbamate on compound **62**. After purification, removal of the Boc group, and then through the use of standard peptide coupling, compound **63** was synthesized. Removal of the Boc protecting group through the use of 10N HCl and desalting afforded the secondary amine (Scheme 4.5).

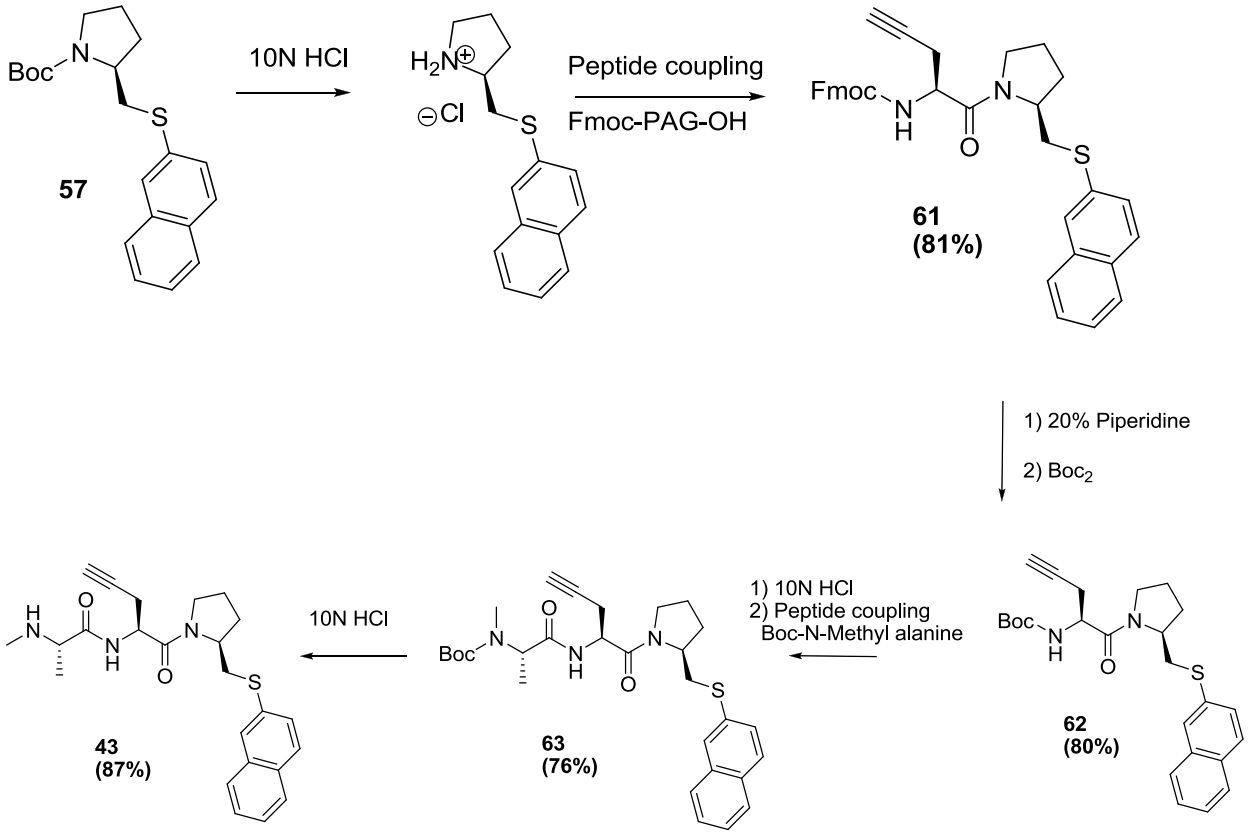

Scheme 4.9 A modified synthesis of compound **43.**

With the increased quantities of intermediates during the synthesis of **43**, treating **63** with modified Glaser coupling conditions[29] allowed for the synthesis of compound **64**. Treating **64** with 10N HCl followed by desalting with the use of a sodium bicarbonate wash, lead to the formation of divalent mimetic **60** (Scheme 4.6).

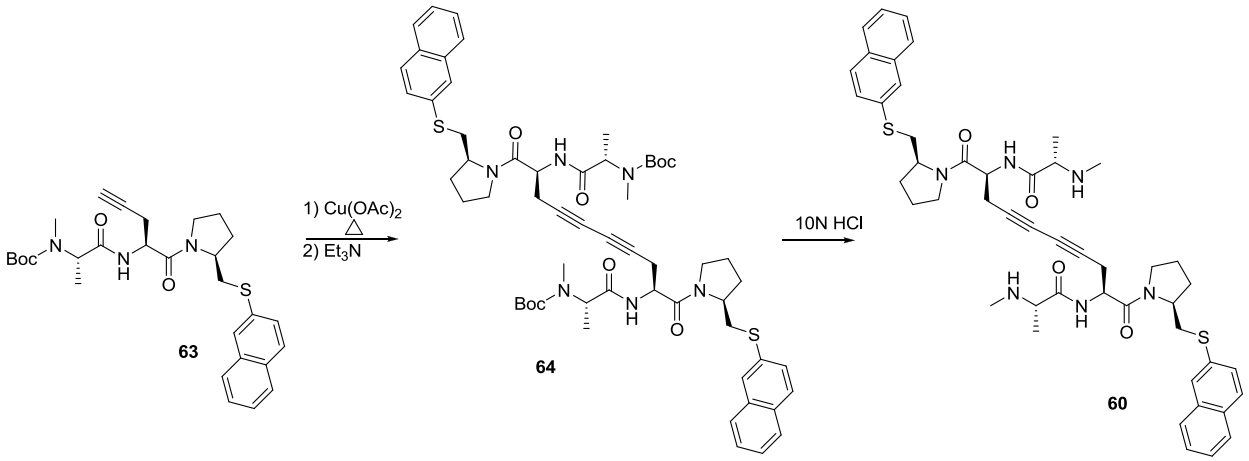

Scheme 4.10 Synthesis of divalent thio-Smac mimetic **60.**

4.4.1 Evaluating compounds **43-45,** and **60** in-vitro for a second trial

The newly synthesized monovalent (**43**) and divalent (**60**) thio-Smac mimetics were introduced into the two new 96 well plates, as shown above in Figure 4.6. The plates where then examined with a bright field microscope before the introduction of each compound, 24 hours after introduction of each compound, and finally 48 hours after introduction of each compound (Table 4.3).

Table 4.3 Pictures of MDA-MB-231 cell line with either no compound and compound after 24 hours, and compound after 48 hours showing apoptotic activity at different concentrations of compounds **43, 44, 45** and **46**

Plate	Compound & Concentration	No Compound	After 24 hrs	After 48 hrs
1	43, 1 μM	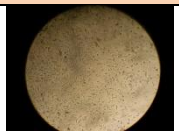	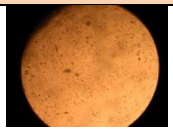	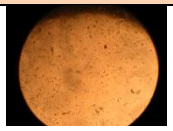
1	43, 1 μM	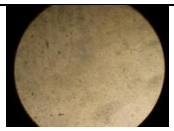	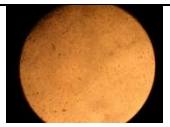	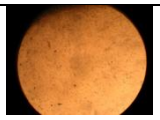
1	43, 100 nM	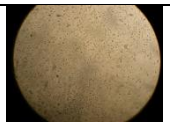	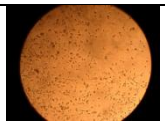	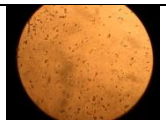
1	44, 100 nM	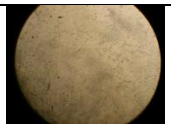	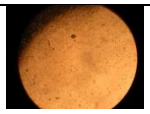	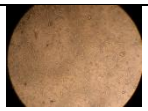
2	43, 100 nM	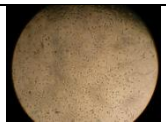	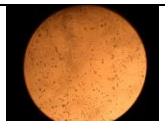	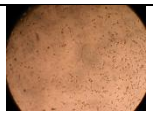
2	60, 100 nM		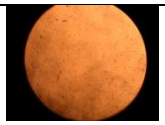	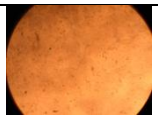
2	60, 10 nM	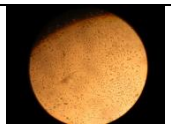	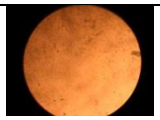	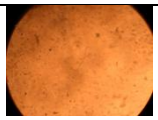

After 48 hours the cell line was then subjected to a 0.01 % Alamar blue solution (Figure 4.7 A) that was added to each well and incubated at 37^{o} C for 48 hours.[30] After 48 hours a visual observation was made to see if a change in colour from had occurred, indicating growth of the cell at that concentration of compound (Figure 4.7 B). Using an

Alamar Blue assay[31] the minimal inhibitory concentration (MIC) of each compound on each plate was quantified using UV-Vis spectroscopy, which was then plotted to help extrapolate EC_{50} value data (Figure 4.8). In plate 2, cell D2 had compound not introduced into the well due to error, therefore it displays substantial cell growth.

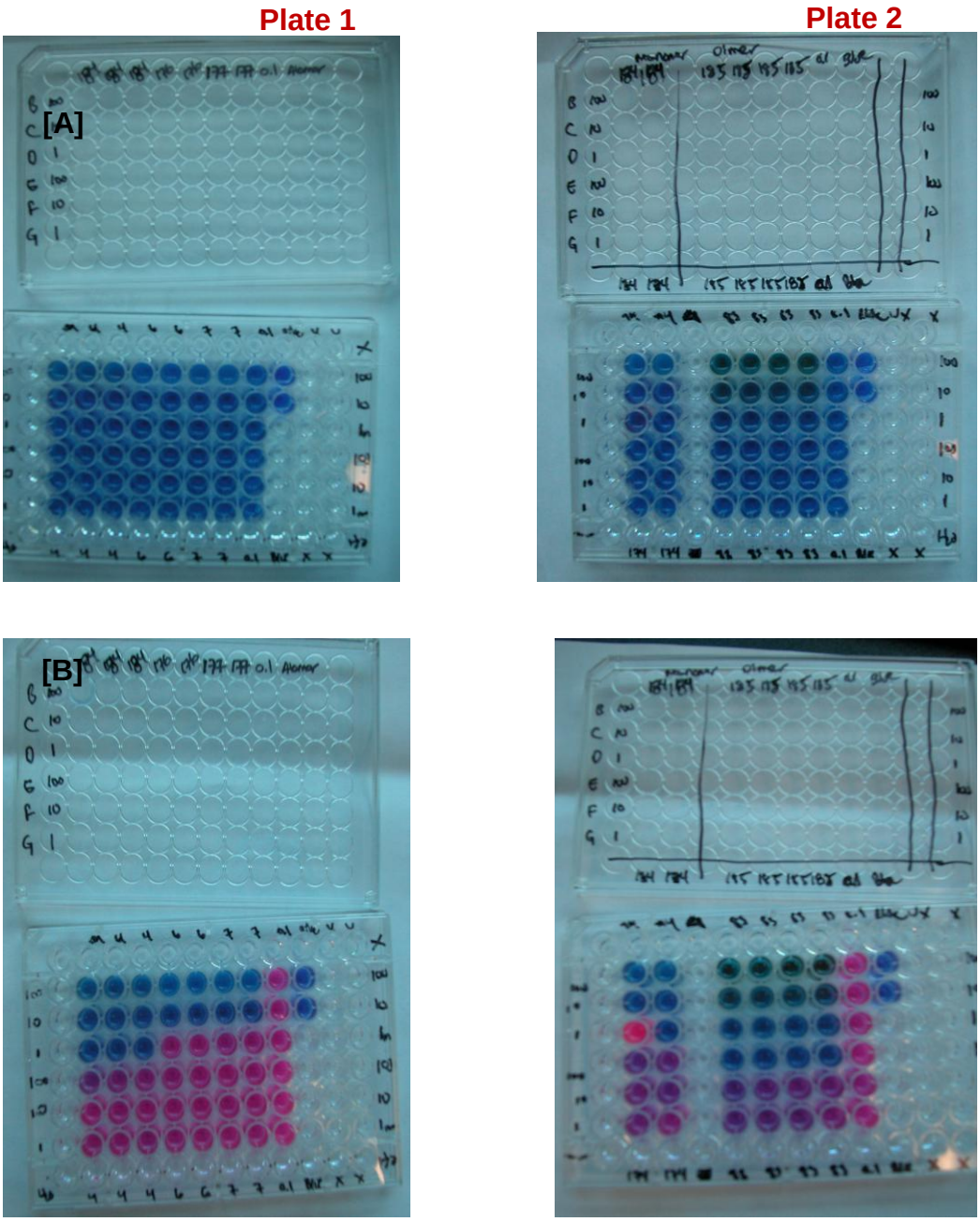

Figure 4.7 [A] Plate 1 and 2 after addition of 0.01% Alamar Blue solution. [B] Plate 1 and 2 after 48 hours of incubation at 37°C.

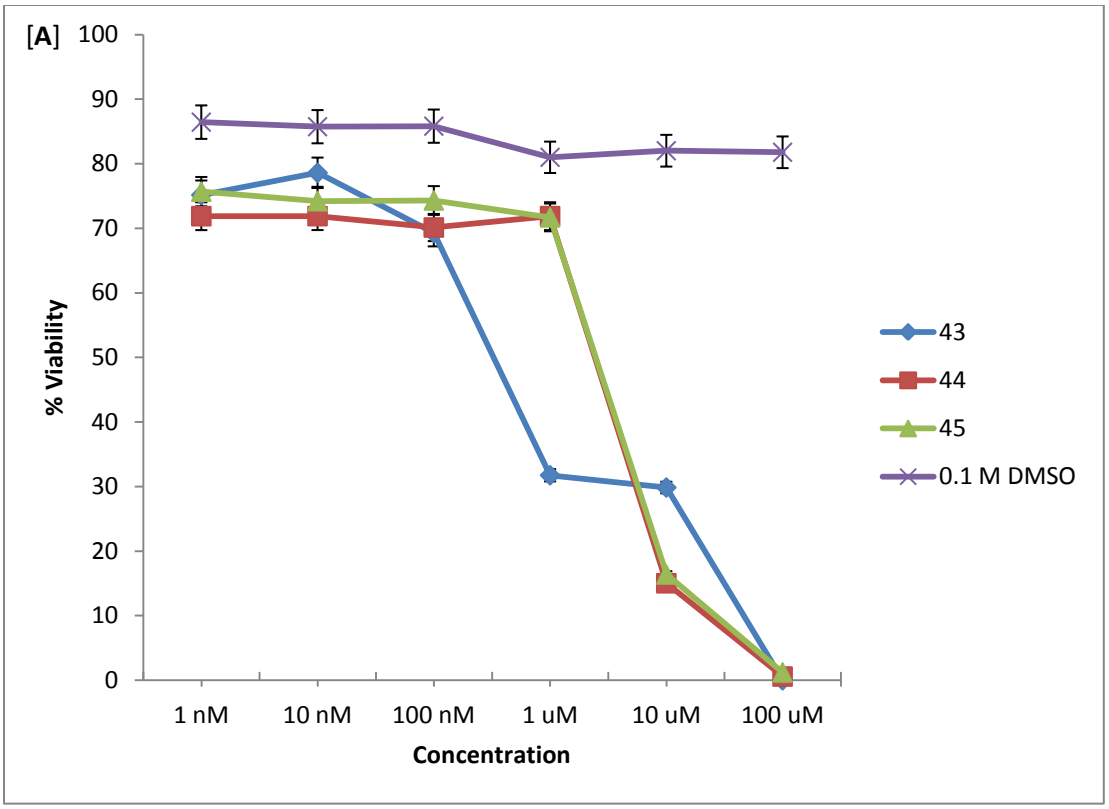

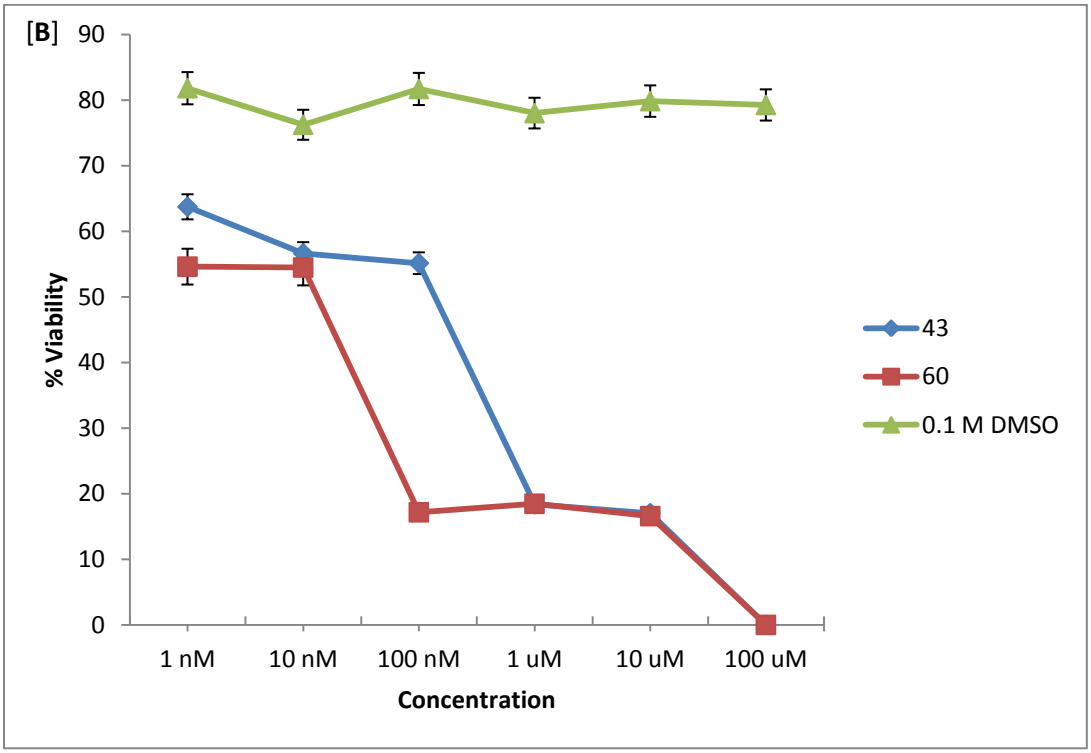

Figure 4.8 [A] Graph generated from newly synthesized **43**, and compounds **44** and **45**. Data obtained from UV-Vis analysis of plate 1. [B] Graph generated from **43** and **60**. Data obtained from Plate 2. EC_{50} values obtained from extrapolation.

From the total of six trials conducted on **43**, and the four trials conducted on **60**, an EC_{50} value of 500 nM and 12 nM was generated respectively. These results, although not the same as the ones in the original trial, were extremely exciting. Not only were we able to synthesize a monovalent Smac mimetic with nanomolar activity, but we were also able to synthesize a divalent bridged mimetic which had comparable activity to **15** developed Aegera Therapeutics. The differences in both **15** and **60** are highlighted in orange (Figure 4.9).

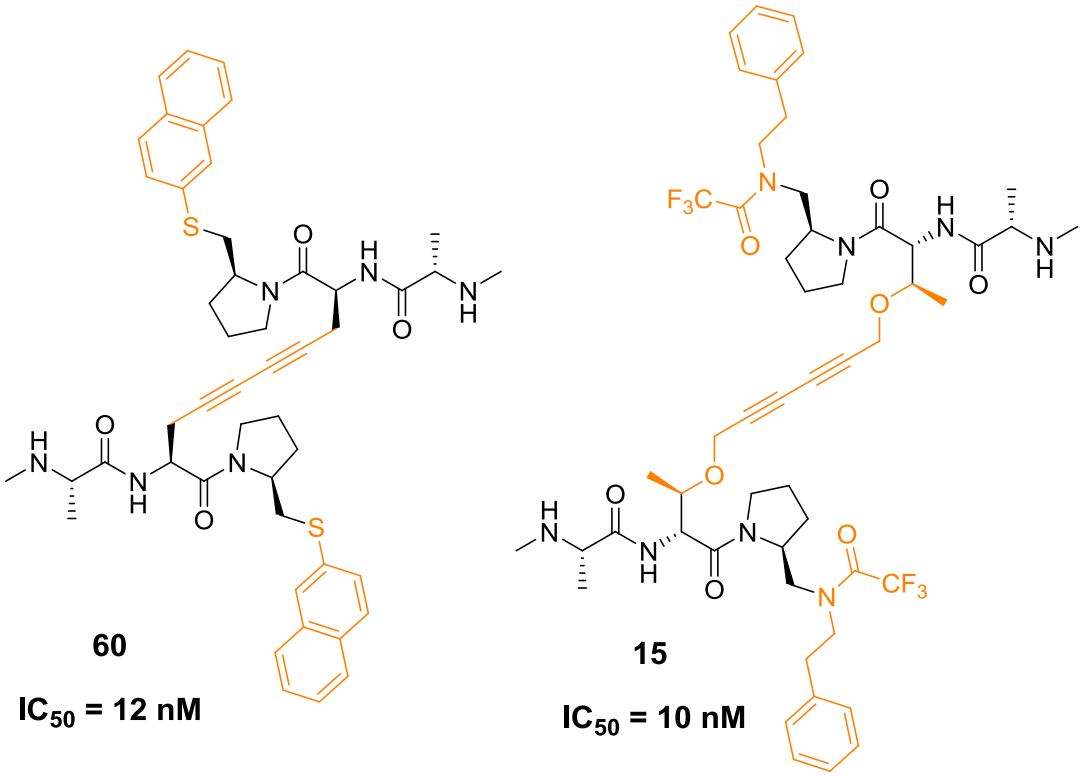

Figure 4.9 Comparison of divalent Smac mimetcs **46** and **15** with comparable nanomolar activity.

Although both molecules have their structural differences, the ability to induce apoptosis in the cell line seems to be fairly similar. We hypothesis that the similarity in

activity could be due to the bio-isosteres in substituent's, modified at positions P2 and P4. It is known that replacement of amine with a thiol and replacement of an oxygen atom with a methylene provide similar biochemical mimicry for drug design.[32] We are now in the process of patenting this compound through the University of Ottawa.

4.5 Chapter Summary

The variation of substituents on the tetrapeptide motif of Smac at positions P2 and P4 has been described extensively, but not exhaustively, by many groups. From the initial design of bridged alkyne compounds, first introduced by Aegera Theraputics, many laboratories have used this as precedence for creating divalent mimetics.

We chose to use this alkyne substituent at P2 to create novel monovalent and a novel divalent Smac mimetic(s). Synthesizing a library of P3-P4 non-peptide based compounds was supported on bio-isosteres for rational drug design. In evaluating the compounds in a first test run gave an EC_{50} values for the most active compound (**43**) at 10 nM. To verify this result compound **43** was again synthesized, in a modified manner to aid in the purification process. To assess the activity of monovalent **43** against its divalent counterpart, compound **60** was also synthesized by our laboratory. Evaluating compound **43** and **60** for six trials gave results with EC_{50} values, obtained through analysis of an Alamar Blue assay, of 500 nM and 12 nM respectively. While this was not the 10 nM activity that was originally observed with **43**, which was believed to have occurred due to an error in cancer cell presence of less than 5,000, it did however verify that compound **43** did deserve further investigation.

Although compounds **60** and **15** (Figure 4.9) have subtle differences, the replacement of substituent's based on bio-isosteres in drug design indicates that further modifications could additionally enhance apoptotic activity. With this knowledge in hand, we may be able to further augment the design and bioavailability of such compounds which can induce apoptosis in pico-molar range, and allow for in-vivo testing. Optimization of functional groups through mimicry should now be the next focus, to continue this project to the next level.

Referencs:

[1] Sun, H.; Nikolovska-Coleska, Z.; Yang, C-Y.; Qian, D.; Lu, J.; Qiu, S.; Bai, L.; Peng, Y.; Cai, Q.; Wang, S.; *Accounts of Chemical Research* **2008**, 41(10) : 1264:1277

[2] Sun, H.; Nikolovska-Coleska, Z.; Yang, C-Y.; Xu, L.; Liu, M.; Tomita, Y.; Pan, H.; Yoshioka, Y.; Krajewski, K.; Roller, P.P.; Wang, S.; *J. Am. Chem. Soc*. **2004**, 126: 16686-16687

[3] Sun, H.; Nikolovska-Coleska, Z.; Yang, C-Y.; Qian, D.; Lu, J.; Qiu, S.; Bai, L.; Peng, Y.; Cai, Q.; Wang, S.; *Accounts of Chemical Research* **2008**, 41(10) : 1264:1277

[4] Bertrand, M. J.; milutinovic, S.; Dickson, K.M.; Ho, W.C.; Boudreault, A.; Durkin, J.; Gillard, J. W.; Jaquith, J. B.; Morris, S. J.; Barker, P. A.; *Mol. Cell*, **2008**, 30, 689-700

[5] Bertrand, M. J.; milutinovic, S.; Dickson, K.M.; Ho, W.C.; Boudreault, A.; Durkin, J.; Gillard, J. W.; Jaquith, J. B.; Morris, S. J.; Barker, P. A.; *Mol. Cell*, **2008**, 30, 689-700

[6] Bertrand, M. J.; milutinovic, S.; Dickson, K.M.; Ho, W.C.; Boudreault, A.; Durkin, J.; Gillard, J. W.; Jaquith, J. B.; Morris, S. J.; Barker, P. A.; *Mol. Cell*, **2008**, 30, 689-700

[7] Sun, H.; Nikolovska-Coleska, Z.; Yang, C-Y.; Qian, D.; Lu, J.; Qiu, S.; Bai, L.; Peng, Y.; Cai, Q.; Wang, S.; *Accounts of Chemical Research* **2008**, 41(10) : 1264:1277

[8] Oost, T.K.; Sun, C.; Armstrong, R.C.; Al-assaad, A.S.; Bentz, S.F.; Deckwerth, T.L.; Ding, H.; Elmore, S. W.; Meadowns, R. P.; Olejniczak, E. T.; Oleksijew, A.; Oltersadorf, T.; Rosenberg, S.H.; Shoemaker, A. R.; Tomaselli, K. J.; Zou, H.; Fesik, S. W.; *J. Med. Chem*. **2004**, 47: 4417-4426

[9] Genentech, Inc. Pyrrolidine inhibitors of IAP. WO2006069063A1; 2005

[10] Cohen, F; Alicke, B.; Elliott, L.O.; et al.; *J. Med. Chem*. **2009**, 52: 1723-1730

[11] Tetralogic Pharmaceuticals Corporation, IAP binding compounds. US7456209B2; **2005**

[12] Novartis AG. Organic compounds. WO2006133147A2; **2006**

[13] M. Cheng et al.; *J. Med. Chem*. **1999**, 42, 5426-5436
[14] Diamond, J.M.; Wright, E.M.; Proc. R. Soc. Lond. B **1969**, 172, 273-316
[15] Li, L.; Thomas, R.M.; Suzuki, H.; De Brabander, J.K.; Wang, X.; Harran, P.; *Science* **2004**, 305: 1471-1474

[16] M.S.S. Palanki, et al. *J. Med. Chem*. **2000**, 43, 3995-4004

[17] Zhao, D. et al.; *J. Org. Chem*. **2006**, 71, 11, 4336-4338

[18] Zhao, D. et al.; *J. Org. Chem*. **2006**, 71, 11, 4336-4338

[19] Sen, S.E.; Roach, S.L; *Synthesis*, **1995**, 756-758

[20] Garegg, P.J.; Ortega, C.; Samuelsson, B.; *Journal of the Chemical Society, Perkin Transaction 1*, **1982**, 681

[21] Rosen, T.; Chu, D.T.W.; Lico, I.; Fernandes, P.B.; Marsh, K.; Shen, L.; Cepa, V.G.; Pernet, A.; *J. Med. Chem*. **1988**, 31, 8, 1598-1611

[22] Luo, S. et al.;. *J. Org. Chem*. **2006,** 71, 9244-9247

[23] Syu, S.; Kao, T.; Lin, W.; *Tetrahedron*, **2010,** 66, 891-897

[24] Slaitas, A.; Yeheskiely, E.; *European Journal of Org. Chemistry*, **2002**, 14, 2391-2399

[25] http://www.smccd.edu/accounts/case/biol230/algae/hemocytometer.pdf

[26] Liu, D.; *Bull. Environmental Contamination Toxicology* **1981**, 26:145-149

[27] Nakayama,GR.; Caton, MC.; Nova, MP.; *J. Immunol Methods*. **1997**, 2 (204), 205-208

[28] http://www.smccd.edu/accounts/case/biol230/algae/hemocytometer.pdf

[29] US Patent 7309792B2 – Harran et al. (**2007**)

[30] Liu, D.; *Bull. Environmental Contamination Toxicology* **1981**, 26:145-149

[31] Nakayama,GR.; Caton, MC.; Nova, MP.; *J. Immunol Methods*. **1997**, 2 (204), 205-208

[32] Meanwell, N.A.; J. Med. Chem. **2011**, 54, 2529-2591

Chapter 5: Conclusion and Future Works

Over the past two years there have been many routs in which this research could have taken; however, two key areas were the main focus of our work. The first was to strengthen the argument that Smac mimetics either bind to both BIR2-BIR3 domains or solely to the BIR3 domain. The second was to synthesize novel mimetics containing bio-isosteres of a highly active compounds through substituent modifications, which could introduce beneficial changes in size, shape, electronic distribution, polarizability, dipole, liphophilicity, and pKa with some or all playing key contributing roles in molecular recognition; creating highly active apoptosis inducer.

In order to accomplish the first objective, we initially synthesized and evaluated divalent Smac mimetics which were previously synthesized and known to induce apoptosis. In doing so allowed for the verification that the previously published compounds did indeed cause cell death, and allowed for the synthesis of control compounds. Based on molecular docking studies and SAR work, as described in Section 1.6, our initial hypothesis was that the ability of Smac mimetics to bind to BIR domains would be dependent on the sequence in which the divalent peptide was synthesized. We synthesized a library of divalent mimetics, in which half the divalent mimetics were synthesized in a forward-reverse fashion while the other half were synthesized in a forward-forward fashion. The evaluation of these mimetics provided new evidence that the sequence in which the peptide is synthesized has no affect on the degree of apoptotic activity. We believe that findings strengthen the argument made by Span et al. that binding is selective for the XIAP-BIR3 domain. Also, that only when

the BIR2 domian is in close proximity and only after binding to the BIR3 domain occurs first, will the Smac mimetic bind to BIR2. The implication of this could allow for future mimetic design towards relieving inhibition directly at BIR3. Further investigation with displacement assays need to be conducted in order to be certain of the selective binding to BIR3 versus BIR2. Since the distance between BIR2 and BIR3 is believed to span 45 Å, ideally the synthesis of bivalent peptides with the ability to span such a distance could provide further insight into how much a factor BIR2 inhibition really is.

For our second objective, we initially hypothesized that using an alkyne substituent at P2 and various substituent's at P4, which could serve as a bio-isostere for well known **15**, could be optimized to produce a much higher active compound. In conducting in-vitro testing and quantifying through the Alamar Blue assay, compounds containing napthanethiol at P4 (**43** and **60**) displayed the highest apoptotic activity. As well, we explored the significance of the phenylethylamine and the trifluoroacetate group in **15** through the synthesis of its analogues (**44** and **45**) to assess their role on apoptotic activity. The apoptotic activity of both these compounds was significantly lower than the parent compound as well as the thiol-based derivatives, indicating the need for a lipophilic substituent at P4. To confirm the hypothesis that a requirement of liphophilic groups at P4 increases activity, a third compound needs to be synthesized in which only the phenylethylamine is present and the trifluoroacetate group is removed. In addition, further testing of these compounds for quality control of drug susceptibility on primary cell lines, such as human mammary epithelial cells (HMEC), is required to ensure the effect is not based on toxicity.

Given that this area of research is quite still new, with less than 12 years from initial discovery, there are numerous paths which can be explored to (1) induce apoptosis and (2) determine the path of progress of Smac mimetics as they are internalized into the cell line. Figure 5.1 shows compounds that were synthesized and not tested, key building blocks that were synthesized, and ideas that should be perused.

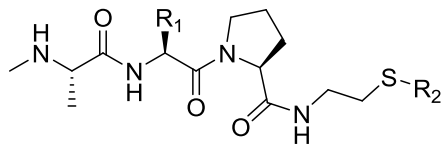

R_1 = amino acids
R_2 = H, S-peptide

Synthesized but not tested

Carbohydrate Synthesized only

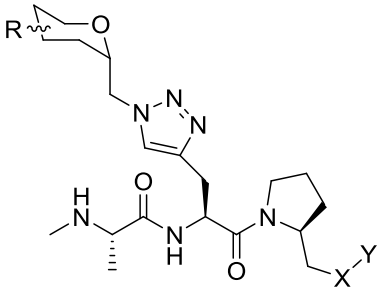

R = any carbohydrate
X = RNH, R_2N, S, SO, SO_2
Y = alkyl, aryl, napthyl, tetrapeptide repeat

Cycloheptalactam Synthesized only

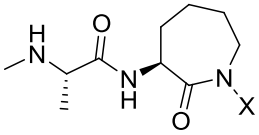

X = Any amino acid, aryl, heteroaryl, napthyl, repeat of peptide

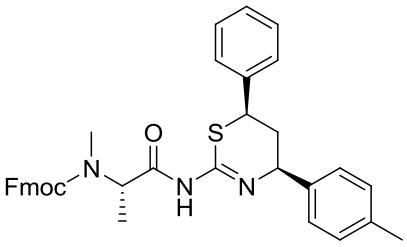

Synthesized but not tested

Figure 5.1 Novel Smac mimetics which should be tested or synthesized further.

By clarifying all the factors that give great activity to **60** a future goal will be to run MD simulations that will help to further design compounds, which could hopefully induce apoptosis in the picomolar range. In synthesizing and/or testing those compounds shown in Figure 5.1, the ability to design “drug-like” candidates for human trials will likely enable the possibility to treat breast cancer in the future.

Chapter 6: Experimental Data and Methods

6.1 General Procedures

6.1.1 Cell Culture

MDA-MB-231 cells, from the mammary gland of a human breast, were obtained from the American Type Culture Collection as ATCC number HTB-26. Cells were grown in Eagle's Medium (MEM) containing 10% heat-inactivated fetal bovine serum (FBS) (Fisher, 361015856, supplier number SH30397-3C), 1% penicillin-streptomycin (Sigma, P4333) in 75 cm^2 flasks (Fisher, 10-126-37) and maintained at 37^oC with 5% CO_2. All cells were removed from the plates using a trypsin-EDTA solution (Sigma, T4174) for use in experiments. The cell line was subcultured and preserved as described.[1]

6.1.2 Viability Assays

Sterile polycarbonate 96-well flat-bottom culture plates (Costar 3596) were used in the Alamar Blue assay. To minimize edge-related anomalies, only the inner wells of each plate were inoculated with medium containing 5000 to 10,000 cells/well; the remaining perimeter wells contained 100 µL of either medium or water/well. The plates where then placed in a humidity-controlled incubator at 37^oC with 5% CO_2.[2] After two days of introduction of compounds into the cell line, one-third the volume of 0.01% resazurin solution was added to each compound-cell containing well. The 96-well plates were incubated as mentioned above for an additional 48 hours. Fluorescence measurements were made on a SpectraMax Absorbance Micro plate reader, set at 600 nm excitation and 690 nm emissions. Readings from blank wells, those containing resazurin but without cells were averaged and subtracted from each test well to give the net result.

6.1.3 Cryopreservation of Cell line

MDA-MB-231 cells, from the mammary gland of a human breast, were cultured and trypsinized as described above. Cells were diluted with MEM and counted using a haemocytometer (VWR, 15170-172). Aliquots containing 1x10^7 cells were added to 15 mL centrifuge tubes and cells were pelleted by centrifugation for 10 min at 2000 rpm. The supernatant was removed and the cells were re-suspended in 1.5 mL MEM. Cell suspensions were transferred to 2 mL cryogenic vials (VWR, CA16001-102) and placed in a "Mr. Frosty" freezing container (Nalgene, 5100-0001, Sigma, C1562). The

[1] Bates, SE., et al. Endocrinology **1990**, 126, 596
[2] Dickson, L. Environ. Sci. Technol.; **1983,** 17, 407

container was placed in an ultra-cold freezer (-80 °C) for 24 h. Samples were then stored in the vapor phase of liquid nitrogen (-196 °C) for 7 days. Following storage, samples were rapidly thawed in a 37 °C water bath with gentle agitation. Thawed samples were transferred to 15 mL centrifuge tubes (Diamed, STK3217P) and slowly diluted to 3 mL by drop wise addition of Eagle's MEM (Sigma, M4655) cell culture medium. After 3 min samples were further diluted to 9 mL. Cells were pelleted by centrifugation for 10 min at 2000 rpm. The supernatant was decanted and the pellet re-suspended in 5 mL MEM.

6.1.4 General Experimental Conditions for Chemical Reactions

All anhydrous reactions were performed in flame-dried or oven-dried glassware under a positive pressure of dry argon or nitrogen. Air or moisture-sensitive reagents and anhydrous solvents were transferred with oven-dried syringes or cannulae. All flash chromatography was performed with E. Merck silica gel 60 (230-400 mesh). All solution phase reactions were monitored using analytical thin layer chromatography (TLC) with 0.2mm pre-coated silica gel aluminum plates 60 F254 (EMD Merck). Components were visualized by illumination with a short-wavelength (254 nm) ultra-violet light and/or staining (ceric ammonium molybdate, ninhydrin, potassium permanganate, or phosphomolybdate stain solution). All solvents used for anhydrous reactions were distilled. Tetrahydrofuran (THF) and diethyl ether were distilled from sodium/benzophenone under nitrogen. Dichloromethane, acetonitrile, triethylamine, benzene and diisopropylethylamine (DIPEA) were distilled from calcium hydride. Methanol was distilled from calcium sulfate. *N,N*-dimethylformamide (DMF) was stored over activated molecular sieves 4Å under argon.

^{1}H (300, 400 or 500 MHz) and ^{13}C NMR (75, 101 or 126 MHz) spectra were recorded at ambient temperature on a Bruker Avance (300, 400, 500), or Varian Inova 500 spectrometer, unless otherwise stated. Deuterated chloroform ($CDCl_3$) or methanol (CD_3OD) was used as NMR solvents, unless otherwise stated. Chemical shifts are reported in ppm downfield from trimethylsilane (TMS) or chloroform corrected using the solvent residual peak, TMS, or $CDCL_3$ as an internal standard. Splitting patterns are designated as follows: s, singlet; d, doublet; t, triplet; q, quartet; m, multiplet and br, broad. Low resolution mass spectrometry was performed on a Micromass Quatro-LC Electrospray spectrometer with a pump rate of 20 µL/min using electrospray ionization (ESI) or a Voyager DE-Pro matrix-assisted desorption ionization-time of flight (MALDI-TOF). Analytical and preparatory scale RP-HPLC were carried out with C-18 columns on a Varian Dynomax HPLC system equipped with a variable wavelength detector (ProStar 330 PDA) or a Waters Delta 600E HPLC system equipped with a variable wavelength detector. Automated solid phase peptide synthesis (SPPS) was performed on APEX 396 (Advanced ChemTech) equipped with a 40 well reaction vessel.

6.1.5 General procedure for Fmoc-group deprotection

Fmoc-amino acids and non-amino acids were dissolved in Piperdine/DMF (1:5) solution and stirred at room temperature for > 1 hour. For SPPS after filteration and several washes complete Fmoc-removal was determined, as described above, before continuing with synthesis. For compounds in solution phase, progress was monitored by thin-layer chromatography. Upon completion of reaction, the solution was concentrated down and azaeotroped with toluene (x 3) before continuing on with addition reactions.

6.1.6 General procedure for Boc-group deprotection

Boc-amino acids and compounds were dissolved in 5N or 10N HCl and stirred at room temperature overnight. The solution was then reduced under pressure. Compounds were left in their salt forms with yields of 85-95% or neutralized with saturated $NaHCO_3$ and extracted with DCM, giving typical yields in range of 82-95%.

6.2 Experimental Procedures and Data

6.2.1 Solid Phase Synthesis of Divalent Smac mimetics (31– 38) Built on either GABA and Ornithine Linkers

All divalent Smac mimetics tethered at P4, with either GABA or Ornithine, were synthesized using conventional Fmoc solid-phase peptide synthesis on an APEX 396 automated synthesizer using acid labile 2-chlorotrityl resin. The procedure[3] for synthesis began with 2-chlorotrityl resin with a loading capacity of 0.60 mmol/g. Attachment of the Fmoc-Orn(Fmoc)-OH (0.5 M), dissolved in DCM, with DIPEA (0.75 M) was added to a reaction vessel containing 2-chlorotrityl resin(115 mg, 0.138 mmol) and the mixture stirred for 2 hours (2 x 1 hour). The resin was filtered and a mixture of MeOH/DIPEA (9:1) was added to destroy excess unbound chloride resin and mixing was continued for an additional 30 minutes. The resin was filtered, washed (3 x DCM, 2 x DMF, 2 x MeOH, 2 x DMF) and allowed to stay suspended in DMF. Cleavage of the Fmoc-group was performed with 20% piperidine in DMF for 45 min followed by two washes of three aliquots of DMF. Complete Fmoc-removal was determined using a Kaiser[4] and TNBS[5] test. Acylation was effected by using 2-5eq. of Fmoc-amino acid/DIPEA (4-10eq.), with HOBT (2-5eq.) and HCTU (2.4-6eq.) in DMF. The desired peptide was synthesized by chain elongation through successive Fmoc-group deprotection and coupling steps. After final coupling, the resin was washed (3 x DMF, 3 x DCM). Cleavage of the divalent peptides was conducted by suspending in a

[3] Barlos, K.; Gatos, D.; Kapolos, S.; Poulos, C.; Schager, W.; Wenqing, Y. Int. J. Peptide Protein Res. **1991**, 38, 555
[4] Kaiser, E.; Colescott, R.L.; Bossinger, C.D.; Cook, P.I.; Anal. Biochem. **1970**, 34, 595
[5] Hancock, W.S.; Battersby, J.E.; Anal. Biochem. **1976**, 71, 261

AcOH/TFE/DCM (1:2:7) mixture and gently agitating for 60 min. The solution was filtered, concentrated, and product precipitated out with diethyl ether.

Divalent peptides tethered with GABA followed a similar procedure as that written above, with the exception of attachment of the first amino acid. Attachment of Fmoc-N-MeAla-OH (0.5 M), dissolved in DMF with HOBT (2-5eq.) and HCTU (2.4-6eq.) for 1 hour, was treated with Piperdine/DMF (1:5) for 45 min while in the presence of the 2-chlorotrityl resin (x 2). The resin was filtered and a mixture of MeOH/DIPEA (9:1) was added to destroy excess unbound chloride resin and mixing was continued for an additional 30 minutes. The resin was filtered, washed (3 x DCM, 2 x DMF, 2 x MeOH, 2 x DMF) and allowed to stay suspended in DMF. The desired peptide was synthesized by chain elongation through successive Fmoc-group deprotection and coupling steps. After final coupling, the resin was washed (3 x DMF, 3 x DCM). Cleavage of the divalent peptides was conducted by suspending in a AcOH/TFE/DCM (1:2:7) mixture and gently agitating for 60 min. The solution was filtered, concentrated, and product precipitated out with diethyl ether.

6.2.2 N-α-N-δ-bis(9-fluorenylmethyloxycarbonyl)-L-ornithine (27)[6]

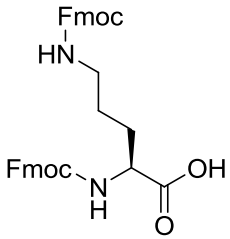

To commercially available Fmoc-ORN(Boc)-OH (10g, 22 mmol), in 30 ml of TFA/DCM (1:1) was mixed at room temperature and stirred for 30 min. After removal of the solvent, the residue was dried under high vacuum for 1 hour. The TFA salt was dissolved in aqueous solution of Na_2CO_3 (10%) (60 ml) and 1,4-dioxane (70 ml) and cooled to 0^{o}C. A Fmoc-OSu (9.65 g, 24.2 mmol) solution in 1,4-dioxane (40 ml) was added via dropping funnel with efficient stirring. The corresponding mixture was allowed to stir overnight at room temperature. The solvent was removed in vacuo and the suspension obtained was diluted with water (150 ml), acidified to pH 3 through the addition of 10% HCl and extracted with CH_2Cl_2 (3 x 75 ml). The organic extracts were combined, dried over $MgSO_4$, filtered and concentrated down, providing the product (12.45g, 98% yield). The crude product was purified by flash chromatography (1% MeOH/CH_2Cl_2) to for a white solid (11.3g, 89%). ^{1}H NMR (400 MHz, $CDCl_3$) δ 7.77-7.70 (4H, m), 7.60-7.48 (4H, m), 7.40-7.31 (4H, m), 7.28-7.23 (4H, m), 4.92 (1H, s), 4.49-4.32 (4H, m, FmocCH_2), 4.17-4.10 (2H, FmocCH), 3.10-2.99 (2H, ddd, J= 4.39, 10.26, 14.39), 1.88-1.55 (2H, m), 1.54-1.23 (2H, m); ^{13}C NMR (101 MHz, $CDCl_3$) δ 173.9, 155.1, 154.9, 143.2, 142.7, 140.3, 140.2, 129.4, 128.9, 127.6, 127.4, 124.6, 124.5,

[6] Reiriz, C.; Castedo, L.; Granja, J.R. J. Pept. Sci. **2008**, 14, 241

123.7, 59.4, 58.7, 54.3, 45.5, 45.2, 39.6, 30.0, 23.5; MS (ESI, MeOH): Calcd for $C_{35}H_{32}N_2O_6$ $[M+H]^+$ = 577.6; $[M+Na]^+$ = 599.6. Found 577.58, 599.65.

6.2.3 (S)-N-methylalanine (105)[7]

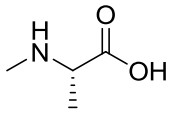

Commercially available Boc-L-Ala (5g, 26.4 mmol) was suspended in 75 ml of toluene, and paraformaldehyde (3.21g) and p-toluenesulfonic acid (0.321g) were added. The mistxure was refluxed until complete disappearance of starting material, determined by TLC, with azeotropic removal of water. The solution was cooled, washed with 1N aqueous $NaHCO_3$ (3 x 25 mL) and dried over $MgSO_4$. Concentration in vacuo gave 4.26g (81% yield) of the oxazolidinone (**104**) as a white crystalline solid. The oxazolidinone (3g, 14.9 mmol) was dissolved in 30 ml (1:1) TFA:DCM and triethylsilane (7.14 ml) was added. The solution was stirred at room temperature overnight and concentrated by a gentle stream of air over mixture, with continual addition of DCM, until a white fluffy powder formed. The white powder was then dissolved in Hexane:MeOH:DCM and heated to dissolved. Upon cooling to room temperature crystallization of product began to occur. After 4 hours the mother liquor was removed, leaving behind a white crystalline solid in its salt form (3.10g, 95% yield). ^1H NMR (400 MHz, CD_3OD) δ 3.9-3.84 (1H, q, J = 7.23, 7.23, 7.21), 3.25 (1H, bs OH), 2.65 (3H, s), 1.48 (3H, d, J = 7.24).

All characterization in accordance to literature.[7]

6.2.4 (S)-N-tert-butoxycarbonyl-2-(hydroxymethyl)-pyrrolidine (49)[8,9]

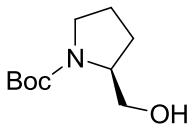

[7] Freidinger, R. et al. **1983**, 48, 77
[8] Zhao, D.; Kuethe, J.T.; Journet, M.; Peng, Z.; Humphrey, G.R.; J. Org. Chem. **2006**, 71, 4336
[9] Reed, P.E.; Katzenellenbogon, J.A. J.Org. Chem. **1991**, 56, 2624

To a heterogeneous mixture of sodium borohydride powder (0.703 g, 18.6 mmol) in isopropyl acetate (100 mL) was added commercially available *N*-Boc-L-proline (2.5 g, 11.6 mmol), at -5 to 0°C in one portion. A gentle evolution of hydrogen gas was observed after the addition. After the reaction mixture was stirred at -5 to 0 °C for 1 h, boron trifluoride etherate (2.92 ml) was added via an addition funnel over 1.5 h maintaining the internal temperature between -5 and 5 °C. The resulting reaction slurry was stirred for an additional 1-2 h at the same temperature and was quenched by the addition of 0.5 N NaOH (200 mL) over 30 min at 0-10 °C. The resulting mixture was heated to 45 °C with vigorous stirring for 10 min to give two clear separated layers which were separated. The lower aqueous layer was back extracted with isopropyl acetate (50 mL). The combined organic extracts were washed with saturated NaCl (200 mL). The organic solution was azeotropically concentrated, and the solvent was switched to heptane. The final volume was adjusted to approximately 230-250 mL. The solution was heated while stirring at 35-40 °C for 1 hour, allowed to rest until reaching room temperature and the product gradually crystallized out (2.13g, 91.4% yield). ^{1}H NMR (400 MHz, $CDCl_3$) δ 4.20 (1H, b, OH), 3.9-3.8 (1H, m), 3.6-3.5 (2H, m), 3.45-3.39 (1H, td, J = 6.96, 6.96, 10.86), 3.3-3.2 (1H, td, J =6.74, 6.74, 10.86), 2.02-1.9 (1H, qd, J = 7.37, 7.37, 7.42, 12.59), 1.86-1.7 (2H, m), 1.6 (1H, bs), 1.44 (9H, s).

All characterization matched with literature.[8]

6.2.5 (S)-N-tert-butoxycarbonyl-2(-4-toluenesulfonyloxy)methylpyrrolidine (50)[10]

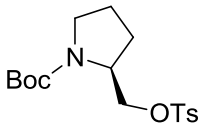

49 (0.500g, 2.48 mmol) was dissolved in 5 ml DCM. To the mixture was added p-toluenesulfonyl chloride (0.710g, 3.72 mmol), 0.52 ml of Et_3N, and DMAP (0.061g, 0.496 mmol) and the mixture was stirred at room temperature overnight. The mixture was transferred into a separtory funnel and washed with 1N HCl (2 x 5 ml). The organic extracts were then washed with a saturated brine solution, dried over $MgSO_4$, and concentrated down in vacuo giving the crude product as a dark, clear, orange viscus oil (0.92g, 110% yield). The crude was purified by flash chromatography giving a clear-orange oil (0.85g, 96% yield). ^{1}H NMR (400 MHz, $CDCl_3$) δ 7.77 (2H, d, J =6.8), 7.33 (2H, m), 4.08 (1H, m), 3.97-3 88 (1H, m), 3 35-3.25 (2H, m), 2.43 (3H, s), 1.95- 1.79 (4H, m), 1.40 (9H, s).

All characterization matched with literature.[10]

[10] Shionogi and Co.; **2006**, patent WO2006/116764A1

6.2.6 (S)-N-tert-butoxycarbonyl-2-(iodomethyl)pyrrolidine (54)[11,12]

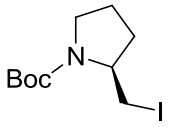

In a flame-dried flask under argon, compound **49** (1.50g, 7.45 mmol) was dissolved in 50 ml distilled toluene. Triphenylphosphine (5.8g, 22.3 mmol), iodine (3.78g, 14.9 mmol), and imidazole (2.03g, 29.8 mmol) were then added in succession, which was stirred overnight at reflux. To quench, 10% HCl was added and the mixture was diluted with 200 ml EtOAc and extracted with EtOAc. The combined organic extracts were washed $NaHCO_3$, brine, then dried over $MgSO_4$. The dried compound was then filtered and then concentrated down in vacuo to afford a crude white solid (2.31g, 99%). Crude **54** was then dissolved in 40 ml Et_2O which causing triphenylphosphine oxide to precipitate out. The dissolved compound was then filtered and concentrated down in vacuo.The crude residue was purified by flash chromatography affording a pale-yellow solid (1.86g, 80%).^{1}H NMR (400 MHz, 40^{o}C, CDCl3) δ 3.87 (1H, m), 3.52-3.14 (4H, M), 2.14-1.79 (4H, m), 1.48 (9H, s). ESI-MS calcd for $C_{10}H_{18}NO_3I$ $[M+Na]^+$: 334.98. Found: 334.95. IR(film): 2972.1, 1652.6, 1395.8, 1363.58, 1163.0, 1107.06, 769.54.

All characterization matched with literature.[12]

6.2.7 (S)-N-tert-butoxycarbonyl-2-(Fluoromethyl)pyrrolidine (55)[13]

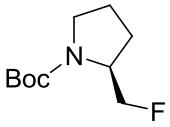

In a flame dried flask, under argon, compound **49** (2g, 9.93 mmol) was dissolved in 30 ml of distilled DCM. To this solution was added 2.77 ml of triethylamine, DMAP

[11] Garegg, P.J.; Ortega, C.; Samuelsson, B.; Journal of the Chemical Society, Perkin Transaction 1, **1982**, 681
[12] Ku, Y.; Cowart, M.D.; Padam, N.; Patent US2004/171845A1, **2004**
[13] Rosen, T.; Chu, D.T.W.; Lico, I.; Fernandes, P.B.; Marsh, K.; Shen, L.; Cepa, V.G.; Pernet, A. J. Med. Chem. **1988**, 31, 1598

(0.121g, 0.993 mmol) and the reaction was cooled to 0°C with an ice-salt bath, 1.93 ml of methanesulfonyl chloride was added drop wise, and the reaction mixture was stirred overnight, allowing the reaction temperature to reach room temperature. The mixture was diluted with DCM, washed with 10% HCl and saturated sodium bicarbonate and brine, dried with $MgSO_4$ and then concentrated down in vacuo to obtain a 3.07g (81.2% crude yield) of a yellow oil. The oil was then transferred to a flame dried flask under argon and 74 ml of 1 M tetra-n-butylammonium fluoride in THF was added to the system. This mixture was then heated to reflux overnight. The mixture was then concentrated down in vacuo, and the residue was taken up in EtOAc and washed with saturated sodium bicarbonate, dried with $MgSO_4$, and concentrated down in vacuo. The crude material was purified by flash chromatography affording **55** as a pale yellow oil. ^{1}H NMR (400 MHz, 40°C, CDCl3) δ 3.87 (1H, m), 3.52-3.14 (4H, M), 2.14-1.79 (4H, m), 1.45 (9H, s). ESI-MS calcd for $C_{10}H_{18}NO_3F$ $[M+H]^+$: 204.21 $[M+Na]^+$: 226.186. Found: 204.18 and 226.16. IR(film): 2972.1, 1689.5, 1395.8, 1365.51, 1164.9, 1005.0, 785.54.

6.2.8 (S)-N-tert-butoxycarbonyl-2-(azidomethyl)pyrrolidine (51)[14,15]

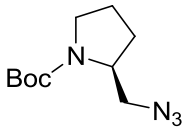

Compound **50** (2.5g, 7.02 mmol) was dissolved in dry DMSO (74 ml) and sodium azide (2.74g, 4.21 mmol) was added. The reaction mixture was heated to 64°C for 20 h, allowed to cool to room temperature and diluted with diethyl ether (200 ml). The organic phase was washed with H_2O (3 x 250 ml) and brine, dried with $MgSO_4$ and the solvent concentrated down in vacuo. The crude product (1.40g, 91% yield) was not further purified, but was used directly for the next reaction. ^{1}H NMR (400 MHz, 40°C, CDCl3) δ 3.88 (1H, m), 3.58-3.10 (4H, M), 2.08-1.72 (4H, m), 1.48 (9H, s). ESI-MS calcd for $C_{10}H_{18}N_4O_3$ $[M+H]^+$: 227.14 $[M+Na]^+$: 249.15. Found: 227.10 and 249.13. IR(film): 2092.62, 1693.38, 1691.46, 1387.69, 1365.51, 1163, 1155.28, 1106.1, 628.75

All Characterization matched with literature.[15]

6.2.9 (S)-N-tert-butoxycarbonyl-2-(aminomethyl)pyrrolidine (52)[16]

[14] Dahlin, N.; Bogevig, A.; Adolfsson, H.; Adv. Synth. Catal. **2004**, 346, 1101
[15] Bellis, E. et al. Synthesis, **2005**, 14, 2407
[16] Slaitas, A.; Yeheskiely, E.; European Journal of Org. Chem. **2002**, 14, 2391

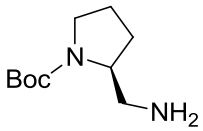

Azide (**51**) (1.40g, 6.19 mmol) in anhydrous THF (60 ml) was reduced with triphenylphosphane (3.40g, 13 mmol) and water (0.245 ml). The reaction mixture was heated to reflux until all the starting material had been consumed. The organic solvent was removed under reduced pressure. Diethyl ether (150 ml) was added to the remaining pale yellow oil, and the pH of the aqueous phase was lowered to 1.75 with 2N HCl. The aqueous layer was separated and washed with diethyl ether (2 x 100 ml), and the pH was then adjusted to 13.0 with 2N NaOH. After extraction with DCM (7 x 100ml), the combined organic phases were dried over $MgSO_4$, filtered, and concentrated down under reduced pressure. Amine (**52**) was obtained as a colourless liquid (0.90g, 73% crude yield) and used without additional purification. ^{1}H NMR (400 MHz,CDCl3) δ 3.82 (1H, m), 3.52-3.27 (2H, m), 3.18-2.62(4H, m), 2.12-1.64 (4H, m), 1.46 (9H, s). ESI-MS calcd for $C_{10}H_{20}N_2O_3$ $[M+H]^+$: 201.29 $[M+Na]^+$: 224.52. Found: 201.27 and 224.48. IR(film): 3480, 3066.61, 3053.11, 2974.03, 1683.74, 1558.38, 1434.94, 1394.44, 1178.43, 1118.64, 740.61, 719.40

All characterization matched with literature.[16]

6.2.10 (S)-N-tert-butoxycarbonyl-2-((4-(4-tert-butylphenyl)-1H-1,2,3-triazol-1-yl)methyl)pyrrolidine (56)[17]

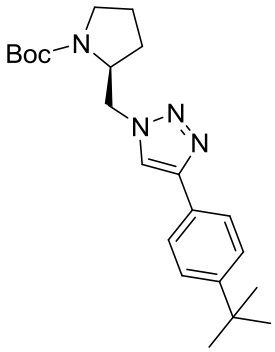

Compound **51** (0.300g, 1.33 mmol) was dissolved in toluene (8 ml) and t-butanol (2 ml). To the dissolved compound was added 4-tertbutyl-phenylacetylene (0.314g, 1.99 mmol), CuI (0.253g, 1.33 mmol), and DIPEA (0.460 ml). The reaction mixture was stirred overnight at room temperature. The solvent was concentrated down under reduced pressure affording a off-white solid (0.508g, crude yield 98%), which was then

[17] Luo, S. et al. J. Org. Chem., **2006**, 71, 9244

purified by flash chromatography to afford a white fluffy solid (0.312g, 62%). ^{1}H NMR (400 MHz,CDCl3) δ 7.74 (2H, m), 7.45 (2H, d, J = 8.44 Hz), 4.72-4.48(2H, m), 4.13 (1H, s), 3.4-3.08 (2H, m), 1.96 (2H, dd, J = 7.07, 15.59 Hz), 1.73-1.71 (1H, m), 1.51 (9H, s, $(CH_3)_3O$), 1.34 (9H, s, $(CH_3)_3C$). ^{13}C NMR (101 MHz, $CDCl_3$) δ 154.8, 151.2, 147.7, 127.8, 125.7, 125.3, 120.1, 79.9, 57.2, 51.4, 47.1, 34.6, 31.2, 28.5, 28.2, 23.3. ESI-MS calcd for $C_{22}H_{32}N_4O_2$ $[M+H]^+$: 385.25 $[M+Na]^+$: 408.26 Found: 385.232 and 408.22.

6.2.11 (S)-N-tert-butoxycarbonyl-2-((naphthalene-2-ylthio)methyl)pyrrolidine (57)[18]

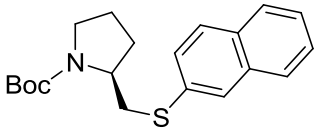

Sodium hydride (60%) (0.253g, 6.32 mmol) was pretreated by washing with hexanes in a flame dried double-neck flask under argon. Hexans were taken out, and distilled THF (10 ml) was added. Thereafter, 2-naphthalenethiol (0.810g, 5.05 mmol) was added and stirred at 0^{o}C. A solution of **50** (0.900g, 2.53 mmol) in dry distilled THF (10 ml) was slowly added over the course of 5 min. The resulting mixture was heated to reflux for until all starting material had been consumed (6 h). The reaction was quenched with water (10 ml), stirred vigorously at 0^{o}C (30 min), and then extracted with DCM (3 x 20 ml). The combined organic layers were dried over $MgSO_4$, filtered, and concentrated down under reduced pressure to afford a crude beige powder (0.810g, 93% crude yield). The crude **57**was purified by flash chromatography to yield the desired product as a white powder (0.64g, 76% yield). %). ^{1}H NMR (400 MHz,CDCl3) δ 7.97 (0.5H, s), 7.83 (0.5H, s), 7.77-7.73 (3H, m), 7.50-7.40 (3H, m), 4.12 (0.5H, s), 3.96 (0.5H, s), 3.64-3.35 (3H, m), 2.93-2.75 (1H, m), 2.04-1.78 (4H, m), 1.43 (9H, s). ^{13}C NMR (101 MHz, $CDCl_3$) δ 153.7, 133.7, 131.8, 128.4, 128.3, 127.9, 127.6, 127, 126.6, 126.3, 125.7, 125.3, 79.7, 56.5, 47.1, 46.6, 37.3, 35.6, 30, 29.5, 28.5, 23.6, 22.7. ESI-MS calcd for $C_{20}H_{25}NO_2S$ $[M+H]^+$: 344.45 $[M+Na]^+$: 377.46 Found: 344.16 and 477.38

All characterization matched literature.[18]

6.2.12 (S)-N-tert-butoxycarbonyl-2-((1-phenyl-1H-tetrazole-5-ylthio)methyl)pyrrolidine (53)[19]

[18] Syu, S.; Kao, T.; Lin, W.; Tetrahedron, **2010**, 66, 891
[19] Sen, S.E.; Roach, S.L. Synthesis, **1995**, 756

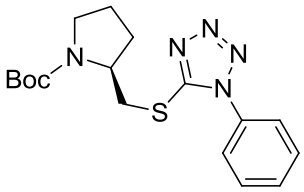

To a flame dried flask under argon, **49** (0.500g, 2.5 mmol) was dissolved in dry THF (20 ml). Thereafter, 1-phenyl-1H-tetrazole-5-thiol (0.89g, 4.99 mmol) and triphenylphosphine (1.31g, 4.99 mmol) was added to the flask. DIAD (0.98 ml, 4.99 mmol) was added dropwise in to the reaction mixture and stirred for 3 hr. To quench the reaction, $NaHCO_3$ (20 ml) was added and extracted with diethyl ether (3 x 15 ml). The combined organic extracts were washed with brine (20 ml), dried with $MgSO_4$, filtered, and concentrated down under reduced pressure affording crude **53** (0.79g, 87% yield) which was then purified by flash chromatography. Giving the final product as a white crystalline solid (0.65g, 72% yield). ^{1}H NMR (400 MHz,CDCl3) δ 7.58-7.51 (5H, m), 4.20-4.17 (1H, m), 3.71-3.34 (4H, m), 2.07-1.82 (4H, m), 1.45 (9H, s). ^{13}C NMR (101 MHz, $CDCl_3$) δ 154.1, 152.6, 133.7, 129.5, 129.1, 125.7, 79.7, 56.5, 46.7, 35.68, 28.5, 23.6, 22.8. ESI-MS calcd for $C_{17}H_{23}N_5O_2S$ $[M+H]^+$: 362.46. Found: 362.43

6.2.13 (S)-N-tert-butoxycarbonyl-2-((3,5-bis(trifluoromethyl)benzamido)methyl)pyrrolidine (58)[20]

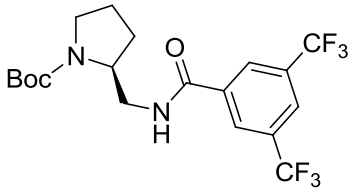

In a flame dried flask under argon, 3,5-bis(trifluoromethyl)benzoic acid (0.206g, 0.799 mmol) was dissolved in distilled DCM and dry acetone (10:1). HBTU (0.364g, 0.959 mmol) and HOBT (0.122g, 0.799 mmol) were added to the dissolved compound and stirred for 45 minutes. To the stirred mixture was added **52** (0.160g, 0.799 mmol), dissolved in dry DCM, and distilled DIPEA (0.278 ml), and the reaction was stirred at room temperature overnight. Upon consumption of the starting material, the solution was diluted with DCM and washed with 10% HCl (2 x 10 ml). The organic phase was then dried with $MgSO_4$, filtered, and concentrated down under reduce pressure. The crude product was purified by flash chromatography to give an amorphous white solid (0.253g, 72% yield). ^{1}H NMR (400 MHz,CDCl3) δ 9.24 (1H, bs), 8.39 (1H, s), 7.95 (1H, s), 4.23-4.17 (1H, m), 3.62-3.57 (1H, ddd, J = 2.99, 4.17, 13.56 Hz), 3.46-3.32 (3H, m),

[20] Slaitas, A.; Yeheskiely, E. European Journal of Org. Chem., **2002**, 66, 891

2.14-1.88 (3H, m), 1.76-1.70 (1H, tdd, J = 3.26, 3.26, 6.14, 12.45 Hz), 1.46 (9H, s). ^{13}C NMR (101 MHz, $CDCl_3$) δ 163.9, 157.6, 136.03, 131.9, 131.5, 127.4, 127.39, 121.5, 80.8, 55.9, 47.7, 47.3, 29.4, 28.1, 23.8. ESI-MS calcd for $C_{19}H_{22}F_6N_2O_3$ $[M+H]^+$: 441.38 $[M+Na]^+$: 464.40. Found: 441.36, 464.38.

6.2.14 (S)-N-tert-butoxycarbonyl-2-((2,2,2-trifluoroacetamido)methyl)pyrrolidine (59)[20]

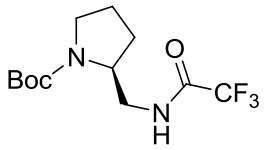

Compound **59** was synthesized using the same procedure as for **58**, and obtained an amorphous white solid (0.430g, 97% yield). ^{1}H NMR (400 MHz,CDCl3) δ 9.04 (1H, s), 4.10-4.05 (1H, m), 3.42-3.28 (3H, ddt, J = 4.34, 12.32, 16.58, 16.58 Hz), 3.21-3.14 (1H, m), 2.08-1.98 (1H, tt, J = 5.44, 5.44, 8.35, 8.35 Hz), 1.92-1.81 (2H, dq, J = 7.79, 13.01, 13.27, 13.27 Hz), 1.64-1.57 (1H, m), 1.42 (9H, s). ^{13}C NMR (101 MHz, $CDCl_3$) δ 157.8, 157.4, 117.45, 80.8, 55.56, 47.31, 46.9, 29.53, 28.29, 23.93. ESI-MS calcd for $C_{12}H_{19}F_3N_2O_3$ $[M+H]^+$: 297.28 $[M+Na]^+$: 320.32. Found: 297.27, 320.28.

General Procedure for Synthesis of **43** and derivatives thereof.

In a flame dried flask under argon, L-Fmoc-propargyl glycine (0.40g, 1.12 mmol) was dissolved in dry DMF. HCTU (0.500g, 1.43 mmol) was added to the dissolved compound and stirred for 45 minutes. To the stirred mixture was added Boc-deprotected version of compound **43** (0.290g, 1.13 mmol) in its HCl salt form, dissolved in dry DMF, and distilled DIPEA (0.416 ml), and the reaction was stirred at room temperature overnight. Upon consumption of the starting material, the solution was concentrated down under reduced pressure, re-suspended with DCM and washed with 10% HCl (2 x 10 ml). The organic phase was then dried with $MgSO_4$, filtered, and

concentrated down under reduce pressure. The crude product (**61**) (0.540g, 81% yield) was not purified at this stage. The crude compound was then dissolved in dry DMF (2 ml), to which 10 ml of 20% piperdine solution in DMF was then added. The reaction was stirred at room temperature until compete disappearance of starting material and then concentrated down under reduced pressure. The crude compound was then re-suspended in dry acetonitrile (5 ml), to which Boc-anhydride (0.233g, 1.07 mmol) and distilled DIPEA (0.375 ml) were added sequentially. The reaction mixture was stirred at room temperature overnight. Upon consumption of the starting material, the solution was concentrated down under reduced pressure, re-suspended with DCM and washed with 10% HCl (2 x 10 ml). The organic phase was then dried with $MgSO_4$, filtered, and concentrated down under reduce pressure. The crude Boc-protected di-amino acid product (**62**) (0.253g, 80%) was then purified by flash chromatography to give a bright-white solid. Boc-protected amino acid(s) were then treated with 5N or 10N HCl at room temperature and stirred until the Boc-protecting group had been fully removed. The HCl slat form of **62** was not purified and continued into the sequential step. In a flame dried flask under argon, N-Boc-N-methylalanine (0.132g,0.65 mmol) was dissolved in dry DMF. HCTU (0.296g, 0.715 mmol) was added to the dissolved compound and stirred for 45 minutes. To the stirred mixture was added Boc-deprotected version of compound **62** (0.220g, 0.65 mmol) in its HCl salt form, dissolved in dry DMF, and distilled DIPEA (0.226 ml), and the reaction was stirred at room temperature overnight. Upon consumption of the starting material, the solution was concentrated down under reduced pressure, re-suspended with DCM and washed with 10% HCl (2 x 10 ml). The organic phase was then dried with $MgSO_4$, filtered, and concentrated down under reduce pressure. The product was then purified by flash chromatography to give **63** as beige amorphous solid (0.260g, 76% overall yield). The beige solid was then used to synthesize **60**, described below, or treated with 10N HCl giving compound **43** (0.028g, 95% yield) which was used without further purification in testing on the cell line.

6.2.15 N-tert-butoxycarbonyl-N-Methyl((S)-1-((S)-2((napthalen-2-ylthio)methyl)pyrrolidin-1-yl)-1-oxopent-4-yn-2-yalamino)-1-oxopropan-2-yl) (62)

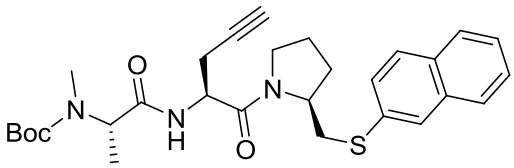

^{1}H NMR (400 MHz,CDCl3) δ major rotamer 8.21 (1H, bs), 8.11-8.01 (3H, m), 7.94-7.54 (4H, m), 5.39-5.12 (1H, m), 4.65 (1H, m), 4.31-4.12 (1H, m), 3.92-3.25 (4H, m), 3.04 (3H, s), 2.79-1.85 (7H, m), 1.75 (9H, s), 1.50 (3H, d, J = 6.76 Hz). ^{13}C NMR (101 MHz, $CDCl_3$) δ major rotamer 175.6, 170, 169.9, 153.6, 133.8, 131.65, 128.34, 127.59,

127.15, 126.73, 126.4, 126.24, 125.4, 79.8, 71.8, 58.97, 57.07, 57.0, 50, 49.8, 46.9, 43.3, 34.7, 30.3, 28.75, 28.4, 24.1, 14.4. ESI-MS calcd for $C_{29}H_{37}N_3O_4S$ $[M+1]^{+:}$ 524.68, $[M+Na]^+$: 547.69, [M-Boc]: 424.68. Found: 524.65, 547.55, and 424.37.

6.2.16 (S)-2-(methylamino)-N-((S)-2-((napthalen-2-ylthio)methyl)pyrrolidin-1-yl)-1-oxopent-4-yn-2-yl)propanamide (43)

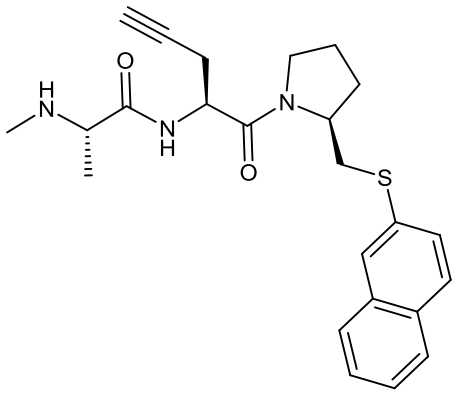

^{1}H NMR (400 MHz,CDCl3) δ 7.9 (1H, s), 7.85-7.73 (3H, m), 7.65-7.2 (4H, m), 4.42-4.03 (3H, m), 3.6-3.47 (4H, m), 2.9 (1H, m), 2.46 (2H, s), 2.02 (3H, d, J = 4.31 Hz), 1.97-1.39 (5H, m), 1.29 (3H, d, J = 6.80 Hz). ^{13}C NMR (101 MHz, $CDCl_3$) δ 174.6, 169, 132.8, 130.6, 127.3, 126.5, 126.1, 125.7, 125.3, 125.2, 78.8, 70.8, 56, 55.9, 42.3, 33.7, 29.3, 27.7, 23.1, 13.4. ESI-MS calcd for $C_{24}H_{29}N_3O_4S$ $[M+1]^{+:}$ 424.58, $[M+Na]^+$: 447.57. Found: 424.38, 447.52.

6.2.17 (2S,2'S)-N,N'-((2S,9S)-1,10-bis((S)-2-((naphthalen-2-ylthio)methyl)pyrrloidin-1-yl)-1,10-dioxodeca-4,6,-diyne-2,9-diyl)bis(2-(methylamino)propanamide) (60)[21]

[21] Harran et al. US Patent **2007**, US007309792B2

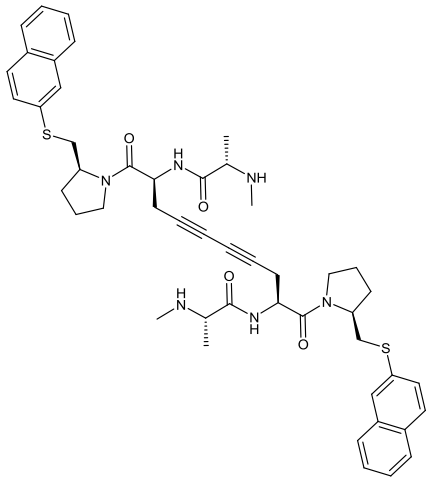

Compound **63** (0.020g, 0.0382 mmol) was dissolved in distilled acetonitrile (5 ml), to this was added $Cu(OAc)_2$ (0.0485g, 0.267 mmol) and the mixture was refluxed (1 h). After 1 hour to the mixture was added triethylamine (0.320 ml) and the reaction mixture was allowed to cool to room temperature and stirred overnight. The solvent was concentrated down under reduced pressure and the Cu(II) salt was removed by filtering over a short ppad of silica gel eluting with DCM:MeOH (9:1) to afford crude **60** boc-protected (0.0367g, 92 yield) as white foam. The crude was not further purified. The boc protected crude (0.0367g, 0.035 mmol) was dissolved in 10N HCl (2 ml), and stirred at room temperature until complete boc removal determined by thin layer chromatography. The solvent was concentrated down under reduce pressure, affording **60** as a yellow foam (0.0296g, 81% yield). The compound was not further purified and tested in-vitro. ^{13}C NMR (101 MHz, $CDCl_3$) δ 170.3, 168.9, 134.1, 131.9, 128.5, 127.8, 127.4, 126.9, 126.6, 126.5, 125.6, 71.2, 66.9, 66.9, 59.2, 57.2, 50.2, 47.1, 43.6, 35, 30.5, 29, 24.4, 14.7. ESI-MS calcd for $C_{24}H_{29}N_3O_4S$ $[M+1]^{+:}$ 845.38 $[M+Na]^+$: 868.42 Found: 845.13, 868.38.

Claims to Original Research

1. Synthesis of novel divalent Smac mimetics (**31-38**) tethered together through an L-ornithine or gama-amino butyric acid, with slight introduction of rigidity, and containing either a forward-reverse sequence or a forward-forward sequence. Allowing to investigate the preference in BIR domain binding based on direction of sequence and limits of rigidity.

2. Synthesis and investigation into propargyl glycine based monovalent Smac mimetics (**39-45**) and bridged acetylene Smac mimetic (**60**) varied at P4, and their ability to induce apoptosis in MDA-MB-231 cancer cell line.

APPENDIX –

Selected NMR Spectra

N-α-N-δ-bis(9-fluorenylmethyloxycarbonyl)-L-ornithine (27), ^{1}H NMR (400 MHz, $CDCl_3$)

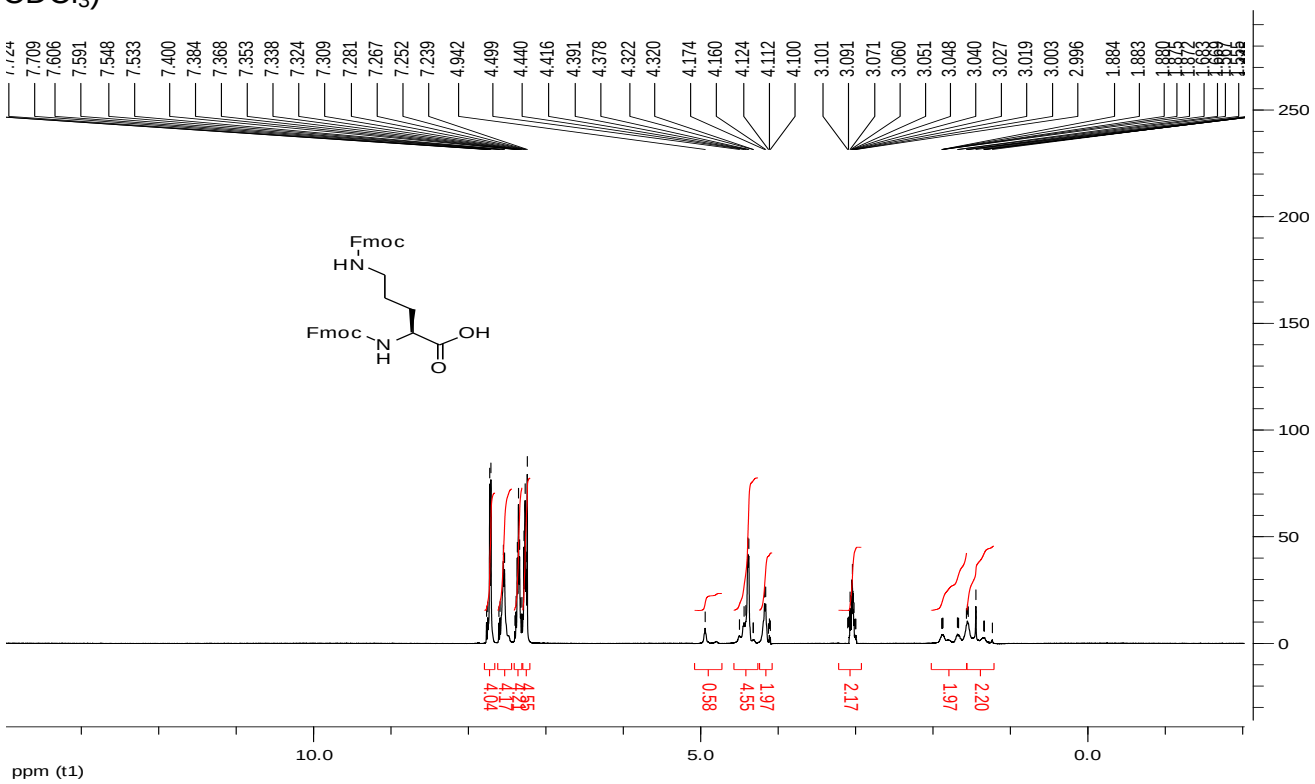

^{13}C NMR (100 MHz, $CDCl_3$

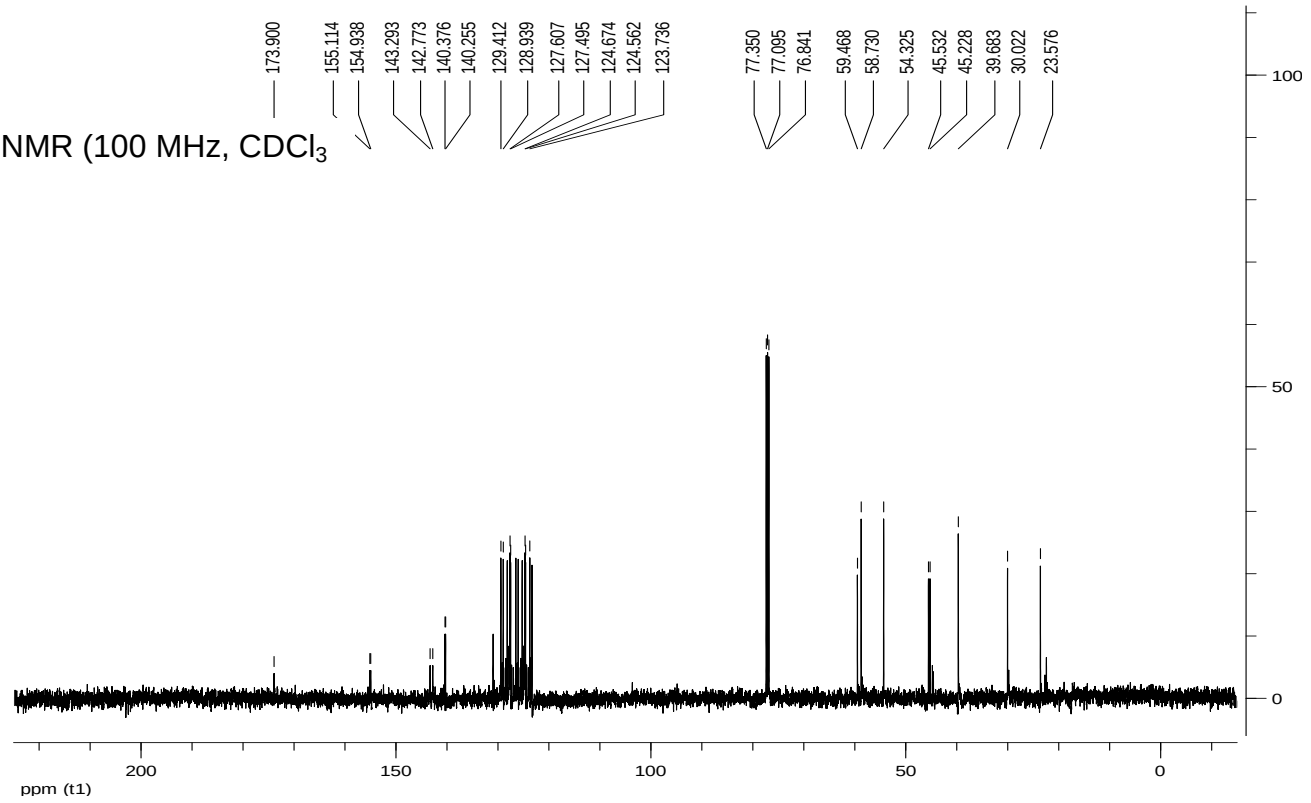

(S)-N-methylalanine (30)

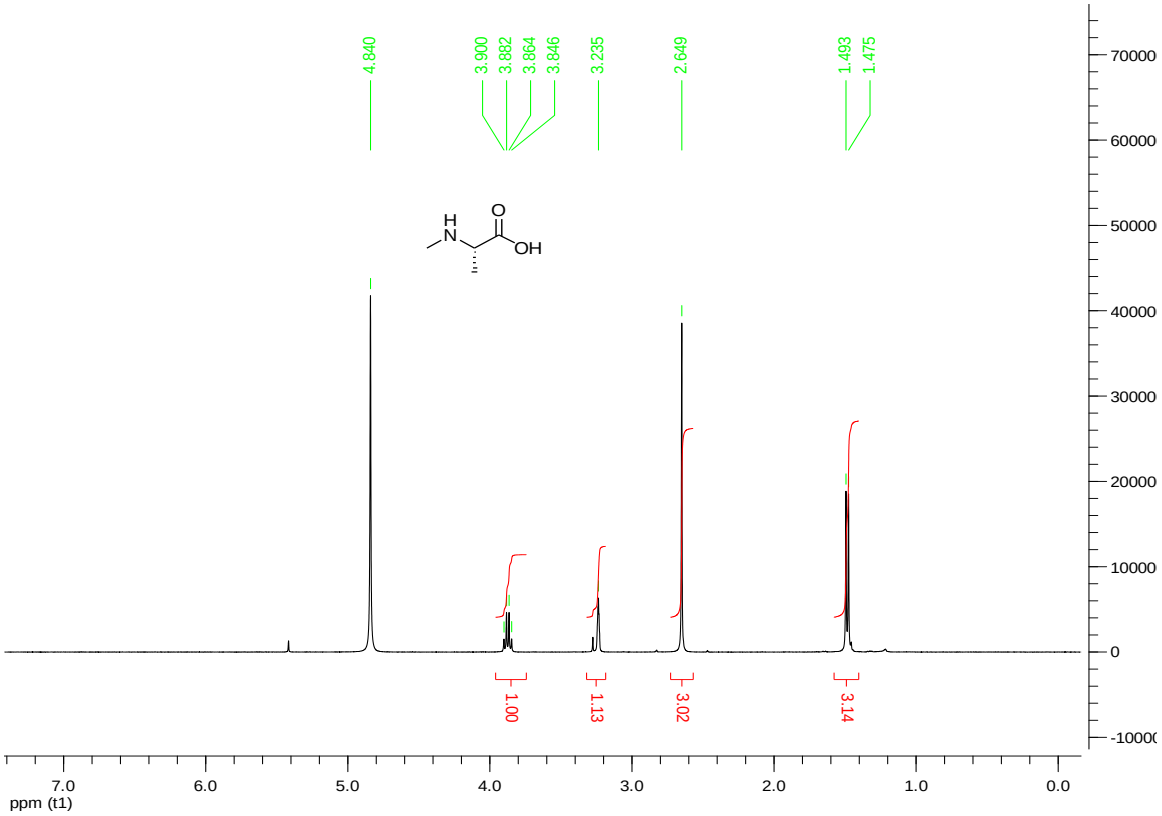

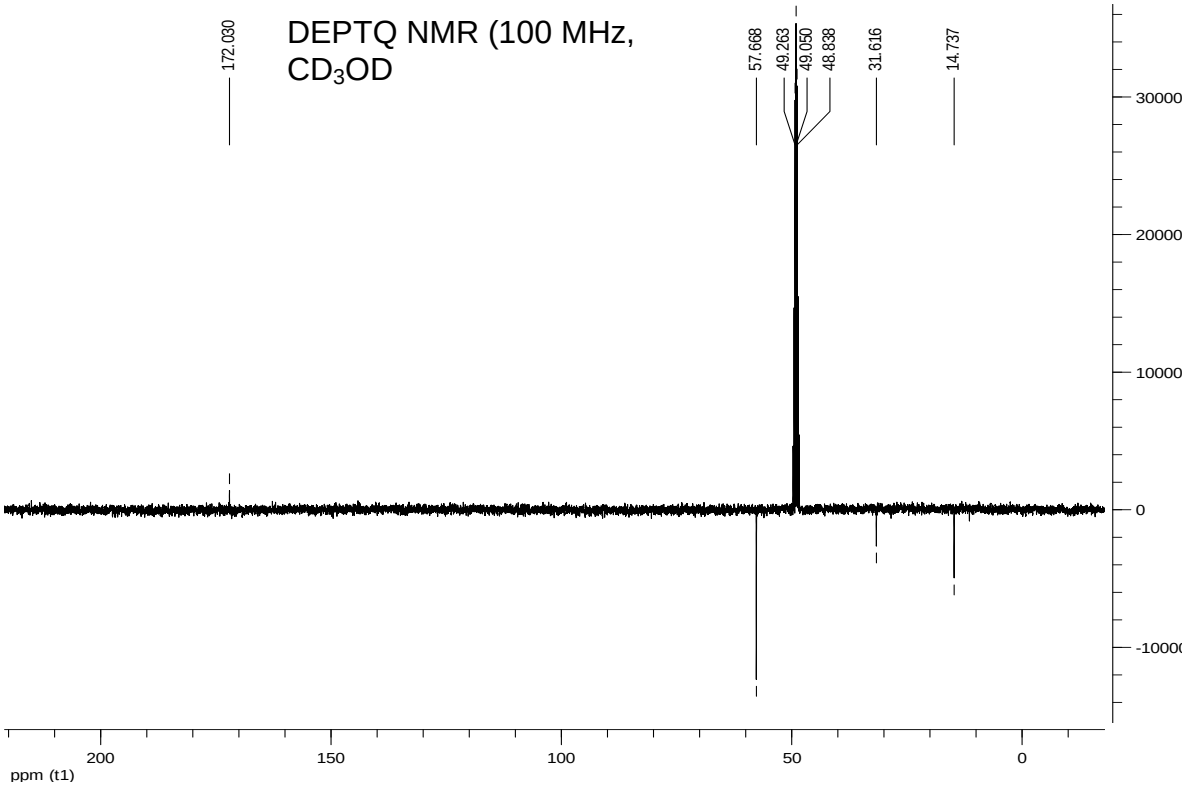

(S)-N-tert-butoxycarbonyl-2-(hydroxymethyl)-pyrrolidine (49)

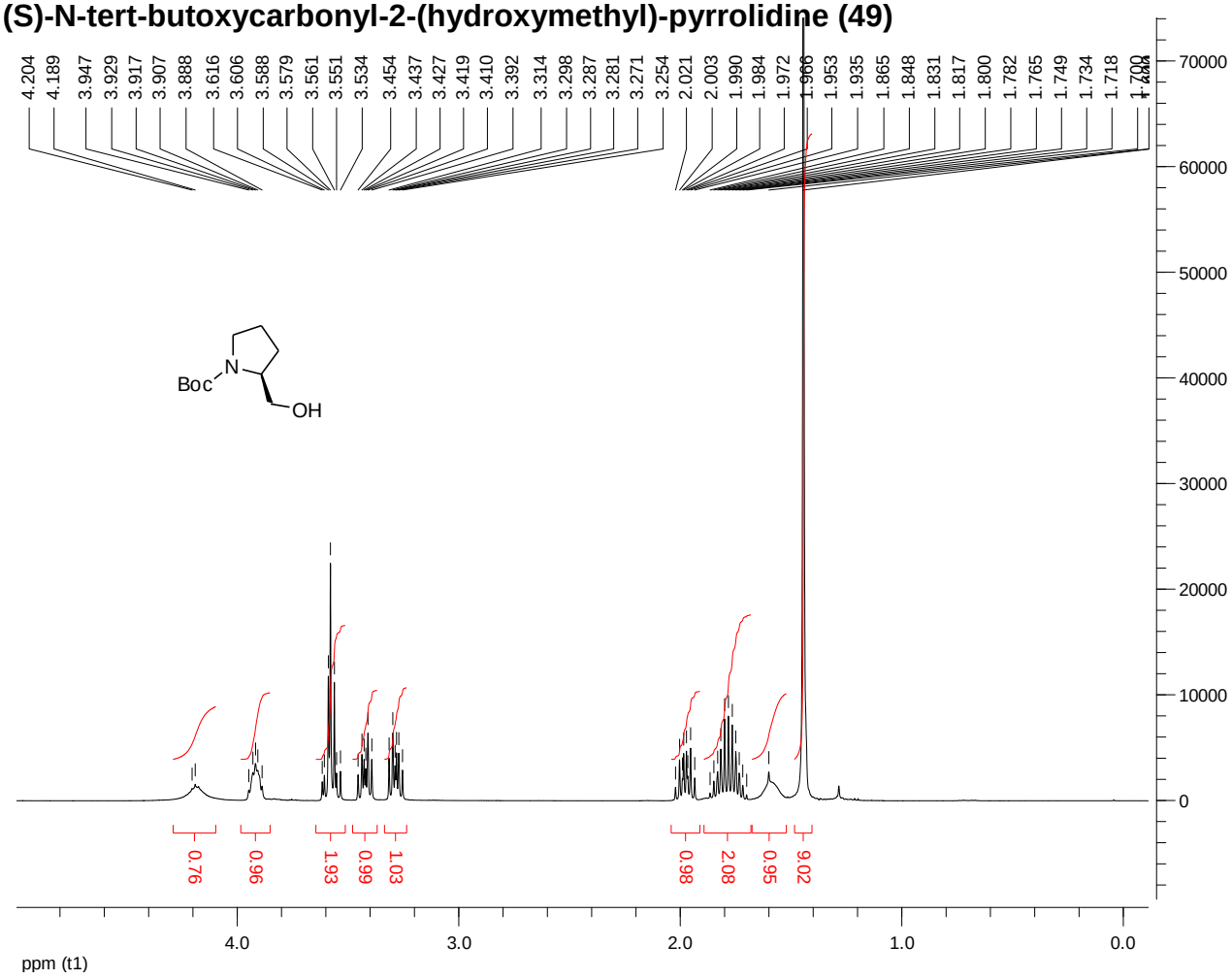

(S)-N-tert-butoxycarbonyl-2-(Fluoromethyl)pyrrolidine (55)

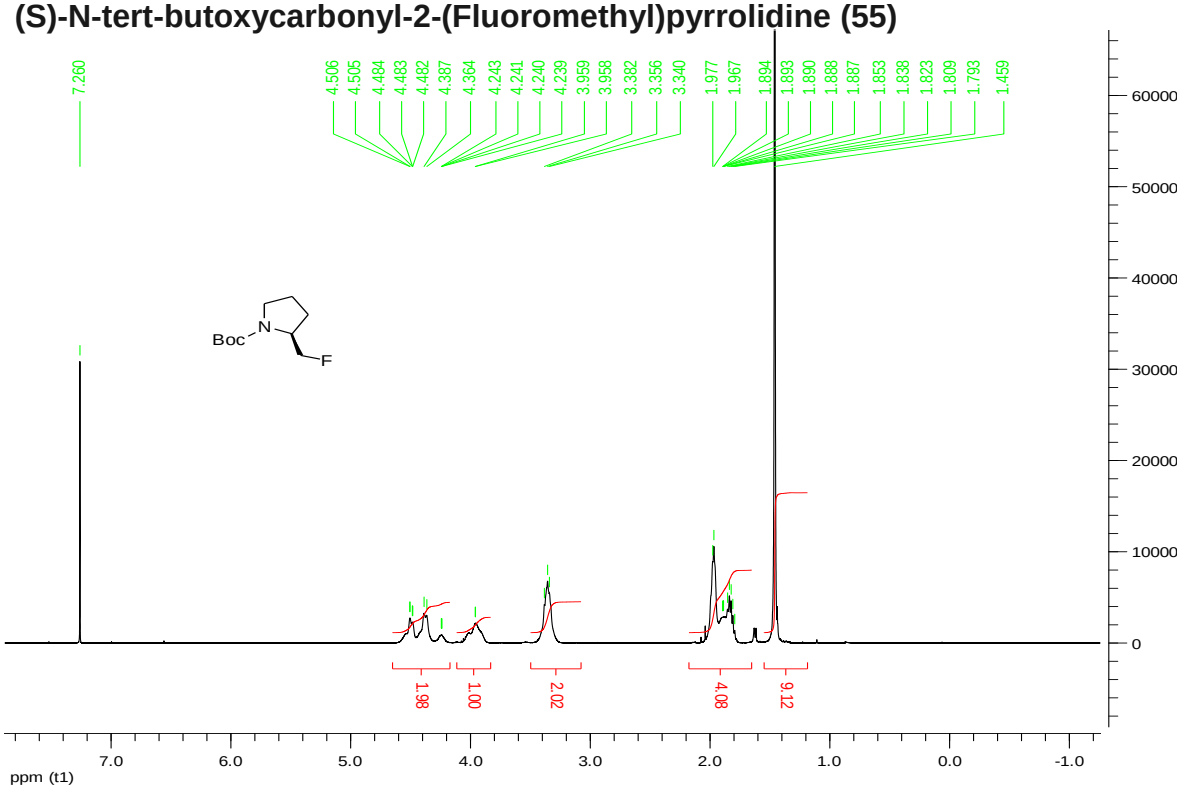

^{13}C NMR (100 MHz, $CDCl_3$)

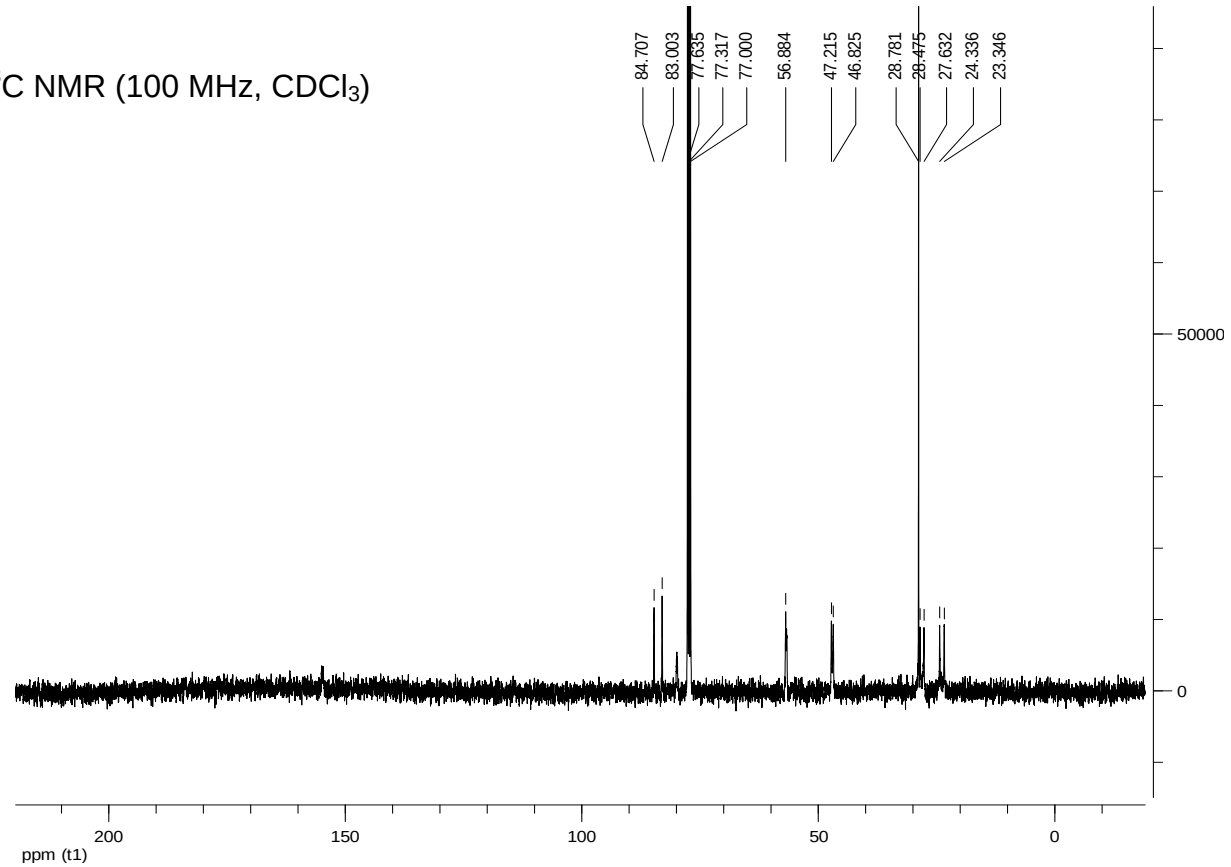

(S)-N-tert-butoxycarbonyl-2-((4-(4-tert-butylphenyl)-1H-1,2,3-triazol-1-yl)methyl)pyrrolidine (56)

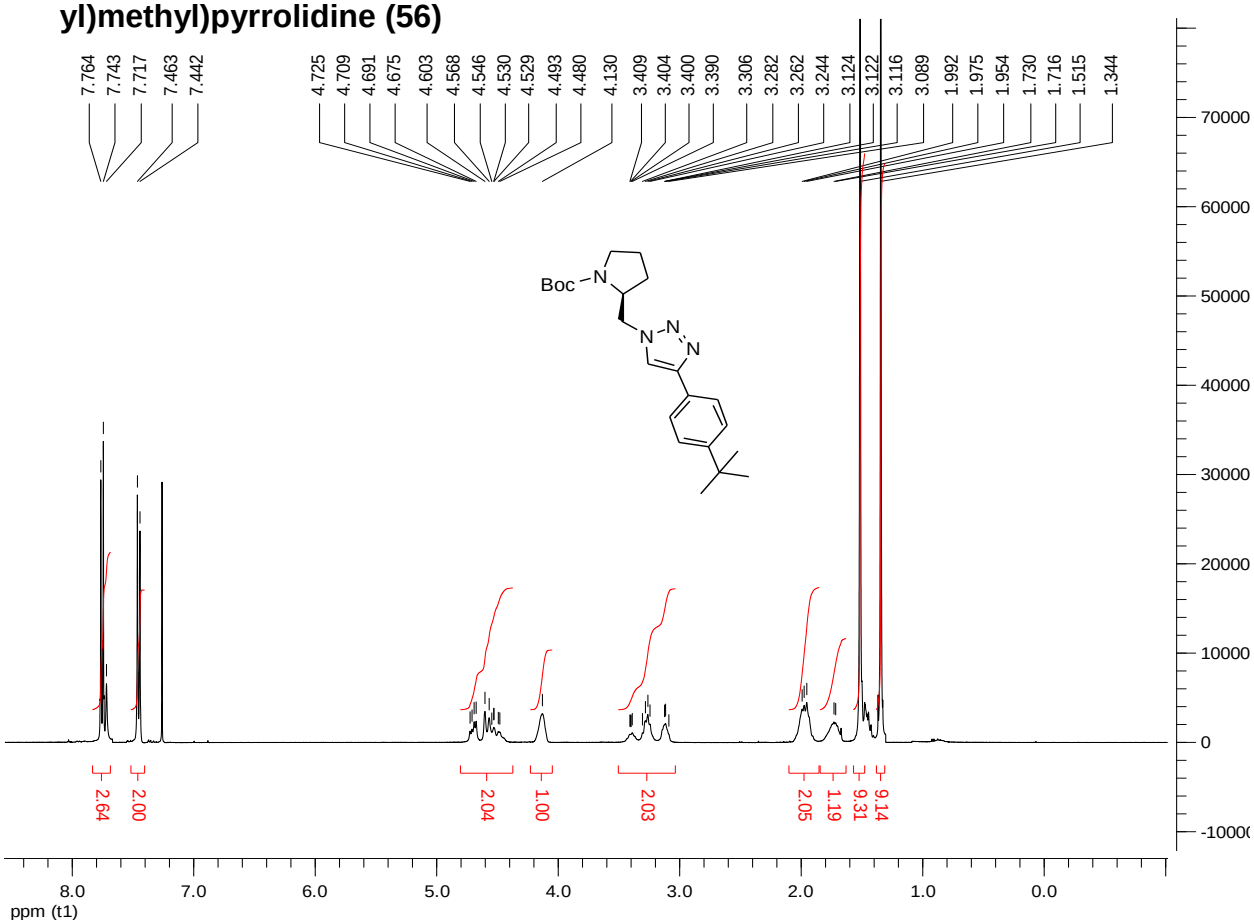

^{13}C NMR (100 MHz, $CDCl_3$)

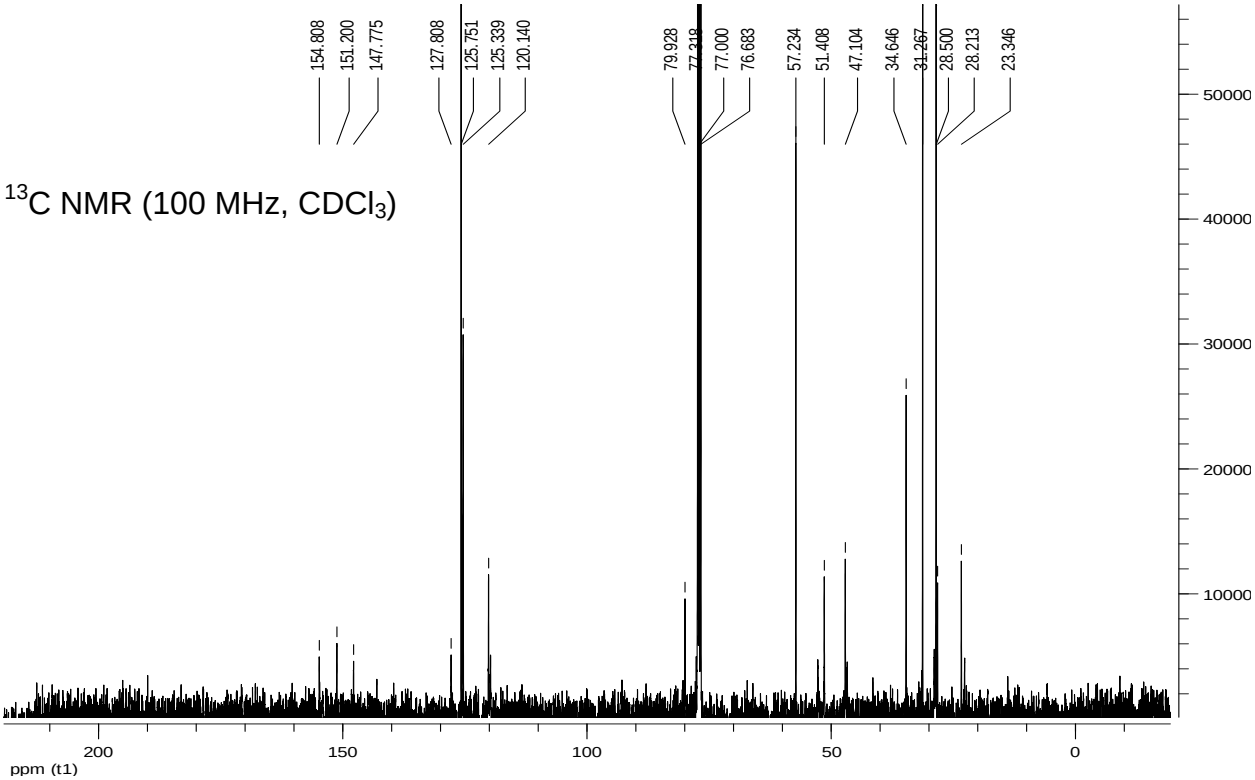

DEPTQ-135 NMR (100 MHz, $CDCl_3$)

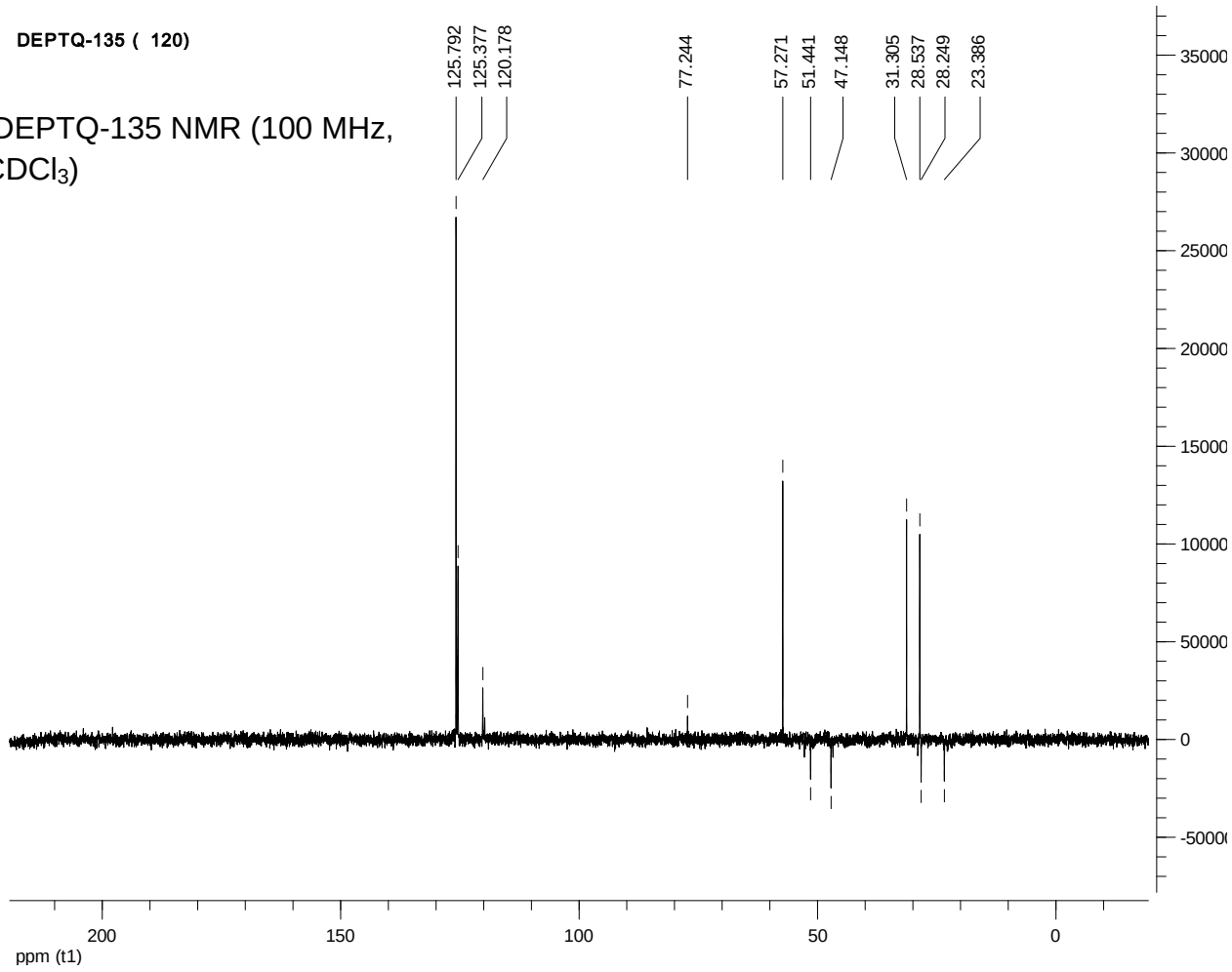

(S)-N-tert-butoxycarbonyl-2-((3,5-bis(trifluoromethyl)benzamido)methyl)pyrrolidine (58)

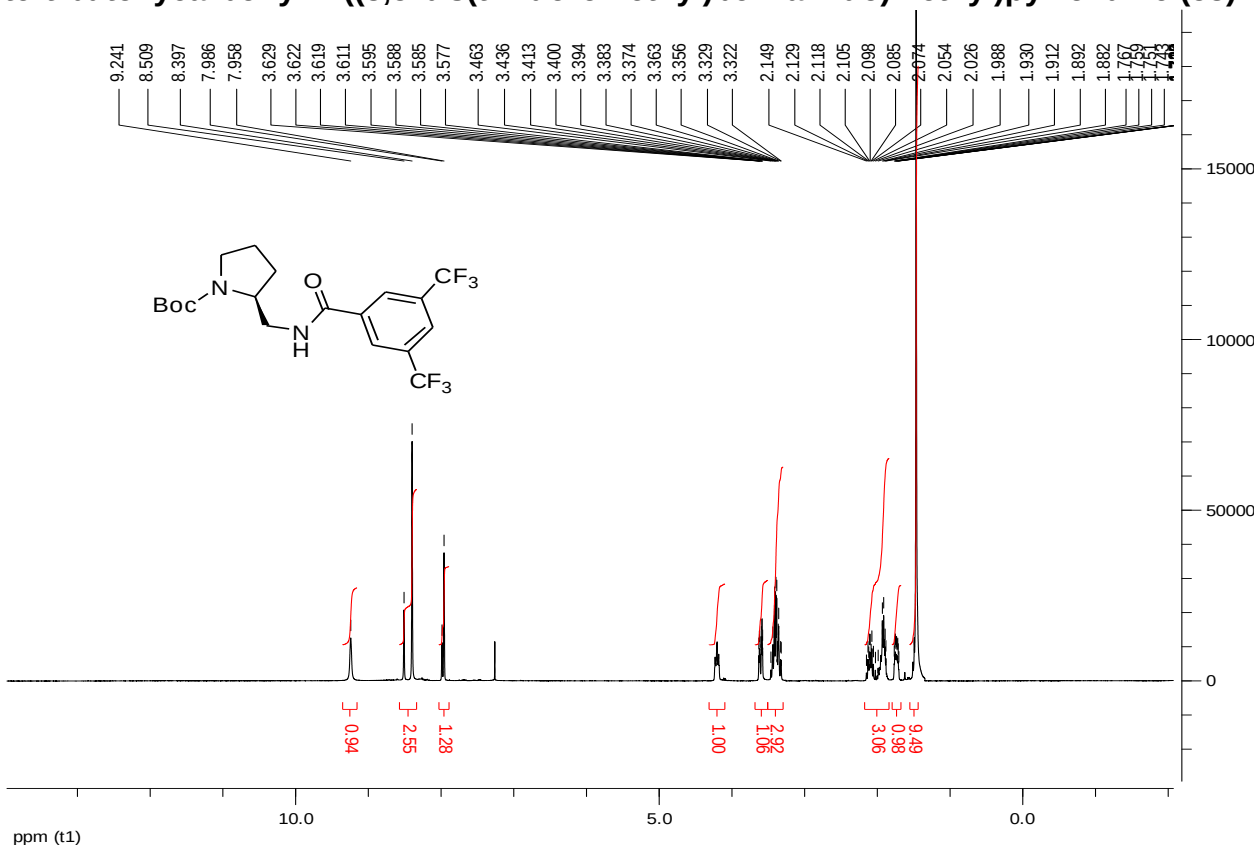

^{13}C NMR (100 MHz, $CDCl_3$)

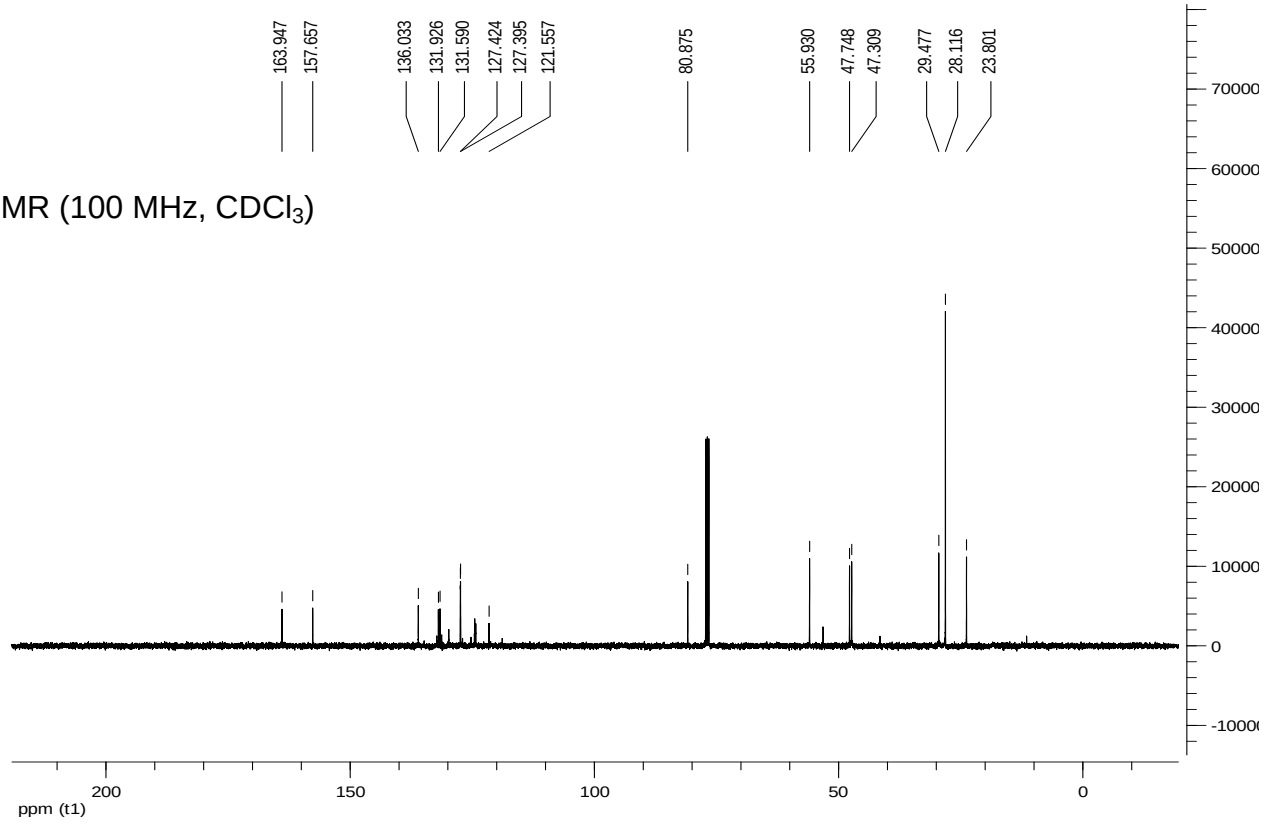

(S)-N-tert-butoxycarbonyl-2-((2,2,2-trifluoroacetamido)methyl)pyrrolidine (59)

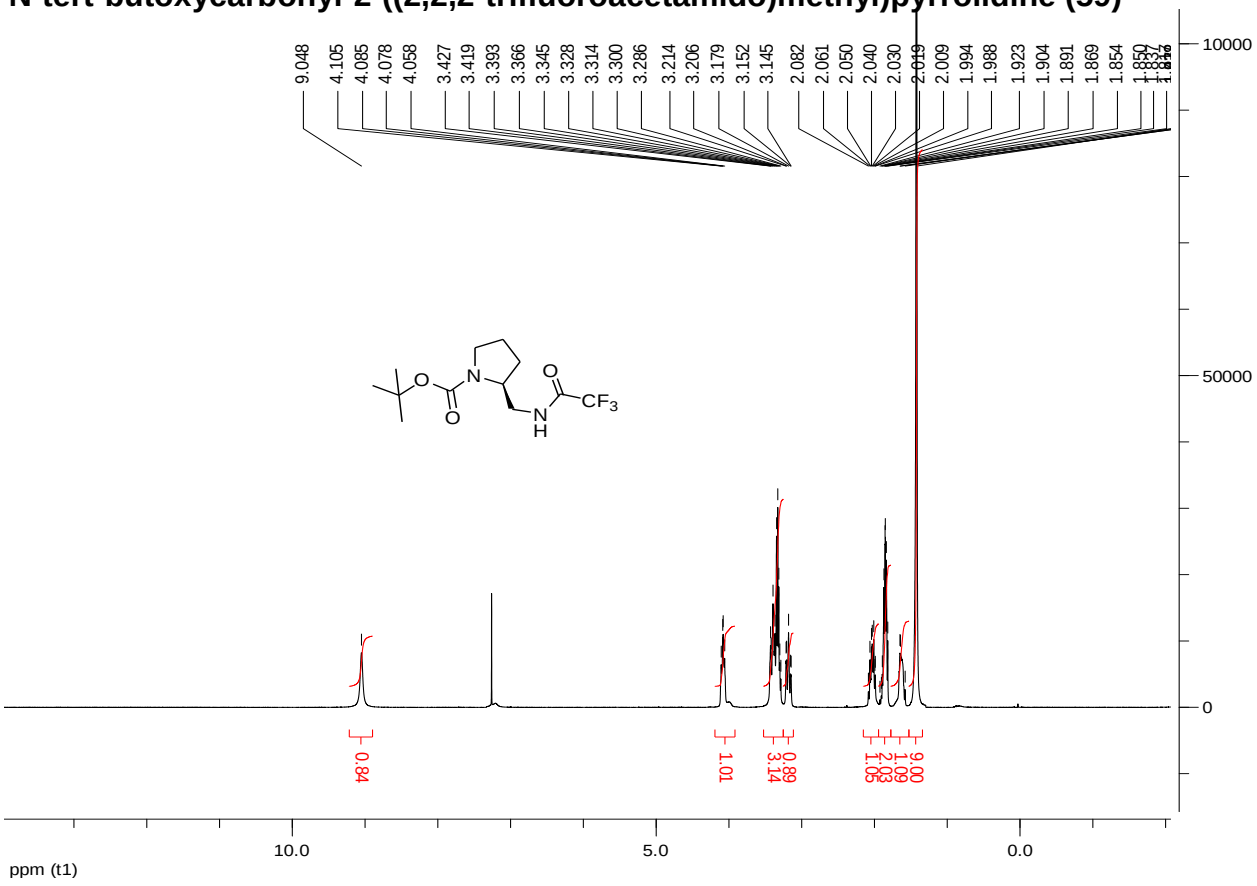

^{13}C NMR (100 MHz, $CDCl_3$)

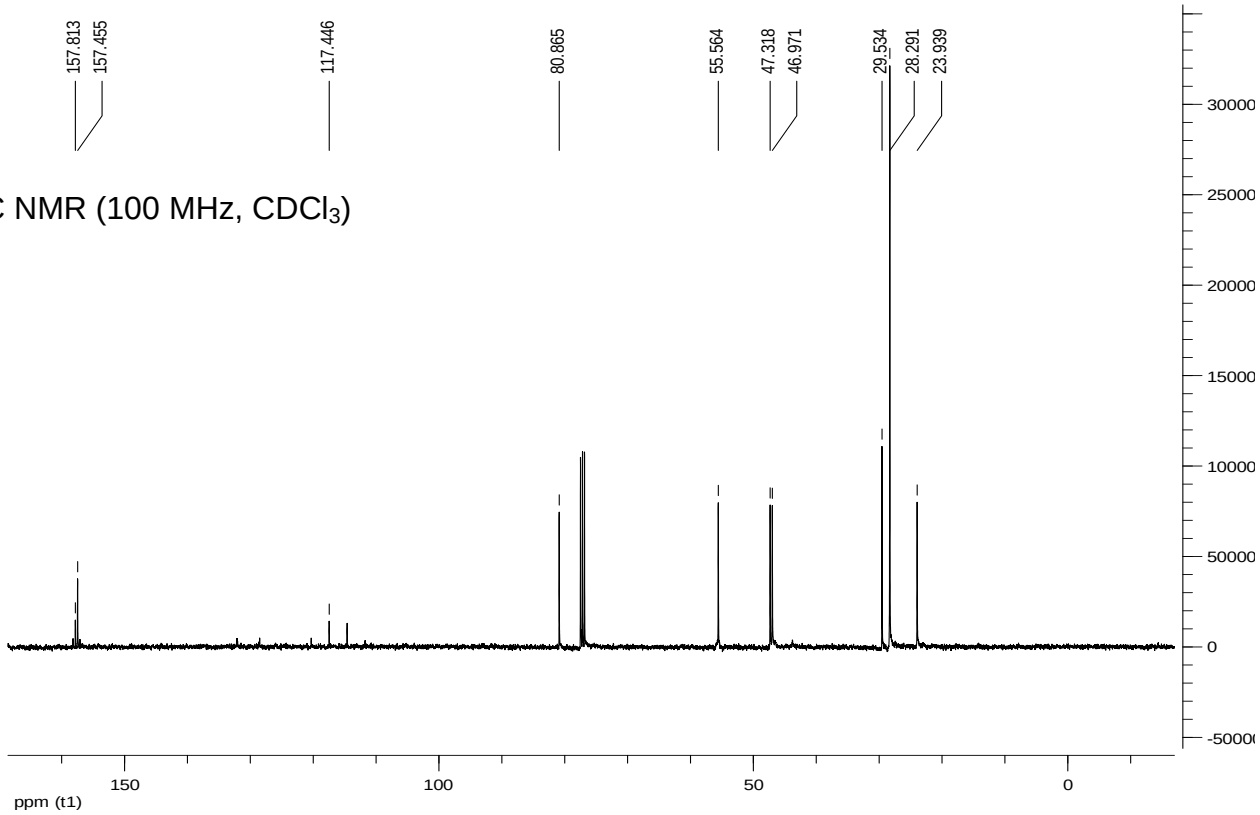

DEPTQ-135 NMR (100 MHz, $CDCl_3$)

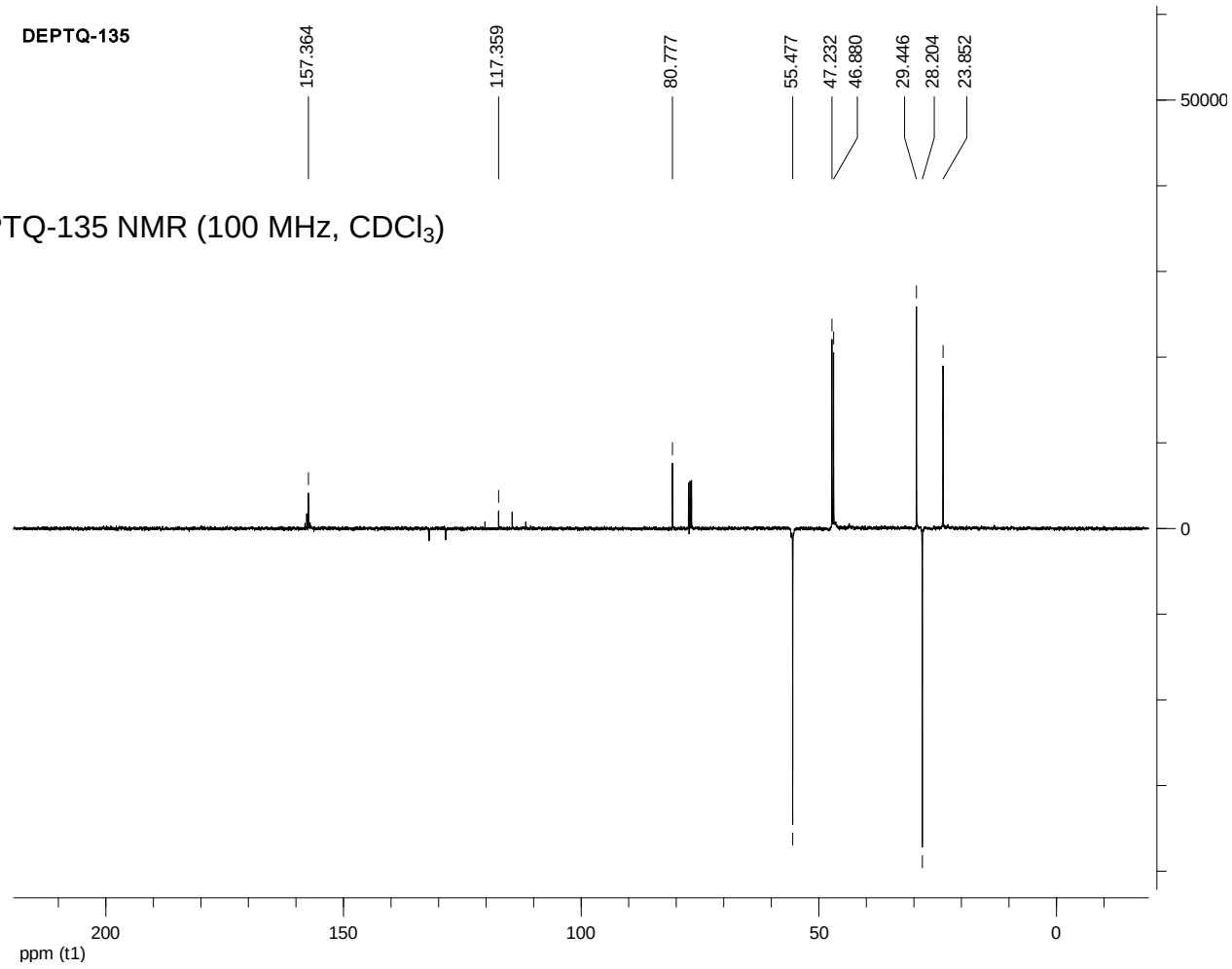

N-tert-butoxycarbonyl-N-Methyl((S)-1-((S)-2((napthalen-2-ylthio)methyl)pyrrolidin-1-yl)-1-oxopent-4-yn-2-yalamino)-1-oxopropan-2-yl) (63)

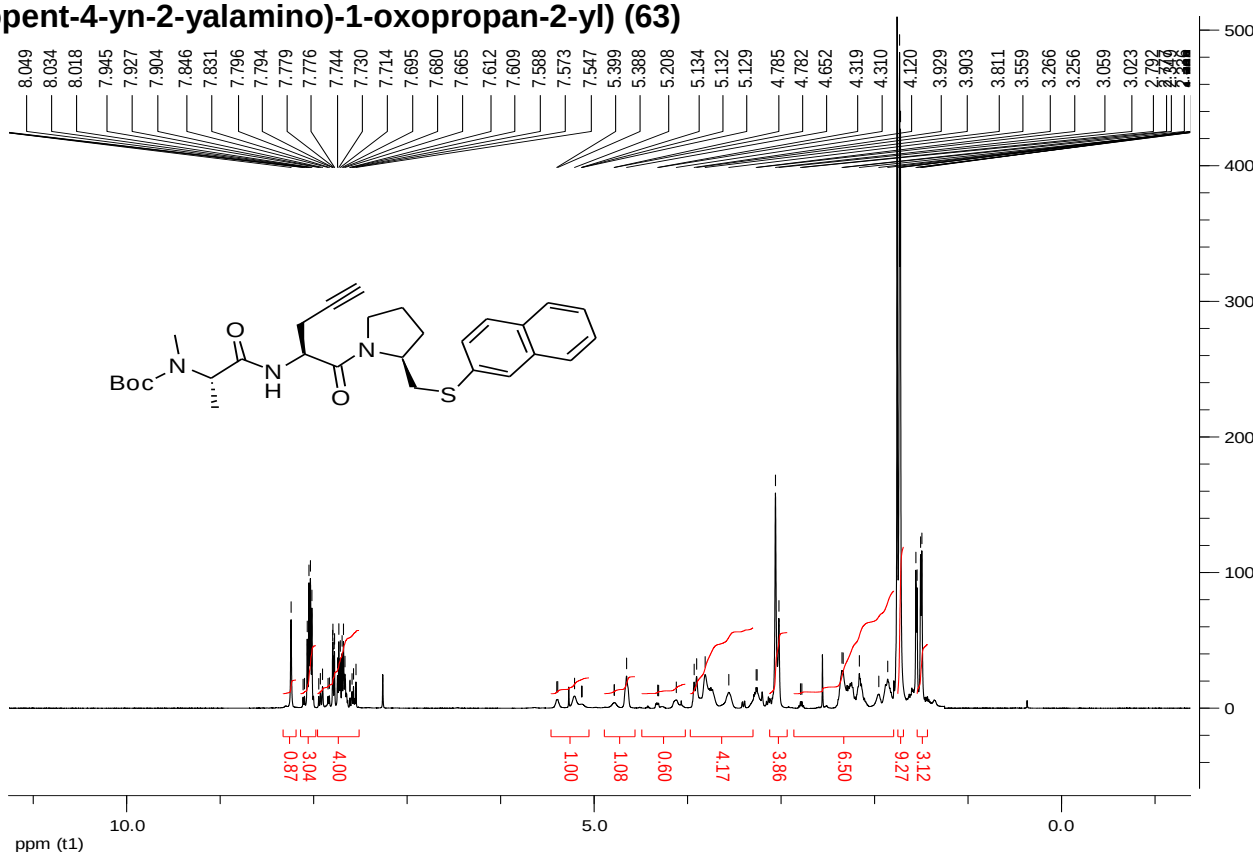

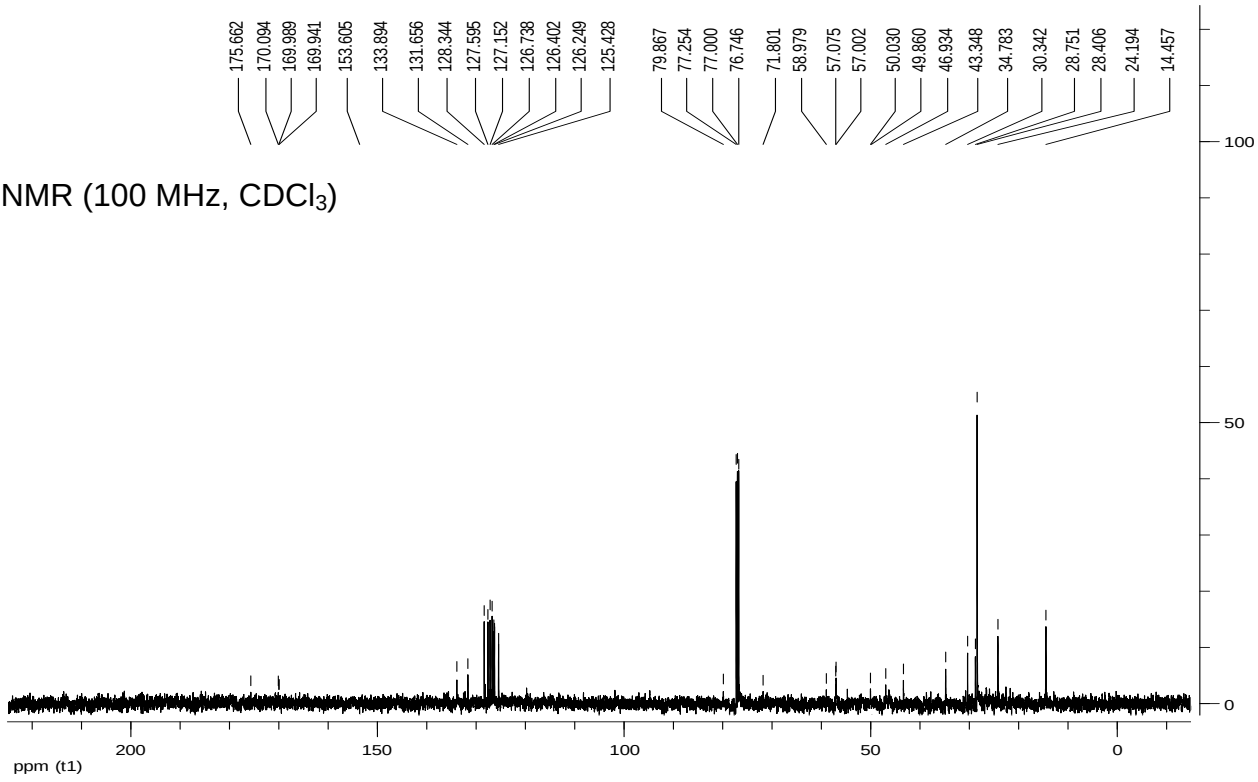

^{13}C NMR (100 MHz, $CDCl_3$)

(S)-2-(methylamino)-N-((S)-2-((napthalen-2-ylthio)methyl)pyrrolidin-1-yl)-1-oxopent-4-yn-2-yl)propanamide (43)

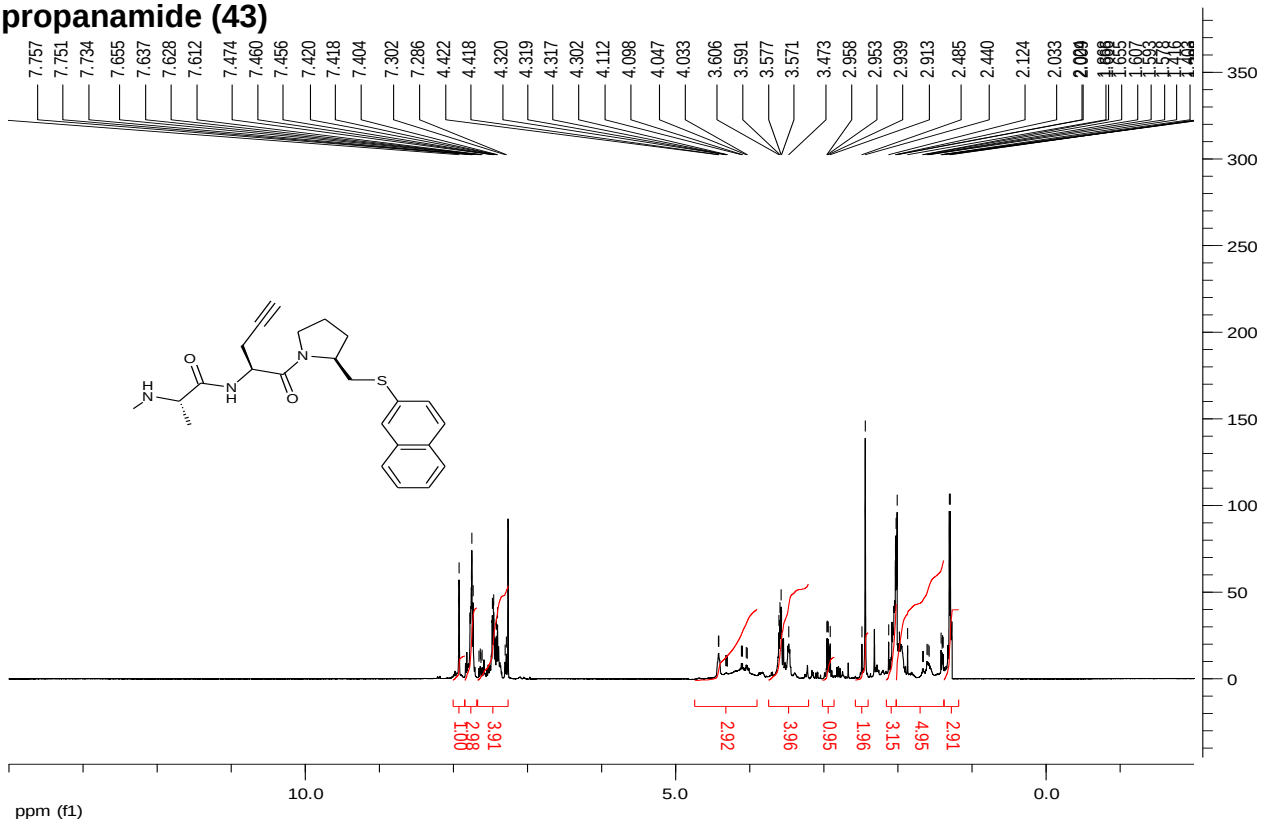

^{13}C NMR (100 MHz, $CDCl_3$)